Russian Original Vol. 36, No. 3, March, 1974
September, 1974

SATEAZ 36(3) 207-322 (1974)

SOVIET ATOMIC ENERGY

АТОМНАЯ ЭНЕРГИЯ
(ATOMNAYA ÉNERGIYA)

TRANSLATED FROM RUSSIAN

CONSULTANTS BUREAU, NEW YORK

SOVIET ATOMIC ENERGY

Soviet Atomic Energy is a cover-to-cover translation of *Atomnaya Énergiya*, a publication of the Academy of Sciences of the USSR.

An agreement with the Copyright Agency of the USSR (VAAP) makes available both advance copies of the Russian journal and original glossy photographs and artwork. This serves to decrease the necessary time lag between publication of the original and publication of the translation and helps to improve the quality of the latter. The translation began with the first issue of the Russian journal.

Consultants Bureau journals appear about six months after the publication of the original Russian issue. For bibliographic accuracy, the English issue published by Consultants Bureau carries the same number and date as the original Russian from which it was translated. For example, a Russian issue published in December will appear in a Consultants Bureau English translation about the following June, but the translation issue will carry the December date. When ordering any volume or particular issue of a Consultants Bureau journal, please specify the date and, where applicable, the volume and issue numbers of the original Russian. The material you will receive will be a translation of that Russian volume or issue.

Subscription
$87.50 per volume (6 Issues)

Single Issue: $50
Single Article: $15

Prices somewhat higher outside the United States.

CONSULTANTS BUREAU, NEW YORK AND LONDON

227 West 17th Street
New York, New York 10011

4a Lower John Street
London W1R 3PD
England

Soviet Atomic Energy is abstracted or indexed in *Applied Mechanics Reviews, Chemical Abstracts, Engineering Index, INSPEC—Physics Abstracts and Electrical and Electronics Abstracts, Current Contents,* and *Nuclear Science Abstracts.*

Published monthly. Second-class postage paid at Jamaica, New York 11431.

SOVIET ATOMIC ENERGY

A translation of *Atomnaya Énergiya*

September, 1974

Volume 36, Number 3 March, 1974

CONTENTS

CONTENTS

(continued)

CONTENTS

(continued)

The Russian press date (podpisano k pechati) of this issue was 2/ 22/ 1974. Publication therefore did not occur prior to this date, but must be assumed to have taken place reasonably soon thereafter.

FIRST CZECHOSLOVAK ATOMIC-ELECTRIC STATION A-1 WITH HEAVY-WATER REACTOR KS-150 (CONSTRUCTION, START-UP, AND INITIAL EXPERIENCE)

V. M. Abramov, B. B. Baturov,
N. V. Bogdanov, V. F. Zelenskii,
V. E. Ivanov, B. L. Ioffe,
G. N. Karavaev, V. A. Mitropolevskii,
M. M. Pchelin, P. I. Puchkov,
Yu. N. Remzhin, G. N. Ushakov,
P. I. Khristenko, J. Keger,
J. Kelner, M. Kozák,
A. Komárek, K. Kostovský,
V. Patrovský, Č. Sklenička,
L. Tomik, A. Ševčik,
and V. Špet'ko

UDC 621.039.524.46.034.3

Planning the working drawings and fabricating the atomic-energy station equipment were assigned mainly to the Skoda factory in Plzen (reactor, etc.); the reactor-vessel metal was produced at the Vitkovitskii factory; the turbocompressors were designed and produced by the CKD (Prague) factory; the steam generators were made at the first Brno metallurgical factory and the Trsebic factory; the primary circuit piping was made by the "Sigma" enterprise. The working project for the station was fulfilled by Energoprojekt (Prague).

The Soviet Union designed and delivered to the station fuel elements, avialite tank for heavy water, the electrical portion and control and safety rods, the KGO system, heavy-water pumps, and several

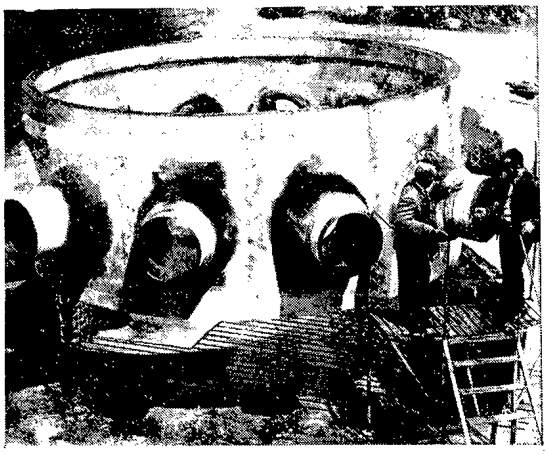

Fig. 1. Ring-shaped part of reactor vessel with forged output branches.

TABLE 1. Completion Dates for Pre-start-Up and Start-Up Operations

Operation	Date	
	planned	actual
Assembly and preparatory work complete and complex testing begun	1/VI 1972	29/V 1972
Complex testing and drying primary circuit	20/IX 1972	20/IX 1972
Physical start-up begun (fuel charging)	5/X 1972	4/X 1972
Station linked to energy system	31/XII 1972	25/XII 1972

Translated from Atomnaya Énergiya, Vol. 36, No. 3, pp. 163-170, March, 1974. Original article submitted October 2, 1973.

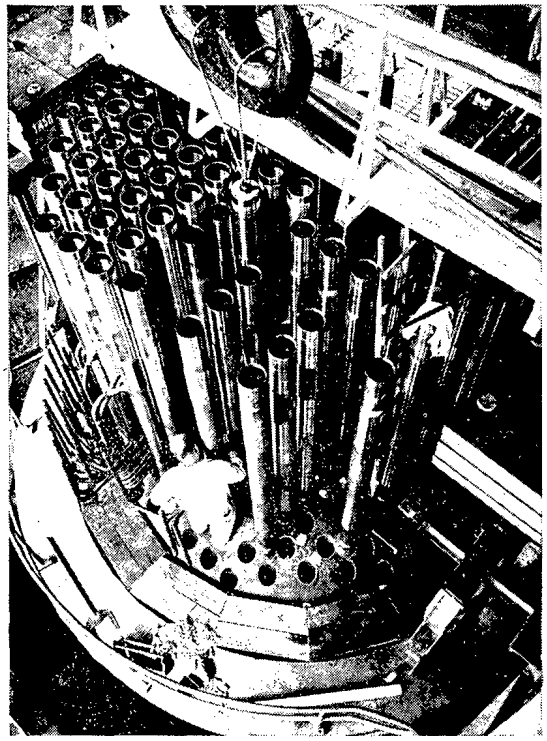

Fig. 2. Welding of standpipes for technical channels and control and safety rod channels to the roof of the assembled reactor vessel.

materials: heavy water, stainless-steel products, and zirconium-alloy sheets and tubes.

During the station construction, Soviet specialists performed a designer's inspection. Moreover, regular consultations between Soviet and Czechoslovak specialists took place.

Special technology was used during preparation of the reactor vessel. The ring-shaped parts (see Fig. 1) were prepared in Plzen at the Skoda factory and were later transported on automatic platforms to the station, a distance of ~400 km. Final welding and heat treatment of the vessel were completed at the station. This technology allows one to assemble the vessel at the station and eliminates various transport problems. Figure 2 shows the vessel already assembled at the station; the standpipes are welded to its roof for technical channels and control and safety rod channels.

To study the brittle fracture of the vessel material on brittle articles, a test setup was constructed at the Skoda factory which produced a tensile force of 8000 tons.

The power-plant construction was complete by the end of 1970, and then began the first stage of complex tests. They were stopped in June, 1971, due to equipment problems and were renewed in 1972. The following deficiencies were observed.

Fuel-assembly mock-ups jammed in 17 technical channels of the reactor. This failure was eliminated by replacing the gaskets in the head of the cassette by guide rings having a certified gap of 0.2 mm.

There was observed five spring failures in the cutoff tubes of technical channels. All 148 springs were replaced.

The device for regulating gas expenditure in the technical channels was observed to operate incorrectly; to correct this, the movement of the device in its lower position was restricted while at the

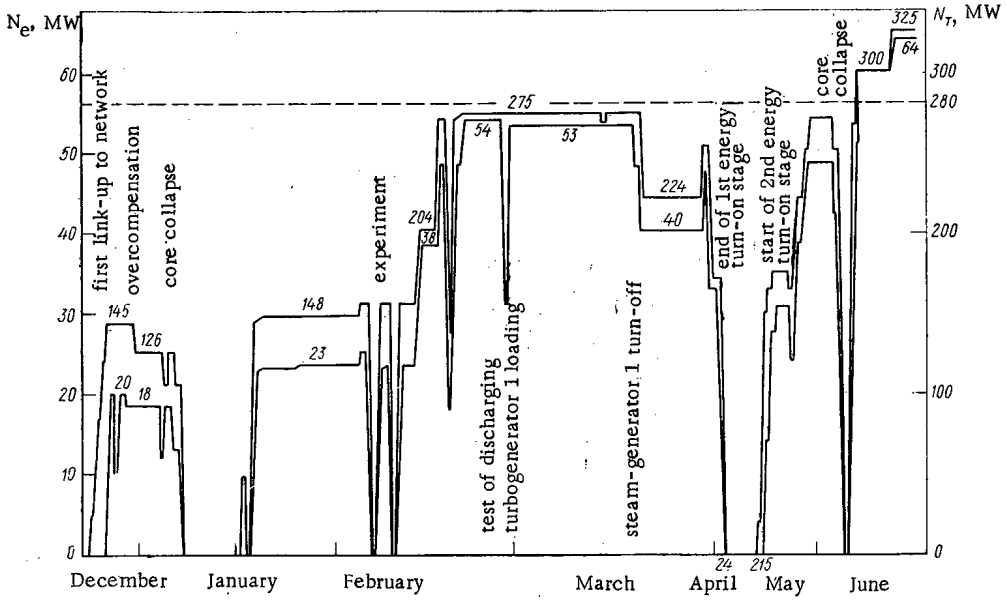

Fig. 3. Chart of station operation in 1972-73.

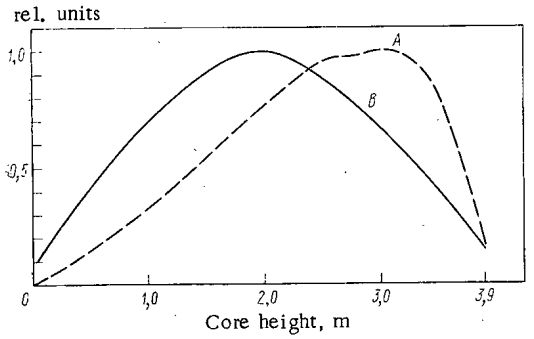

Fig. 4

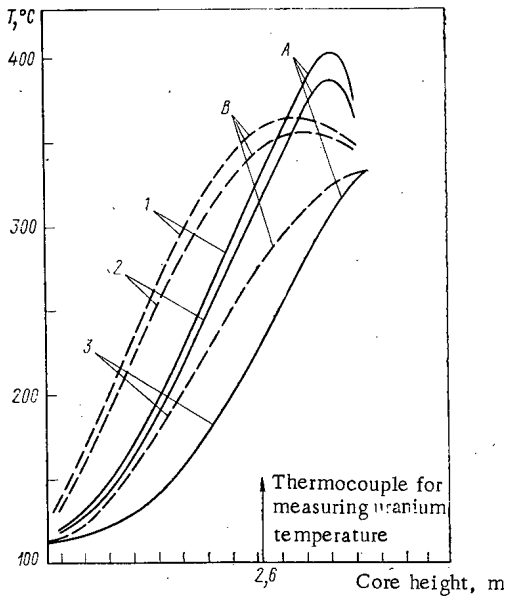

Fig. 5

Fig. 4. Neutron density distribution over reactor-core height: A) at beginning of operating period; B) after replacing compensating rods.

Fig. 5. Temperature distribution of rod at radius 39.45 cm in fuel elements having diameter 112 mm: ——) neutron distribution shown in Fig. 4, curve A; -----) cosinusoidal neutron distribution; 1) uranium temperature; 2) coating temperature; 3) gas temperature. Reactor parameters: N = 255, 6 kcal/sec; G = 4.83 kg/sec; t_1 = 114°C; t_2 = 324°C; P_1 = 29.7 abs. atm.

same time minimum expenditure of heat-transfer agent through the fuel elements was ensured.

Due to nonobservance of the electric-spark operating modes, microfractures appeared in the windows of the cutoff tubes. To eliminate internal stress, we increased the radius of curvature at the window corners.

In the first stage of complex testing, oil leaked from the compressors into the primary circuit due to breakdown in the sealing system of one turbocompressor. The oil was vaporized by the compressors and reached working parts in the primary and heavy-water circuits. Since the oil's (T5K) solubility in water is less than 10 mg/liter, it accumulated on the surface of the water in the avialite tank.

To remove the oil a wet method was used with water solution of detergent "Slovafol 910" (alkyl polyglycol ether) in concentration 2-4 g/liter with additional 0.1-0.5 g/liter polyphosphates (tripolyphosphate and hexamethylphosphate) to increase the washing efficiency.

TABLE 2. Evironmental Radiation Monitoring at Station

Type of monitoring	Number of monitored sites		
	biological monitoring		constant technical monitoring
	constant	periodic	
Power (dose)	123	—	50
Radioactive-gas concentration	59	252	18
Radioactive-aerosol concentration	30	110	148
Concentration of radioactive substances in vapor and water	—	—	30
^{131}I concentration	1	—	—

The steam-generator loops were degreased, i.e., the turbocompressor and auxiliary circuits of the reactor: the distillation apparatus for D_2O, the apparatus for scrubbing CO_2 (distillation and filters), and the apparatus for igniting the incendiary mixture. The heavy-water circuit and the avialite tank were degreased using the solution without additional polyphosphates, since corrosion experiments on avialite in a detergent solution with commerical polyphosphate showed that the solution is corrosive. Degreasing using the solution was accomplished by circulating it at a temperature of 80-85°C. The circulation time was 4-30 h.

The reactor and the inseparable parts of its piping were not degreased due to the danger of moistening the biological shield's graphite stack which can hold approximately 10 tons of water. The removable parts

TABLE 3. Radiation Doses of Station Workers

Period	Number of workers monitored	Dose (mrad)		
		below 100	100–200	200–500
December 1972	558	83	1	—
February 1973	400	39	4	—
April 1973	545	40	4	2

(the technological channels, the control and safety rods, etc.) were degreased outside the reactor in detergent solution and in alcohol; the accessible reactor parts were wiped and drained.

After degreasing by the wet method, a significant amount of moisture remained in the circuits; this decreased significantly (from 1000 to 400 ppm) by the second stage of complex testing due to water-vapor condensation in the condensers of the incendiary-mixture combustion circuit. The drying process began immediately after complex testing. For complete circuit drainage, taps were placed at the lowest points of the circuit before the start of complex testing.

Drying proceeded according to a special program. The first and heavy-water circuits were divided into sectors: reactor; gas loops; D_2O cooling loops; CO_2 scrubbing and incendiary-mixture combustion; distillation apparatus and freezers; high-pressure tanks and low-pressure D_2O tank; D_2O level maintenance circuit; D_2O filling circuit; gas housekeeping. Individual sectors were dried by repeating 3-4 times the cycles: filling with dry gas or air; heating the sectors by specially set up electric heaters, hot water, steam, or gas heat of compression to 55-60°C; evacuation of the circuits to 10^{-1}-10^{-3} torr with simultaneous heating.

The circuits were evacuated using stationary and portable vacuum pumps which were attached sequentially to individual sectors. The gas moisture was measured in every cycle. The D_2O cooling loops were attached to the reactor during the last drying cycle and evacuation was accomplished through nitrogen freezers for observing the formation of ice.

In the final drying stage, dry CO_2 gas with moisture less than 50 ppm was used until obtaining its stable values. After the drying, helium tests of the heavy-water circuit equipment hermeticity were conducted. Then, all systems were filled with dry CO_2 gas having moisture less than 20 ppm and tests were made on the primary circuit at pressure 54 kg/cm^2 and temperature 80°C. The moisture in the circuit was no greater than 70 ppm. Some deterioration of D_2O isotope for 0.18% H_2O was observed after energy start-up and gas-circuit heating to 280-300°C; this is explained as due to removing the moisture adsorbed by the inner surfaces of the primary circuit, which has area 57000 m^2 (if one takes into account the porous surface of oxide films, this is many times greater). Moreover, some surfaces were not degreased, which could decrease the efficiency of evacuation.

A detailed chart, approved by an intergovernmental commission at the beginning of March, 1972, was worked out for completing the great volume of assembly work, equipment repair, and system adjustment. Putting it into effect demanded great efforts from all organizations which participated in the work. Conditions created by the appropriate CSSR organizations aided the successful completion of the problem: active help to the group of Soviet specialists; creative attitude toward fulfilling the assembly and adjustment work by the station operational personnel.

The collectives and working groups from the CSSR suppliers worked successfully on a high level of quality; this was confirmed during the power start-up process; all basic operations were completed on or ahead of schedule (see Table 1). The sequence of operations was determined by a network chart produced using a computer.

Energy Turn-On. The energy turn-on program planned for three stages with gradually increasing technical parameters and power. Preparations for energy turn-on began in 1970 with working out of documentation and safety questions and the training of personnel. Documents of equipment readiness for use were worked out, discussed, and approved for all station systems by a commission. A medical department conducted multiple inspections and confirmed that the station was ready for turn-on.

About 50 workers successfully completed training at Soviet atomic-energy stations at Novovoronezhsk and Beloyarsk. A factory school operated for two years for workers with lower qualifications. Workers with higher educations studied in courses for raising their qualifications. After acquiring knowledge in the field of operating atomic-electric stations, the personnel took exams several times. Practical experience was obtained also during complex equipment testing and during planned periods of systems training.

TABLE 4. Volume and Frequency of External Environmental Radiation Monitoring

Type of monitoring	Number of sites monitored	Monitoring periodicity
Background gamma radiation	7	2 times per year
Radioactive-aerosol concentration	11	1 time per week
Radioactive precipitates	11	1 time per month
Radioactivity:		
soil	4	2 times per year
drinking water	4	2 times per year
milk	5	6 times per year
surface water	7	2 times per year

An inspection was conducted before energy start-up; it included eliminating leaks in the armature; cutting off some auxiliary circuits to guard against moisture from them contaminating the D_2O and CO_2; repeated x-ray monitoring of all welded joints with which work was being conducted; pressing the circuits and observing their tightness; helium testing of the heavy-water cooler hermeticity; repeated test of some technical equipment. Special working groups and commissions for monitoring and submission acceptance were formed for these ends. The appropriateness of these measures was confirmed when the station was started up without incident.

The reactor was brought to critical power on December 21, 1972. On December 22, after successful repeat monitoring of the reactor shielding, its power was raised to 17 MW (thermal), i.e., 3% of nominal.

Steady operation at this power was used for equipment monitoring, and after completion of this program the power started to be raised to 10% (56 MW), achieved on December 23. After another equipment test on December 24, the power was again raised to 17.5% (100 MW), and on December 25, 1972, it reached the intended level — 22.5% (113 MW thermal). At this power on the same day two turbogenerators were linked to the energy system; each had electrical power of 8 MW.

The station operated at this power until January 7, 1973, when it was stopped due to vibration of one turbocompressor. A planned shutdown for some experiments had been intended for the following day. By January 18, 1973, the station had again been brought up to the energy capacity at which it operated until April 2, 1973.

During the start-up, January 17, 1973, at 10% capacity there occurred an emergency reactor shutdown due to turn-off of two turbocompressors caused by a 110-kV drop in the voltage of their supply network. Figure 3 charts the power for the first period in which the station was used, up to the middle of June, 1973.

First Results of Use. The first experience using the reactor and the station and the successful start-up and adjustment work showed that the efforts of Soviet and Czechoslovak specialists had had positive results. During the start-up process, there were no serious equipment failures, while minor defects were fewer than for classical stations having the same power.

From December 25, 1972, until April 22, 1973, i.e., from the moment of linking the first generator to the network, there occurred in all four emergency stoppages of the reactor; one of these was according to plan in order to test the stress in the piping during "heat impact" while three were due to failures in the external energy system.

Reactor. The experimental data confirm that the reactor has surplus reactivity allowing it to achieve higher fuel depletion than that projected; the measurement, regulating, and reactor-shielding systems work reliably in all modes of use; all the systems of auxiliary technical circuits also work reliably. Impurities in the heat-transfer agent do not fundamentally raise the limits indicated in the project and do not have a noticeable effect on the efficiency of equipment and fuel elements; the variation in isotope content of heavy water is insignificant and within the expected limits.

In the first period of use, due to the large reactivity surplus at nonsteady reactor operating modes and a significant quantity of compensating rods which were not fully loaded, we observed distortion in the neutron field over the reactor height (Fig. 4, curve A). This led to a shift in the maximum temperature

and the rod-shaped thermocouple indicators were lower by 40-50°C (see Fig. 5) than the true fuel-element temperatures. This made more difficult raising the reactor power and observing fuel loading.

By replacing four compensating rods with rods having cadmium only in their lower half, and four shortened rods with full-length rods we were able to approximate the neutron distribution to cosinusoidal distribution (see Fig. 4, curve B).

The thermotechnical and hydrodynamic conditions in the reactor core was studied. For this purpose, 19 experimental cassettes were lowered into the reactor; they were supplied with sensors for heat-transfer agent expenditure, covering temperature and cores in the axial and radial directions, neutron flux over the reactor-core height, and power (measured with calorimetric detectors). These measures will serve to optimize the reactor-core temperature conditions.

Also studied were the structural and radiation stability of the fuel elements, their radiation growth, the behavior of the structural-element coverings and the materials under operating conditions.

Attention was given to questions of reactor-material corrosion, in particular, the effect of organic acids produced by radiolysis of CO_2 and D_2O in the reactor, on corrosion of the heavy-water tank.

The first use period showed that the reactor operation is fully reliable. All its systems operate normally.

Fuel. Despite the fact that many tests of the fuel-element assemblies on loops and tests stands in the USSR and CSSR had confirmed their reliability, there was still some uneasiness before the station start-up concerning them. During the complex-testing period, only one assembly was tested in the reactor over 500 h at gas temperatures 70-115°C, pressure 20-64 abs. atm, and moisture 260-280 ppm. The condition of the assembly and the fuel elements was satisfactory. Until June 22, 1973, the average fuel depletion reached 1500 MW·day/ton, and the maximum was 2700 MW·day/ton.* The system for measuring temperature of fuel elements and gas leaving the reactor channels worked reliably. During the entire period of using the reactor, there was only one instance of damage to fuel-element coverings; this is evidence of the promise and reliability of the fuel.

CO_2 and D_2O System. At all stages of reactor start-up, the following were chemically monitored: composition of CO_2 delivered to the station; composition of CO_2 in the primary circuit; composition of gas entering the incendiary-mixture combustion circuit; chemical and isotope composition of D_2O in the heavy-water circuit.

The constant contact between CO_2 and heavy water necessitates high CO_2 purity. During periodic monitoring, the moisture, oil, and mechanical-impurities content and the CO_2 chemical composition were determined.

The composition of the CO_2 delivered to the station was:

	wt. % (min)
CO_2	99.6
	wt. % (max)
O_2	0.2
N_2	0.2
CO	0.02
Ar	10^{-4}
	wt. ppm (max)
H_2	2
H_2O	20
Hydrocarbon C_1—C_8	5
Oil	5
H_2S, NH_3, P	1
HCl	0.2
B	0.1
Cu	0.1

*In the fall of 1973, the reactor power with two units operating reached 75 MW, and fuel depletion reached maximum 5000 MW·day/ton.

The moisture in CO_2 in the circuit was in the complex-testing period about 750 ppm. After drying the primary circuit it did not exceed 150, and the average was 70 ppm. After energy start-up, the moisture with respect to heavy water was 900, and with increased power it decreased to 750 ppm. At the same time, the gas moisture with respect to heavy water beyond the incendiary-mixture assembly was 270 ppm.

Regular monitoring of the oil content in the gas is simultaneously monitoring of the turbocompressor operation. Therefore, most of the samples were taken at the output from the turbocompressors. The oil content in the gas is 2-5 $mg/n \cdot m^3$.

The mechanical-impurities content in CO_2 was ~ 20 mg/ton. The deuterium concentration in CO_2 at the output from the space over the D_2O surface in the heavy-water tank did not exceed 0.05 vol. % D_2. Deposition of the incendiary mixture was two orders of magnitude lower than projected.

Before arrival at power, the chemical composition of D_2O practically did not change: conductivity 0.79 μmho/cm, iron content 0.3 mg/liter, aluminum content 0.1 mg/liter.

The chemical-impurities content, especially aluminum and organic substances, began to increase rather rapidly after the reactor reached power; this confirmed the assumption tested on the KS-60 loop and at the reactor of the Institute for Atomic Research (CSSR), concerning radiolysis of CO_2 and water. Mainly organic acids are formed, and this leads to decreased p_D value for D_2O, equal to 4.7 (after freeing it from CO_2). The organic substances accumulate in condensate in the incendiary-mixture combustion circuit, where p_D for D_2O varies from 1 to 2.

Avialite corrosion is monitored by the growth of corrosion products in D_2O and the measurement of the corrosion rate and its character by electrochemical sensors on the hot and cold collectors of the heavy-water circuit. Beginning with the second half of the first stage of energy start-up, we observed stable aluminum content in D_2O and decreased rate of corrosion as measured by the sensors.

Operation of Other Station Equipment. During the first stage of energy start-up at 30 abs. atm pressure, the CO_2 losses from the primary circuit were 90-100 kg/h; in the second stage at 52 abs. atm, they were 180 kg/h. There were no deficiencies in the piping or armature.

In May, 1973, corrosion damage was found in the stainless-steel piping of one section of the heavy-water heat exchanger due to high chloride content (greater than 30 mg/liter) in the cooling water.

A characteristic of the KS-150 reactor is the combination of gas and heavy-water circuits, which allows increased reactor reliability, since the pressure in the gas and heavy-water circuits are in constant equilibrium. However, this structural decision makes high demands on the purity of the heat-transfer agent. The D_2O and CO_2 interaction products which accumulate during their irradiation are drawn off with the D_2O condensate from the incendiary-mixture combustion apparatus (quantity of condensate 2 liters/h). At present, methods are being devised to purify the condensate from organic products and to regenerate them.

The turbocompressors worked reliably. This is confirmed by the above-indicated low oil content in the gas, five times less than allowable. Despite these good results, the turbocompressor construction and automatic equipment still do not completely exclude small amounts of oil from entering the primary circuit.

Steam generators Nos. 1, 2, 5, and 6 operated in the normal mode, while Nos. 3 and 4 were in the readiness mode to dissipate heat in case of accidental cooling. At the end of the first stage of energy start-up, leaks were observed in the water heater of steam generator No. 1. A loop was cut out and corrosion and erosion phenomena were observed on the pipe plate (from the water side). The cause of this has not been finally determined.

In the second stage of energy start-up, there were observed about 40 loose welds (out of 120,000) in various parts of steam generators Nos. 1, 2, 5, and 6. Complete inspection and repair on the steam generators were completed in two months.

The transport and technical section includes two loader—unloaders (one reserve). The cassettes are lifted into the cooling zone and lowered by a crane having capacity 5 tons.

Toward the beginning of energy start-up, some automatic loader—unloader control operations were performed with insufficient reliability. It was decided in the first stage to work with the loader—unloader at zero reactor power but at operational pressure and with reduced gas circulation. The limited used of the loader—unloader was caused also by the absence of special dowels in the technical-channel seals which

would protect the gasket from being crumpled when the cassette was moved into the loader—unloader. These devices will be mounted according to the reactor overload; this will ensure that the loader—unloader works according to the overall program. The loader—unloader worked well in all operations at zero reactor power.

The electrical equipment in the first stage of energy start-up provided the station's own needs from three independent sources. The supply system for electrical devices of category 1 worked reliably; the diesel-generator station worked satisfactorily. Strict dispatcher measures will be taken in the second stage; one hydrogenerator of the Madunitsa hydroelectric station and two diesel generators (for turning the reverse-block turbocompressors) will operate continuously.

Some Conclusions from Station Use. During the period under consideration the station produced 100 million kW·h of electrical energy at power-use factor 0.75 and readiness factor 0.83. The emergency shielding was activated three times in all (external impulses). All this shows the station's reliability. The fuel was used at covering temperatures 450°C and higher. The real prerequisites exist for obtaining fuel-expenditure depths significantly greater than those projected. The control and safety rods and KGO systems worked satisfactorily. All dynamic technical equipment worked reliably. The heavy-water and gas-circuit chemical modes presented new problems concerned with producing organic acids and concerned with corrosion questions.

Monitoring the radiation environment at the station and outside it is accomplished by the biological and special—technical monitoring system (see Tables 2-4).

The maximum γ-radiation dose power was observed within the D_2O system; in the service corridors it was 100 mCi/h. Radioactive gases were noted only in two unattended rooms, with maximal concentration $9 \cdot 10^{-9}$ Ci/liter. The presence of radioactive aerosols was observed only in one room with maximal concentration $6 \cdot 10^{-13}$ Ci/liter. The activity of aerosols and gases exhausted through the chimney was on the average $2.5 \cdot 10^{-3}$ Ci/day. The isotopes ^{89}Sr, ^{90}Sr, and ^{131}I were not observed in the emissions.

The average irradiation dose for workers at the station over five months was low: none of the workers exceeded the allowable monthly dose. Great attention was paid to monitoring the populated areas near the station. This work was done by the external-dosimetry laboratory. Monitoring was extended to a region 35 km in radius. The point for determining the background was 55 km from the station.

From the first period of using the station, we can conclude that the equipment shielding was effective and that there were no changes in the radiation environment in the surrounding areas.

CONCLUSIONS

In energy reactors similar to the KS-150 but larger, high fuel-expenditure levels (native metallic uranium) are entirely attainable. Thanks to the high conversion ratio, they can simultaneously produce plutonium for fast reactors in quantities approximately double the unit yield of thermal reactors using enriched uranium.

Another method for developing such reactors [1, 2] may be to use in them a ring with equilibrium concentration of Pu and ^{238}U with additional ^{235}U contained in native uranium or diffusion-plant waste. In this case, they would be able to burn significant quantities of ^{238}U and, using their plutonium many times, also produce transuranic elements.

LITERATURE CITED

1. P. I. Khristenko, At. Énerg., 20, No. 1, 26 (1966).
2. P. A. Petrov and P. I. Khristenko, in: Proceedings of the VII Congress of the World Energy Conference [in Russian], Vol. 12, Izd. Sov. Natsional'nogo Komiteta (1969), §. 3, p. 340.

FUEL-CHANNEL POWER MONITORING SYSTEM FOR THE REACTOR USED IN THE SECOND UNIT OF THE BELOYARSK NUCLEAR POWER STATION

B. G. Dubovskii, A. Ya. Evseev,
V. V. Ezhov, V. A. Zagadkin,
V. F. Lyubchenko, I. G. Batenin,
L. G. Andreev, V. M. Malyshev,
M. G. Mitel'man, K. N. Mokhnatkin,
N. D. Rozenblyum, É. I. Snitko,
and G. A. Shasharin

UDC 621.039.562: 621.039.517

One of the most important problems arising at the present time in connection with the use of nuclear reactors is that of equalizing the power distribution in the active zone of the nuclear reactor and keeping it at its optimum. An efficient system for monitoring the power distribution will increase the reliability of the reactor and improve its economic indices.

In this paper we shall present some basic data relating to the construction of a fuel-channel power monitoring system for the reactor in the second unit of the Beloyarsk Nuclear Power Station, together with experience in its use. As sensors for the system we chose direct-charge detectors [1, 2].

In constructing the system we adhered to the basic principle that the arrangement of the sensors in the active zone should not interfere with the normal working of the reactor. In view of this we refrained from placing sensors in empty cells instead of fuel channels, which would reduce the power of the reactor; we also restricted their installation of sensors in the evaporating channels, since in this case the sensors would lie in the coolant of the first circuit, reducing its flow in the channel in question and greatly complicating the assembly and operation of the system.

For siting the sensors we chose the central apertures of the steam-superheating channels; this necessitated the manufacture of direct-charge detectors capable of working at 700°C. Experience showed that no electrical terminals were capable of working reliably at high temperatures and humidities close to the active zone of the reactor; the construction of the detectors had to be such that the coupling line formed a single unit with the detector, any terminals or clamps lying well outside the reactor. A detector satisfying this requirement (and also a number of others imposed upon detectors lying inside the zone) has now been developed and successfully undergone production tests [1]. The main characteristics of detectors

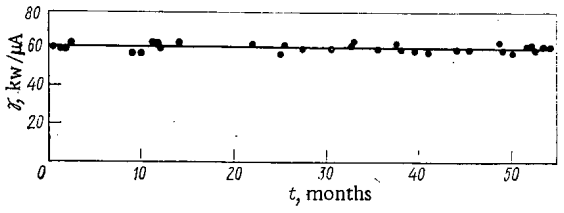

Fig. 1. Time dependence of the sensitivity of the direct-charge detectors.

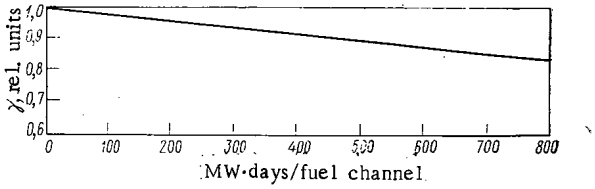

Fig. 2. Fall in the sensitivity of the direct-charge detectors as the energy of the fuel channels becomes depleted.

Translated from Atomnaya Énergiya, Vol. 36, No. 3, pp. 171-173, March, 1974. Original article submitted April 19, 1973.

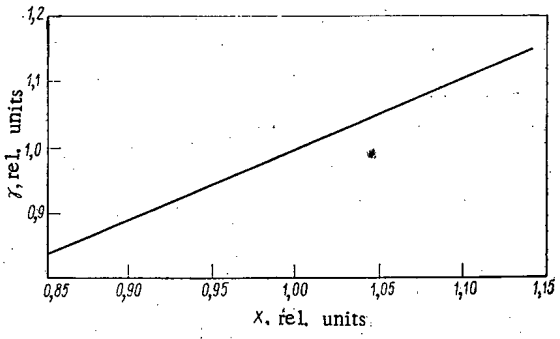

Fig. 3

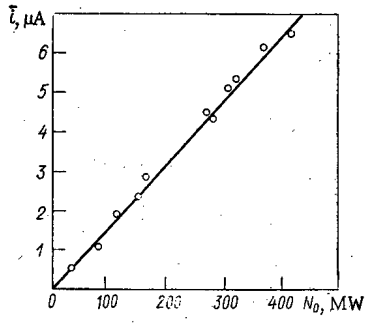

Fig. 4

Fig. 3. Sensitivity of the direct-charge detectors as a function of the uranium enrichment in the steam-superheating channels.

Fig. 4. Mean current of the direct-charge detector as a function of the thermal power of the reactor.

of the DPZ-7 type used for monitoring the power of the fuel channels in the Beloyarsk Nuclear Power Station are:

Diameter of sensitive element, mm	6
Length of sensitive element, mm	6000
Length of coupling line, mm	15,000-17,000
Initial sensitivity to thermal neutrons, $A \cdot cm^2 \cdot sec/neutron$	$(7.8 \pm 0.6) \cdot 10^{-19}$
Initial sensitivity to hyperthermal neutrons, $A \cdot cm^2 \cdot sec/neutron$	$(19.8 \pm 1.8) \cdot 10^{-19}$
Change in sensitivity due to the burn-up of the emitter material, $\% \cdot A/sec$	0.013 ± 0.0016
Calibration characteristic relative to the neutron flux density	Linear
Nonidentity, %	±2
Probability of faultless operation for 10,000 h	0.8
Working temperature, °C	700
Diameter of emitter (rhodium), mm	0.5

The apparatus used for measuring the currents of direct-charge detectors with ranges of 0-15 and 0-3 μA (having a basic error of ±1.5 and ±2.5% respectively and an input resistance of no greater than 1 kΩ) enables the currents of 100 direct-charge detectors to be recorded on an automatic-recording ÉPP-09M3 potentiometer. The direct-charge detectors are connected to the apparatus in groups of 20. Provision is made for the average current of each group to pass out to a single-point automatic recorder. The switching system comprises a relay device enabling any group of direct-charge detectors to be connected to the input unit on a signal from the control unit. The time required to read all the sensors is determined by the writing speed of the ÉPP-09M3. Provision is made for measuring the resistance of the detectors.

The system for monitoring the power of the fuel channels in the reactor of the second unit of the Beloyarsk Nuclear Power Station consists of 92 direct-charge detectors, uniformly distributed about the active zone; 72 are placed in the steam-superheating channels and 20 in the evaporator channels in order to record a reasonably complete power distribution over the reactor. The system was assembled in June 1970 after the successful operation of twelve experimental direct-charge detectors installed in March 1968.

During the operation of the system it was essential to determine the sensitivity of the direct-charge detectors as fuel-channel power sensors, and also the changes taking place in this sensitivity as the campaign proceeded. In view of the fact that no standard method existed for determining the power of the fuel channels in the Beloyarsk Nuclear Power Station to a high accuracy, the following method was adopted for determining the quantities in question.

The thermal power of the reactor and also the thermal power of all 266 steam-superheating channels was determined by a thermotechnical method, with an error of ±4%. Knowing the mean current of the direct-charge detectors placed in the steam-superheating channels, the sensitivity of the direct-charge detectors as sensors of fuel-channel power may be determined from the formula

$$\gamma = \frac{W}{N\bar{i}}, \tag{1}$$

where W is the power of the steam-superheating channel zone, N is the number of such channels, $\bar{i}$ is the mean current of the direct-charge detectors, determined with due allowance for the period during which these have been in place (correction for burn-up).

The maximum permissible error in the experimental determination of the mean sensitivity of the direct-charge detectors was calculated from the formula

$$\delta\gamma = \delta W + \delta i + \delta\bar{i}, \tag{2}$$

where δw, $\delta\bar{i}$, δi are the maximum errors in the determination of the thermal power of the steam-superheater channel zone, the arithmetic mean current of the detector, and the measured current of the direct-charge detector respectively ($\delta\gamma$ equals ±8%).

Figure 1 shows the change in the value of γ with time. Within the limits of experimental error (±5%) the value of γ remains constant for 54 months

$$\gamma = 61 \pm 5 \text{ kW}/\mu\text{A}$$

Unfortunately, the direct-charge detectors cannot always be placed in a "fresh" fuel channel. Sometimes the detectors of the monitoring system are placed in channels which have already been in operation for a considerable time. This situation may arise from either the installation of the monitoring system in a working reactor or the replacement of a direct-charge detector which has become unserviceable. Since the sensitivity of a failed direct-charge detector has diminished as a result of burn-up at the end of its period of service, in order to compare the readings of the old and new detectors it is essential to introduce a correction into the reading of the new one. This may be conveniently effected in practice by referring the readings of all the direct-charge detectors to the case in which they are installed in a "fresh" channel. The fall in the sensitivity of the direct-charge detectors as the energy of the channels in which they lie becomes depleted is shown in Fig. 2.

The maximum acceptable error in the determination of the relative power of the fuel channel in which the detector is installed may be calculated from the formula

$$\frac{\Delta W}{W} = \frac{\Delta i}{i} + \delta_{DCD} + \delta_c \tag{3}$$

where i is the current of the direct charge detector, δ_{DCD} is the nonidentity factor of the direct-charge detector, δ_c is the nonidentity of the steam-superheating channel.

The effect of the nonidentity of the steam-superheating channels on the readings of the direct-charge detector, mainly due to differences in the ^{235}U charge of the channels, was determined by a calculation carried out by Z. M. Kurova. Figure 3 shows how the coefficient γ depends on the enrichment of the fuel in the steam-superheating channel. Taking a reserve of $\delta_c = 5\%$ we obtain the maximum error in the determination of the relative power of the fuel channel containing the detector as ±9%.

An extremely vital service characteristic of the direct-charge detectors is their reliability. The factory-guaranteed service life of the DPZ-7 detectors placed in the steam-superheating channels is one year with a confidence probability of $P^* = 0.8$. In actual fact only 10% of the detectors fail for various reasons over a year's operation of the system.

The operation of the system during 1970-1972 showed that its incorporation enabled the power of the fuel channels to be operatively balanced and an optimum distribution readily to be achieved, as well as detecting and eliminating surges of power in the active zone. Thus, after the reactor had been brought up to a power of 150 MW, one of the compensating rods proved to have been into the active zone, although its position indicator suggested that the rod had been completely extracted. Analysis of the readings of the direct-charge detectors nearest to the rod enabled the error to be exactly determined and duly eliminated.

The sum of the currents (the mean current) of the direct-charge detectors situated in the active zone of the reactor is proportional to the neutron flux integrated over the volume of the reactor and hence to its thermal power, as indicated in Fig. 4, which gives the thermal power of the reactor (horizontal axis) as a function of the mean current of the direct-charge detectors (vertical axis). The scatter in the experimental data is due to the error in determining the thermal power of the reactor. The system under consideration may also be used for monitoring the total power of the reactor.

At the present time an analogous monitoring system is being installed in the reactor of the first unit in the Beloyarsk Nuclear Power Station.

LITERATURE CITED

1. E. N. Babulevich et al., "Direct-charge detector for determining the neutron flux in power reactors," At. Énerg., 31, No. 5, 465 (1971).
2. M. G. Mitel'man et al., "Direct-charge detectors (present state)," in: Metrology of Neutron Radiation in Reactor and Accelerators, Vol. 1 [in Russian], Standarty, Moscow (1972), p. 115.

ON CHOOSING THE OPTIMUM PARAMETERS FOR A NUCLEAR HEAT-SUPPLY STATION

Yu. D. Arsen'ev, Yu. S. Bereza, M. E. Voronkov, and S. I. Mukhanov

UDC 621.039.003

An analysis of existing models representing the development of nuclear power in the Soviet Union and elsewhere shows that, in view of the predicted nuclear-fuel breeding coefficients, fast reactors may completely satisfy the requirements of nuclear heat-supply stations as regards nuclear fuel. According to predictions regarding the development of electric power systems, the loading coefficients of these stations will gradually diminish, and this casts a certain doubt on even the possibility of using fast reactors in the basic part of the loading graph in the year 2000 [1]. Hence the use of atomic heat and electric power plants occupying the basic part of the load instead of nuclear heat-supply stations may prove unfavorable, since these will displace fast reactors into the variable zone of the loading graph. In addition to this, the use of fast reactors with low coolant parameters for atomic heat and electric power plants reduces the specific development of electrical power in heat consumption [2, 3].

It should be emphasized that the low parameters of nuclear heat-supply stations enable us to obtain a higher level of plutonium breeding than that obtained in nuclear power stations, which is important during the first stages of the adoption of fast reactors, in which the optimum duration of the fuel campaign of the nuclear heat-supply stations may be taken as minimal, while, as secondary nuclear fuel is created by virtue of the fast reactors, the accumulation of plutonium in the nuclear heat-supply stations will play a smaller and smaller part. Thus, in addition to fulfilling their direct energy functions, nuclear heat-supply stations may to a certain extent promote the optimum use of nuclear fuel when this is in either short or copious supply. The question as to the most efficient type of nuclear heat-supply station thus becomes very important, all the more so in view of the fact that the constructional parameters of nuclear heat-supply stations should differ very substantially from those of nuclear power stations [4].

The program of development of nuclear power stations in the USSR includes the extensive use of water-cooled water-moderated power reactors (VVÉR series) [5-8]. In the circuit of a nuclear heat-supply station the coolant passes from the reactor into a steam generator-water supply heater in which the supply water is heated by secondary steam not having any radioactivity. Essentially the system is of the three-circuit type (Fig. 1). Furthermore, the pressure of the supply water is higher than the pressure of the steam in the vessel of the steam generator-water heater, and this practically eliminates the danger of radioactive contamination.

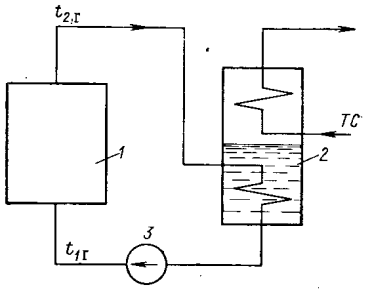

Fig. 1. Thermal system of a nuclear heat-supply plant with a water-cooled water-moderated reactor: 1) Reactor; 2) steam generator-water supply heater; 3) circulating pump; TC — thermal circuit.

Translated from Atomnaya Énergiya, Vol. 36, No. 3, pp. 174-177, March, 1974. Original article submitted October 13, 1972; revision submitted June 18, 1973.

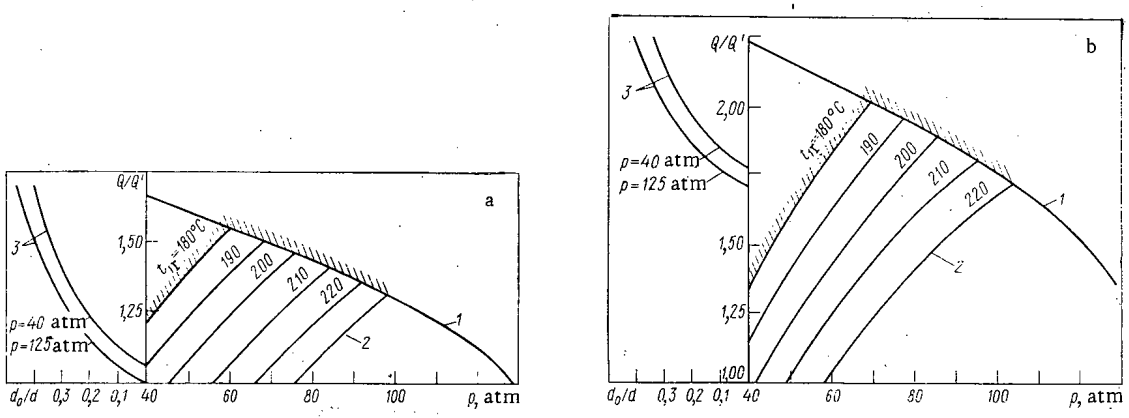

Fig. 2. Thermal characteristics of the active zone: a) Regular fuel elements of a VVÉR-440 reactor with an external diameter of 9.1 mm; b) fuel elements with a reduced diameter of 7.14 mm; 1) limit of thermal power as defined by the boiling crisis; 2) thermal power Q/Q' as a function of pressure for various coolant temperatures at the entrance into the active zone; 3) change in the axial aperture of the fuel tablet of diameter d_0 as a function of thermal power.

The active zone of a power reactor differs in temperature from that of the reactor in a nuclear heat-supply station. The lower temperature of the coolant in the heat-supply station enables the thermal power of the reactor to be boosted. For purposes of analysis we took the standard zone of VVÉR-440 reactor having a thermal power of Q' = 1180 MW. From the condition of constant temperature in the center of the fuel element and in the can, we calculated the temperature conditions for standard fuel elements with an external diameter of 9.1 mm. The ultimate possibilities of boosting the power of the active zone by reducing the parameters were considered for rod fuel elements of diameter 9.1 and 7.14 mm (126 and 216 rods per cassette respectively). The dimensions of the fuel elements were determined from the condition that the water/uranium ratio and the amount of fuel in the active zone should remain constant.

The heat-evolving surface of the cassettes containing fuel elements of reduced diameter increased by 34% in comparison with the fuel elements of diameter 9.1 mm (the thermal power of the rod-type fuel elements increased for constant temperatures of the center of the fuel unit and the can). For fuel elements of this type the necessary reserve (margin) required to avoid approaching the melting point of the fuel was provided by introducing a technological aperture in the center of the fuel unit (tablet). The magnitude of the relative aperture is shown as a function of the reactor power (Q/Q') in Fig. 2a and b (curve 3) for fuel-element wall temperatures of 249 and 330°C (p = 40 and 125 abs. atm, respectively).

From the equations of thermal balance and the condition that the temperature at the wall should be approximately equal to the saturation temperature at the specified pressure we obtain a relationship between the reactor power and the pressure for various temperatures of the coolant at the entrance into the reactor (curves 2). For all types of fuel elements we calculated the relationships limiting the reactor power in respect of boiling crisis. Curve 1 was obtained with due allowance for the maintenance of a constant margin relative to the crisis, which was taken the same as in the nominal working mode of the VVÉR-440 unit.

On using the reactor for heat supply, the temperature at the entrance into the reactor cannot be below the specified $t_{1r} > t_l$. The value of t_l is determined by the maximum temperature in the thermal network and the temperature head in the heat exchanger. It follows from Fig. 2 (curve 1) that the boosting of the thermal power is limited by the development of the heat-outflow crisis, and (on retaining the constant margin with respect to the crisis, $Q_{cr}/Q' = 1.6$) increases with falling pressure.

For a constant geometry of the active zone the choice of optimum coolant pressure may be based on the specific expenditure (cost) equation:

$$E = \frac{P + P_a}{Q\eta\tau}(K_0 + K_1 + K_2 + K_3 + K_4) + E_f + E_{ser} \text{ roubles/Gcal} \qquad (1)$$

where P is the reduction factor, P_a is an amortization factor allowing for a reduction in respect of capital and current repairs and renovation, η is the efficiency of the nuclear heat-supply plant, τ is the annual number of hours' use at steady power, K_0 is the capital outlay for the whole reactor section allowing for

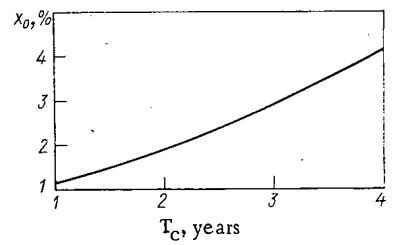

Fig. 3

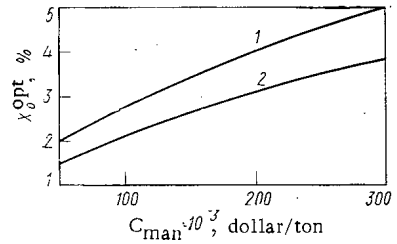

Fig. 4

Fig. 3. Dependence of the initial enrichment of the fuel x_0 on the required effective duration of the campaign for a constant reactor power.

Fig. 4. Dependence of the optimum enrichment of the fuel x_0^{opt} on the net cost of the natural uranium C_n and of manufacturing the fuel element C_{man}: 1) $C_n = 20 \cdot 10^3$ dollar/ton; 2) $C_n = 60 \cdot 10^3$ dollar/ton.

shielding and all expenses in construction except for expenditure on the vessel (the quantity K_0 does not depend on the power of the reactor Q and the pressure of the coolant p), K_1 is the capital outlay for the reactor vessel, proportional to the coolant pressure p, K_2 is the capital outlay on the steam generator in respect of coolant, proportional to the surface of the generator, i.e., the thermal power Q and the pressure p, K_3 is the capital outlay on the steam generator without K_2, including the auxiliary equipment and the structural part, proportional to Q, K_4 is the capital outlay on the system for heating the customer's water, proportional to Q, E_f is the fuel component of the specific expenditure [9], E_{ser} is the service (running) component of the specific expenditure (auxiliary materials and wages).

For the construction of the active zone taken E_f = const; neglecting the slight change in the service (running) component (i.e., assuming E_{ser} = const), we may use the base-point method [10] and reduce the optimization formula (1) to the dimensionless form

$$y = \delta\left(\frac{1}{Q}\right) + \theta_1'\delta\left(\frac{p}{Q}\right) + \theta_2'\delta p, \tag{2}$$

where $\delta(1/Q) = Q'/Q - 1$; $\delta(p/Q) = pQ'/p'Q - 1$; $\delta p = p/p' - 1$ are the relative changes in the physical links; $\theta_1' = K_1'/K_0'$; $\theta_2' = K_2'/K_0'$ are the economic similarity criteria, constituting the capital-outlay ratios in the problem under consideration.

All the primed quantities characterize an arbitrary version of the calculation at the base point, in no way affecting the ultimate optimization. We took p' = 60 abs. atm and Q' = 1180 Gcal and determined the physical links for active zones with a coolant temperature of $t_{1r}' = 180°C$ at the entrance into the reactor. For the analysis we took the ranges $\theta_1' = 0.05$–0.25 and $\theta_2' = 0.01$–0.1, and for these values we plotted the curves $y = f(\theta_1'; \theta_2'; \delta p)$, the minimum of which determined the desired value of p_{opt}/p'.

For the ranges of variation of θ_1' and θ_2' just indicated the $y = f(\delta p)$ curves have an economic optimum limited by the boiling crisis [11, 12].

Thus for thermal-network water temperatures of 150/70°C and a head of 30° in the steam generator the optimum pressure in the active zone is 60 and 70 abs. atm for fuel elements of diameter 9.1 and 7.14 mm respectively.

Allowing for possible constructional changes in the active zone, let us now consider the question of optimizing the fuel component of the cost of power in the reactor used for nuclear heat-supply stations.

We are interested in finding the initial enrichment of the fuel (determining the duration of the fuel campaign) which minimizes the fuel component of the energy of the nuclear heat-supply station for various values of the cost of natural uranium and the expenditure incurred in the manufacture of the fuel cassettes.

Allowing for the regeneration of worked-out fuel, the fuel component may be expressed thus [9]:

$$E_f = C_n\left(1 + \frac{pT_c}{\varphi}\right) = \frac{1.16}{24\eta B}\left(C_n\frac{x - x_0}{x_n - x_0} + C_{en} + C_{man} - C_{wo}\right)\left(1 + \frac{pT_c}{\varphi}\right), \tag{3}$$

where C_f is the fuel component of the net cost of thermal power, allowing for the net cost of the worked-out fuel, roubles/Gcal; T_c is the duration of the campaign, years; φ is the nuclear power station load

coefficient; B is the average depth of burn-up, MW · day/ton of U; η is the efficiency of the nuclear heat-supply station; C_n, C_{en}, C_{man}, are the specific net costs of natural uranium, enriched uranium, and the manufacture of the fuel assemblies per ton of fuel in the cassettes respectively, roubles/ton; C_{wo} is the net cost of the worked-out fuel, including the net cost of the residual uranium and the accumulated plutonium, less the expenditure incurred in the transportation and chemical reprocessing of the fuel, roubles/ton; x_1, x_0, x_n are the initial enrichment of the uranium in the assemblies, the spent material of the gas-diffusion plant, and the amount of ^{235}U in the natural uranium respectively, %.

The specific net cost of enrichment depends considerably on the degree of enrichment [13]:

$$C_{en} = a_0 + a_1 x_0 + a_2 x_0^2, \text{ roubles/ton,} \tag{4}$$

The duration of the campaign T_c, depending on the enrichment of the original charge, was determined by a physical calculation (Fig. 3).

This relationship may be approximated by the equation

$$T_c = b_2 + b_3 x_0 + b_4 x_0^2, \text{ years,} \tag{5}$$

where $b_2 = 0.1$; $b_3 = 0.97$; $b_4 = 0$.

The depth of burn-up increases with increasing enrichment and is determined by the equation

$$B = b_0 + b_1 x_0, \text{ MW · days/ton U,} \tag{6}$$

where $b_0 = 4.4 \cdot 10^3$; $b_1 = 1.03 \cdot 10^4$.

Since the specific yield of plutonium increases on reducing the depth of burn-up B, which according to (6) depends on the initial enrichment of the fuel x_0, in the problem under consideration the net cost of the worked-out fuel may be expressed by the equation

$$C_{wo} = b_5 + b_6 x_0 + b_7 x_0^2, \text{ roubles/ton U.} \tag{7}$$

It should be noted that the results of the physical calculation for the nuclear heat-supply plant agree satisfactorily with the results of [14].

Substituting (4)-(7) into (3) and minimizing the result, we obtain the optimum enrichment

$$x_{opt} = \sqrt{(A_1 C_n^2 + 2A_1 (A_2 + x_0) C_n + A_2^2 + \beta^2 - \frac{C_{man} + a_0 + b_5}{a_2 - b_7}} - (A_2 + A_1 C_n + \beta), \tag{8}$$

where

$$A_1 = \frac{1}{2(a_2 - b_7)(x_n - x_0)}; \quad A_2 = \frac{a_1 - b_6}{2(a_2 - b_7)}.$$

The quantity $\beta^{-1} = d\alpha/dx \cdot 1/\alpha$ is a weak function of x_{opt}, where $\alpha = 1/B(1 + (p/\varphi)T_c)$. From (5) and (6) we obtain

$$\beta^{-1} = \frac{b_3 + 2b_4 x_0}{\frac{\varphi}{p} + b_2 + b_3 x + b_4 x_0^2} - \frac{b_1}{b_0 + b_1 x_0}.$$

Equation (8) is solved by the method of iterations.

Generalizing non-Soviet data relating to the costs of the fuel cycle [13] we take the following ranges of variation of the original indices: $C_n = (20\text{-}60) \cdot 10^3$ dollar/ton; $C_{man} = (50\text{-}300) \cdot 10^3$ dollar/ton; $a_0 = 29.4 \cdot 10^{-3}$; $a_1 = 39.4 \cdot 10^3$; $a_2 = 2.64 \cdot 10^3$.

For the open fuel cycle ($C_{wo} = 0$) with $x_0 = 0.2\%$ and $x_n = 0.71\%$ we obtain $A_1 = 371 \cdot 10^{-6}$; $A_2 = 7.45$.

With these indices and $p/\varphi = 0.15$ we plotted the curves of Fig. 4, showing the way in which the optimum enrichment x_0^{opt} depends on the expenditure incurred in manufacture for various net costs of the natural uranium. It follows from this graph that the expenses incurred in manufacture constitute the decisive factor of x_0^{opt}, while the net cost of natural uranium influences the optimum enrichment much less markedly. Allowance for the value of the plutonium produced leads to an increase in x_0^{opt}.

The analysis was carried out for the active zone of the VVÉR-440; however, the conclusions also apply to the active zones of other reactors of this type of various powers.

Thus we have determined the ranges of pressure of the coolant for nuclear heat-supply stations with water-cooled water-moderated reactors; these vary in accordance with the technological-economic indices of the stations. For the coolant parameters of the corresponding nuclear heat-supply stations we have indicated the ranges of boosting applicable to the thermal power of the reactor as compared with a reactor of the power type. We have determined the way in which the optimum enrichment of the fuel for nuclear heat-supply stations depends on the cost of the natural uranium and the expenditure on fuel manufacture.

LITERATURE CITED

1. G. Bainbridge and A. Farmer, Symp. on Economic Integration of Nuclear Power Stations in the Electrical Power System, IAEA, Vienna (1970), SM-139/18.
2. E. Ya. Sokolov, Teploénergetika, No. 10, 2 (1971).
3. L. S. Gornostaev and G. A. Kruglov, ibid., 7.
4. Yu. D. Arsen'ev, M. E. Voronkov, and N. M. Sinev, At. Énerg., 35, No. 3, 197 (1973).
5. G. V. Ermakov, Teploénergetika, No. 4, 7 (1971).
6. A. M. Petros'yants et al., At. Énerg., 31, No. 4, 315 (1971).
7. V. V. Stekol'nikov et al., At. Énerg., 25, No. 5, 408 (1968).
8. V. P. Denisov et al., At. Énerg., 31, No. 4, 323 (1971).
9. V. V. Batov and Yu. P. Koryakin, Economics of Nuclear Power [in Russian], Atomizdat, Moscow (1969).
10. Yu. D. Arsen'ev, Theory of Similarity in Engineers' Economic Calculations [in Russian], Vysshaya Shkola, Moscow (1967).
11. G. N. Kruzhilin and D. A. Labuntsov, Izv. Akad. Nauk SSSR, Énergetika i Transport, No. 3, 86 (1969).
12. A. I. Klemin and M. M. Stringulin, Some Problems Regarding the Reliability of Nuclear Reactors [in Russian], Atomizdat, Moscow (1968).
13. J. Bader et al., Power Engng., 73, No. 12, 26 (1969).
14. S. A. Skvortsov, At. Énerg., 28, No. 4, 294 (1970).

COMBINED PULSED METHOD OF MEASURING HIGH REACTIVITIES FOR REACTORS WITH REFLECTORS

É. A. Stumbur, A. G. Shokod'ko,
V. I. Zhuravlev, I. P. Matveenko,
and Z. N. Milyutina

UDC 621.039.55:621.039.519.4

Recently the pulsed α method of measuring reactivities, based on recording the asymptotic transient neutron field $\varphi_{as} = \varphi_0(\mathbf{r}, \mathbf{v})e^{-\alpha_0 t}$ formed in a subcritical reactor after irradiation of the latter from a pulsed source, has become more and more widely employed [1, 2].

The fundamental advantage of this method lies in the fact that the results obtained on measuring the quantity α_0 are independent of the positioning and energy characteristics of the source and detector.

However, the method used in practice for determining the reactivity $\rho \equiv (1-k_{eff})/k_{eff}$ in fractions of β_{eff} by comparing α_0 with the critical decrement α_0^{cr} (Simmons—King [1]) $(\rho/\beta)_{SK} = \alpha_0/\alpha_0^{cr} - 1$ is only justified if the time of generation of the prompt neutrons depends weakly on k_{eff}. For reactors with reflectors this is not the case: furthermore, when, with increasing degree of subcriticality, the asymptotic decrement α_0 is determined mainly by the life-time of the neutrons in the reflector, the α method becomes entirely inapplicable [3].

In addition to the α method, there are also a number of integrated pulse methods of measuring reactivity (methods of Sjöstrand, Garelis—Russell, and Gosani [1, 2]) using various kinds of time integral of the neutron flux $\varphi(\mathbf{r}, \mathbf{v}, t)$ excited in the reactor by a pulsed source. Basic to these methods is a separation of the over-all integral of the neutron flux F into the "prompt" component F_p and the "delayed" component F_d, the latter being due to the decay of the emitters of delayed neutrons (subject to the condition $\alpha_0 \gg \lambda_i$ and a constant decay rate of the emitters).

$$F(\mathbf{r}, \mathbf{v}) \equiv \int_0^\infty \varphi(\mathbf{r}, \mathbf{v}, t)\, dt = F_p(\mathbf{r}, \mathbf{v}) + F_d(\mathbf{r}, \mathbf{v}). \quad (1)$$

TABLE 1. Experimental and Calculated Reactivities*

Assembly	α_0, sec^{-1}	(ρ/β) from k_{eff}	(ρ/β) from (3)	(ρ/β) on various assumptions				
				a	b	c	d	e
A^{exp}	1597±40	—	5,15 †	5,25 †	5,13±0,04	5,25±0,04	5,32±0,05	5,17±0,05
A_{calc}	1588	4,91 (k_{eff}=0,9622)	4,91	5,03	5,03	5,09	5,10	5,00
B^{exp}	3020±100	—	28,1±0,7	27,8±0,7	31,2±0,5	30,9±0,5	32,3±0,5	28,3±0,7
B_{calc}	2970	26,2 (k_{eff}=0,8225)	26,2	26,7	29,5	30,0	30,5	26,3

* The errors of the experimental values are the mean square errors.

† Values arbitary, since the difference in the local ratios Q_p/Q_d and C_p/C_d were not found, detailed measurements of $Q_p(x)$ and $Q_d(x)$ not being made.

Translated from Atomnaya Énergiya, Vol. 36, No. 3, pp. 178-181, March, 1974. Original article submitted March 7, 1973.

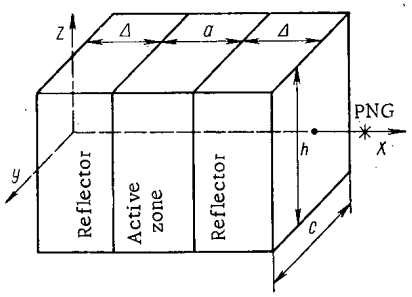

Fig. 1

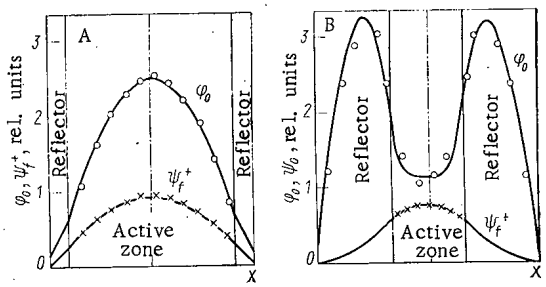

Fig. 2

Fig. 1. Arrangement of the assembly and experiment: h = 30 cm, c = 28 cm; assembly A: a = 37 cm; assembly B: a = 13.6 cm.

Fig. 2. Asymptotic neutron distributions φ_0 and value functions of the function neutrons ψ_f^+ for assemblies A and B: ——) calculation; ○, ×) experiment. The errors in the experimental values are indicated by the size of the characters (○, ×).

Integrated pulsed methods (in contrast to the α method) enable us to obtain the values of $(\rho/\beta) \equiv \rho/\beta_{eff}$ simply from measurements at a specified subcritical state without the necessity of bringing the system to criticality for measuring α_0^{cr}.

However, a common disadvantage of the integrated pulsed methods is the fact that the resultant reactivity depends very considerably on the disposition of the pulse source and detector. This is an inevitable consequence of the difference in the spatial behavior of F_p and F_d, especially for reactors with reflectors, in which case integrated methods give ambiguous results [4-6].

An analysis of the integrated pulsed methods [5, 7] shows that the integrated fluxes $F_p(\mathbf{r}, \mathbf{v})$ and $F_d(\mathbf{r}, \mathbf{v})$ are related by

$$\chi \hat{Q} F_d - \hat{L} F_d = -\chi_d \hat{Q} F_p. \tag{2}$$

Here $\hat{Q}$ is the operator of fission processes, $\hat{L}$ is the operator of all other transport processes [4]; $\chi \equiv \chi_p + \chi_d$ is the spectrum of fission neutrons, including the prompt $\chi_p = (1-\beta)f_p$ and delayed $\chi_d = \Sigma \beta_i f_i$ neutrons.

Equation (2) leads to a general expression for determining the reactivity from the integrated fluxes F_p and F_d [7]:

$$(\rho/\beta) = \frac{\int \Psi_f^+(\mathbf{r})\, Q_p(\mathbf{r})\, d\mathbf{r}}{\int \Psi_f^+(\mathbf{r})\, Q_d(\mathbf{r})\, d\mathbf{r}}, \tag{3}$$

where $Q_p(\mathbf{r})$ and $Q_d(\mathbf{r})$ are the densities of the fissions due to the components F_p and F_d of the integrated flux; $\Psi_f^+(\mathbf{r}) \equiv \int \chi(\mathbf{v})\psi^+(\mathbf{r}, \mathbf{v})\, d\mathbf{v}$ is the value of the fission neutrons based on the solution $\psi_f^+(\mathbf{r}, \mathbf{v})$ of the critical equation for the specified subcritical reactor.

$$\frac{1}{k_{eff}} \hat{Q}^+ \chi \psi^+ - \hat{L}\psi^+ = 0. \tag{4}$$

It was shown in [4, 7] that all the foregoing integrated methods (Sjöstrand, Gosani, Garelis—Russell, and others) constituted different forms of approximation to the general relation (3), only valid for certain particular cases. The same conclusion was reached by the authors of [8], who confirmed this by a series of numerical experiments.

A combined integrated method of determining reactivity was therefore proposed in [7], based on a strict realization of Eq. (3) by measuring the distributions of $Q_p(\mathbf{r})$ and $Q_d(\mathbf{r})$ over the active zone in pulse experiments, and also a direct measurement of the spatial behavior of the value function $\Psi_f^+(\mathbf{r})$.

In the present investigation we tested the combined method experimentally for two assemblies of a subcritical reactor with an interchangeable reflector (Fig. 1). The active zone, made in the form of a parallelepiped, was a highly-enriched uranium-water lattice (of the type described in [9]). On the two sides of the assembly were beryllium reflectors.

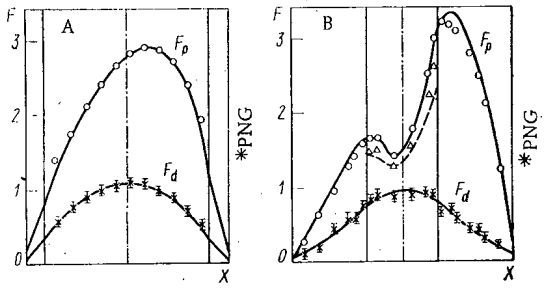

Fig. 3

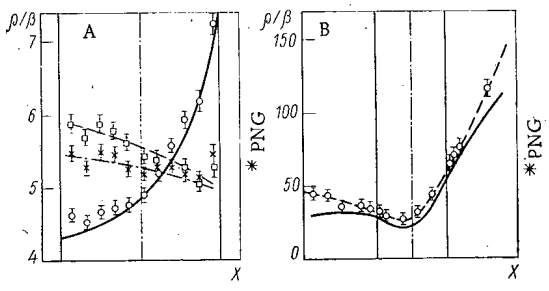

Fig. 4

Fig. 3. Distribution of the integrated fluxes F_p and F_d for assemblies A and B: ——) calculation; ○, ×) experiment (for a 1/v detector) Δ) experiment (for a ^{235}U detector). The experimental errors for F_p are indicated by the size of the characters (○, Δ).

Fig. 4. Dependence of the reactivities (ρ, β) of assemblies A and B determined by different methods on the position of the detector x: ——) calculation; ○) experiments for $(\rho/\beta)_{Sj}$; ×) $(\rho/\beta)_{GR}$; □) $(\rho/\beta)_{Go}$.

In assembly A ($\rho \approx 5\beta$) the reflectors were of thickness $\Delta = 4$ cm. In assembly B ($\rho \approx 30\beta$) the active zone was thinner and the reflectors thicker; $\Delta = 20$ cm. The other dimensions of the assemblies were the same. The target of the pulsed neutron generator (PNG) was placed to one side beyond one of the reflectors, which certainly created an unfavorable asymmetry in the initial neutron distribution (and correspondingly in F_p) along the x axis.

The neutron fluxes in the assemblies were measured with a pulsed fission chamber containing ^{235}U and an SNM-12 boron counter. The transient neutron distributions were recorded with an AI-256 analyzer (in the "slow" analysis mode).*

For both assemblies we measured the values of the asymptotic decrement α_0, the asymptotic neutron distributions $\varphi_0(\mathbf{r}, \mathbf{v})$ (from the readings of the 1/v detector) shown in Fig. 2, and the spatial distributions of the integrated fluxes F_p and F_d (Fig. 3).

The values of the reactivities obtained by the Sjöstrand $(\rho/\beta)_{Sj}$, Gosani $(\rho/\beta)_{Go}$ and Garelis—Russell $(\rho/\beta)_{GR}$ methods depend greatly on the position of the detector and therefore have a great scatter: in assembly A from 4.5 to 7.3β, and in assembly B over the whole system from 25 to 125β and within the active zone from 25 to 50β (Fig. 4). We see that the use of ordinary integrated methods leaves a considerable indeterminacy in the reactivity values.

In order to use Eq. (3) of the combined integrated method we measured the spatial dependence of the value $\Psi_f^+(\mathbf{r})$ by the method of the "influence function." On placing a neutron source $S(\mathbf{r}, \mathbf{v}) \equiv S_0\chi(v)\sigma(\mathbf{r}_S - \mathbf{r})$ in the subcritical system, the neutron flux $\vartheta(\mathbf{r}, \mathbf{v}|\mathbf{r}_S)$ at the point $\mathbf{r}$ is described by the equation

$$\chi\hat{Q}\vartheta - \hat{L}\vartheta = -S_0\chi\sigma(\mathbf{r}_S - \mathbf{r}). \tag{5}$$

Together with (4), this gives an integral equation for $\Psi_f^+(\mathbf{r})$:

$$\int \Psi_f^+(\mathbf{r})\, Q(\mathbf{r}|\mathbf{r}_S)\, d\mathbf{r} = \frac{S_0}{\rho}\Psi_f^+(\mathbf{r}_S), \tag{6}$$

where $Q(\mathbf{r}|\mathbf{r}_S)$ is the density of fissions at the point $\mathbf{r}$ for a source at $\mathbf{r}_S$.

In practical experiments the readings of the detector (in a small volume δV_i around the point $\mathbf{r}_i$) have the values $C(\mathbf{r}_i) = \eta Q(\mathbf{r}_i)$ where η is the efficiency of the detector with respect to the density of fissions in the material of the active zone. A "point" source of fission neutrons may be conveniently simulated† by a small quantity of ^{252}Cf introduced into the selected volume δV_S. The results of such experiments (for all possible combinations of the disposition of the detector $\mathbf{r}_i$ and the source $\mathbf{r}_S$ in the active zone) may be used by expressing (6) in the form of a system of linear equations

*The experimental arrangements (shielding from background, characteristics of the pulsed source and detectors, etc.) were analogous to those employed in [9].

†In the experiments this source was replaced by a ^{238}Pu—Be source; the equivalence of this to the fission source was confirmed by a multigroup calculation.

$$\sum_{i=1}^{N} \tilde{\psi}_i C_{iS} \delta V_i = \xi \tilde{\psi}_S \delta V_S; \quad S = 1, 2 \ldots N. \tag{7}$$

Here $\tilde{\psi}_i$ is the value of the neutrons Ψ_f^+ averaged over the volume δV_i, C_{iS} is the reading of the detector in the volume δV_i for the positioning of the source in δV_S. The constant $\xi \equiv (S_0/\rho\eta)$ may be found as the greatest eigenvalue of the matrix of coefficients of the system (7); its determination and the subsequent evaluation of $\tilde{\psi}_i$ are quite simple if one uses small computers (such as the Nairi) for N = 10-20 (the number of points of disposition of the source and detector may be considerably reduced on allowing for the symmetry of the system). The results of such measurements of Ψ_f^+ are presented in Fig. 2.

For the assemblies under consideration we made a series of calculations of the neutron fluxes, values, and functionals: α_0, k_{eff}, β_{eff} etc. The calculations were carried out in the $2P_0$ approximation (for an 18-group representation of the neutron spectrum) in a plane one-dimensional geometry (allowing for the transverse dimensions by introducing an effective leak DB_{yz}^2). Homogenization of the active zone and correction of the cross sections in the thermal group were carried out as in [9].

The equivalence between computing models and the experimental assemblies may be estimated by reference to the agreement between the calculated and measured values of α_0, a quantity which, in contrast to k_{eff}, is accessible to direct experimental determination and may be obtained numerically by solving the equation

$$\chi_p \hat{O}\varphi_0 - \hat{L}\varphi_0 + \frac{\alpha_0}{v}\varphi_0 = 0. \tag{8}$$

The solution of Eq. (4), leading to the values of k_{eff} and $\Psi_f^+(\mathbf{r})$, as well as the determination of F_p and F_d was carried out in the usual manner by the iteration of sources [10].

Thus the complete set of these computed results enabled us to calculate all the required forms of (ρ/β) for the various integrated methods. The results of all the experiments and calculations are presented in Table 1.

Together with the value of reactivity based on Eq. (3), relating to the combined pulse method, Table 1 also gives the values of (ρ/β) obtained for the following different approximations to Eq. (3):

a) on the assumption that $\Psi_f^+ \equiv 1$, i.e., without allowing for the value function, as proposed in [8];

b) using the readings of the 1/v detector, i.e., the quantity $C_{p,\,d}(\mathbf{r}) \equiv \int (1/v) F_{p,\,d}\, dv$ instead of $Q_p(\mathbf{r})$ and $Q_d(\mathbf{r})$;

c) using approximations a) and b) simultaneously;

d) averaging $(\rho/\beta)_{Sj}$ over the active zone;

e) in Eq. (3), substituting the hard-to-determine $\Psi_f^+(\mathbf{r})$ by its palliative $Q_d(\mathbf{r})$, which may be quite naturally obtained from pulse experiments (in the flux F_d the dominant contribution is that arising from the fundamental harmonic [6], which for a uniform active zone is close to the Ψ_f^+ distribution).

We see from the table that the calculated prototypes of the assemblies were somewhat less subcritical than the experimental versions. At the same time they were fairly close both as regards the neutron distributions (Figs. 2 and 3) and as regards the reactivity values.

This comparison leads to the conclusion that, even for an unfavorable disposition of the pulse source, the combined integrated method yields a fairly accurate value of the reactivity.

The most convenient practical approximation of this method is that indicated in e), i.e., calculating the reactivity by means of the formula

$$(\rho/\beta) = \frac{\int Q_p(\mathbf{r})\, Q_d(\mathbf{r})\, d\mathbf{r}}{\int [Q_d(\mathbf{r})]^2\, d\mathbf{r}}, \tag{9}$$

giving the reactivity values to an error of 2%.

The methods set out in a)-d) (for reactors with highly-efficient reflectors) lead to considerably greater errors (5-15%).

LITERATURE CITED

1. E. Garelis, in: Pulsed Neutron Research, IAEA, Vienna, Vol. II, p. 3.
2. I. F. Zhezherun, in: Theoretical and Experimental Problems of Transient Neutron Transport [in Russian], Atomizdat, Moscow (1972), p. 224.
3. É. A. Stumbur et al., ibid., p. 275.
4. É. A. Stumbur, I. P. Matveenko, and A. G. Shokod'ko, ibid., p. 245.
5. C. Masters and K. Cady, Nucl. Sci. and Engng., 29, 272 (1967).
6. C. Preskitt et al., ibid., p. 283.
7. É. A. Stumbur, At. Énerg., 29, No. 3, 212 (1970).
8. G. Kasaly and A. Fischer, J. Nucl. Energy, 26, 17 (1972).
9. E. A. Stumbur et al., At. Énerg., 25, No. 1, 13 (1968).
10. G. I. Marchuk, Methods of Calculating Nuclear Reactors [in Russian], Gosatomizdat, Moscow (1961).

RELATIONSHIP BETWEEN THE HIGH-TEMPERATURE RADIATION EMBRITTLEMENT OF AUSTENITIC STAINLESS STEELS AND NICKEL ALLOYS AND FOCUSING PROCESSES

I. A. Razov, L. R. Ul'pe, and L. D. Shokhor

UDC 539.2:539.16.04:669

The high-temperature radiation embrittlement of austenitic stainless steels and nickel alloys greatly reduces their short- and long-term ductility, their time to failure in creep-strength tests, and their steady creep velocity [1-3].

Presently-existing hypotheses as to the reasons for this phenomenon are not entirely supported by experiment. Thus the "carbide" hypothesis [4, 5], according to which high-temperature embrittlement may be explained by the precipitation of carbides along the grain boundaries, is not confirmed by the experimental data of [6], according to which the high-temperature embrittlement still remains after heat treatment leading to the resorption of the carbides. Also unsatisfactory are the "vacancy" hypothesis [7] and the hypothesis of grain-boundary pinning preventing migration [8], since irradiation with electrons and γ-quanta (which create a large number of vacancies) does not produce high-temperature embrittlement [9]. The most satisfactory theory is the "helium" hypothesis [1, 2]. According to this, high-temperature embrittlement is due to helium bubbles formed at the grain boundaries by the reaction $^{10}B(n, \alpha)^{7}Li$ involving thermal neutrons. This point of view is experimentally supported by the following facts: a reduction in the dose of thermal neutrons brought about by the screening of the samples, or irradiation in reactors with a different spectrum of thermal neutrons, leads to a reduction in the high-temperature radiation embrittlement [9]; the reduction in the relative elongation of the irradiated material is related to the boron content of the sample (Fig. 1) [10]; an electron-microscope examination of irradiated samples [1, 2, 11] showed that many helium bubbles were indeed formed at the grain boundaries.

TABLE 1. Amount of Helium Formed in Stainless Steel 304 (Boron content 14 ppm) on Irradiation in the ATR and FFTF Reactors for 1000 Days

ATR			FFTF		
Φ(thermal) = 8·10²² neutrons/cm² $\Phi(E > 0.18\text{MeV}) \approx 6{,}1 \cdot 10^{22}$ neutrons/cm²			Φ(thermal) < 1,7·10¹⁹ neutrons/cm² $\Phi(E > 0{,}18\text{MeV}) = 6{,}6 \cdot 10^{21}$ neutrons/cm²		
chemical element	content		chemical element	content	
	ppm	%		ppm	%
Fe	18,1	34,5	Fe	77	51,4
B	14,0	26,7	N	42,4	28,3
N	7,9	15,1	B	13,1	8,8
Ni	6,9	13,2	Ni	9,6	6,4
Cr	5,5	10,5	Cr	7,6	5,1
Total	52,4	100	Total	149,7	100

Translated from Atomnaya Énergiya, Vol. 36, No. 3, pp. 182-185, March, 1974. Original article submitted February 7, 1973.

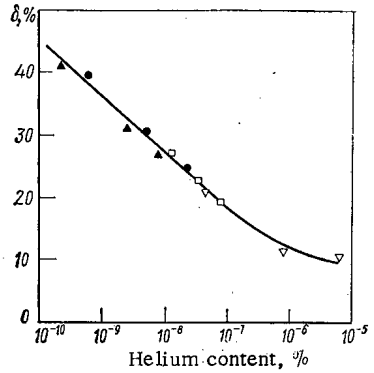

Fig. 1

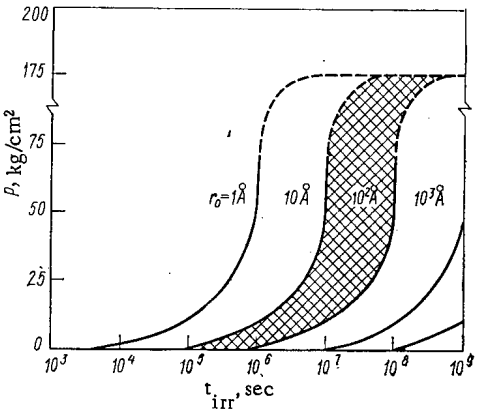

Fig. 2

Fig. 1. Dependence of the relative elongation δ on the amount of helium transformed by the reaction $^{10}B(n, \alpha)^{7}Li$ according to Martin and Weir [10]. T_{test} = 700°C; deformation (strain) rate $\dot{\varepsilon}$ = 0.2%/min; steel 304; original boron content: ▲) 15 parts/billion; ●) 110 parts/billion; □) 150 parts/billion; ▽) 3900 parts/billion.

Fig. 2. Dependence of the pressure P in bubbles of various initial radii on the irradiation time t (the shaded region corresponds to the most probable values of the radii of the bubbles).

However, a number of experimental facts cannot be satisfactorily explained by the helium hypothesis. Thus, during the neutron irradiation of stainless steel, helium is formed by a (n, γ) reaction not only in boron but also in many other elements (Table 1) [12]. The high-temperature embrittlement does not depend on the quantity of helium diffusing to the grain boundaries [12] from the matrix along dislocations. The existence of this diffusion process was proved experimentally by Woodford [2]. By using various forms of heat treatment, the distribution and dimensions of the gas bubbles at the grain boundaries were varied, but this did not lead to any change in the high-temperature embrittlement [2].

All this makes it rather doubtful whether the helium bubbles formed at the grain boundaries are responsible for the high-temperature radiation embrittlement of austenitic stainless steels and nickel alloys. On the other hand, the relationship between the embrittlement and the boron content is quite obvious.

The hypothesis now proposed is based on the possible formation of nonequilibrium helium bubbles at the grain boundaries; these develop during neutron irradiation mainly as a result of focusing processes. The grain boundaries of the material may weaken as a result of the considerable helium pressure inside the bubble. Nonequilibrium bubbles were found in [1] on irradiating copper foil with α-particles.

Let us separate out a layer of thickness l along a grain boundary of the metal, this thickness corresponding to the maximum range of a focuson. Then all the neutrons scattered in this zone with an energy $E < E_f$, $\beta < \beta_f$ (energy and maximum focusing angle) create focusons [13] and the extreme atoms of the corresponding chains at the grain boundary receive moment P directed at the same angle α to the boundary. However, neutrons with energy $E > E_f$ or a collision angle $\beta > \beta_f$ only cause the displacement of a few neighboring atoms. Thus we have, as it were, a filtering boundary layer which selects neutrons satisfying the focusing condition, and transmits the momenta almost losslessly, orienting them strictly with respect to the boundary. The existence of a component of momentum P_s tangential to the grain boundary leads to preferential jumps of the atoms in this direction. In general only the energy of the grain boundary is increased. However, if an ejected atom with momentum P_s collides with a helium atom formed by a $^{10}B(n, \alpha)^{7}Li$ reaction involving thermal neutrons, then it will transmit energy to the helium atom sufficient to overcome the potential barrier around the nonequilibrium bubble. Nonequilibrium bubbles may be formed from equilibrium bubbles. Nuclei for nonequilibrium bubbles may also be provided by fine pores and complex defects formed by the interaction of fast neutrons with atoms of the crystal lattice.

Let us suppose that the helium atoms are displaced along the grain boundary at a certain average velocity W, corresponding to their directional jumps as a result of the process just described. Then the number of absorbed helium atoms occurring in the time t to t + dt in a layer extending a distance x along

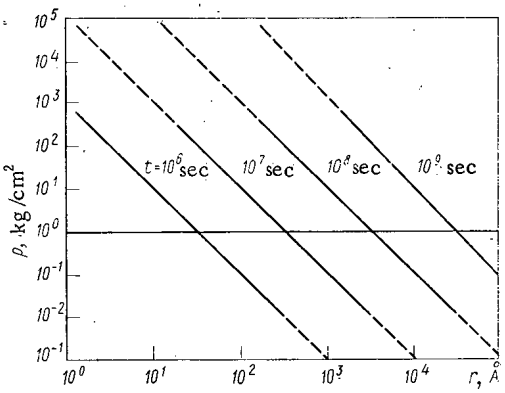

Fig. 3. Pressure in bubbles of various initial radii r at the instant $t = t_0$.

the boundary with thickness δ and width s (grain size) equals

$$d\Gamma(x, t) = \Gamma_0(x, t)[1 - e^{-2m\delta r(x, t)x}]\,dt, \tag{1}$$

where m is the number of capture centers in unit volume, $\Gamma_0(x, t)$ is the "flux" of helium atoms generated and moving along the grain boundary. The number of helium atoms absorbed in the layer from x to x + dx in a time t is equal to

$$\frac{\partial\Gamma(x, t)}{\partial x}\,dx = V_0\frac{s\delta m}{v}\,dx, \tag{2}$$

where v is the volume occupied by one helium atom, V_0 is the volume of bubble so formed with a normal pressure of P_0 within it. Using Eqs. (1) and (2) together with the relation between the volume V_0 and the observed volume $V_d = (4/3)\pi r^3(x, t)$, we obtain:

$$\gamma r^2\left[r\frac{\partial P}{\partial t} + 3P\frac{\partial r}{\partial t}\right] = \frac{\partial\Gamma_0}{\partial x}[1 - e^{-2\delta mrx}] + \Gamma_0 \cdot 2\delta m e^{-2\delta mrx}\left[x\frac{\partial r}{\partial x} + r\right], \tag{3}$$

where $\gamma = (4/3)\pi(1/P_0)(s\delta m/v)$.

In general, in order to determine P(x, t), we must know r(x, t) and $\Gamma_0(x, t)$. We obtain $\Gamma_0(x, t)$ from the following considerations: The number of captured neutrons in the layer δ, or the number of helium atoms being formed, equals

$$dn = I_0(1 - e^{-n_B\sigma\delta})\,dt, \tag{4}$$

where I_0 is the flux of incident thermal neutrons on the grain boundary, n_B is the number of boron atoms in unit volume, σ is the cross section for the capture of a neutron by a boron nucleus. Using (4) and the obvious relations for a layer of small thickness $n_B(t) = n_0 - n(t)/\delta$, where n_0 is the original number of boron atoms in unit volume, we obtain an expression for the number of helium atoms formed

$$n(t) = n_0\frac{\delta}{\eta}[1 - e^{I_0\sigma\tau}], \tag{5}$$

where η is the volumetric proportion of grain boundaries. In deriving (5) it was assumed that for boron $n_B\sigma\delta \ll 1$. If we now use (5) and assume $t < x/W$ we obtain an expression for $\Gamma_0(x, t)$:

$$\Gamma_0(x, t) = \frac{s\delta}{\eta}n_0W[1 - e^{-I_0\sigma t}]. \tag{6}$$

Capture centers are mainly provided by complex radiation defects, hence the number of centers of formation of "nonequilibrium" helium bubbles depends on the irradiation time: $m = \varphi(t)$. In general we must also allow for the dependence of the radius of a nonequilibrium bubble on the gas pressure within it, due to the deformation of the surrounding material $r = f(P)$. Together with the unknown relationship r(x), the facts impede the solution of Eq. (3).

In order to estimate the helium pressure in a nonequilibrium bubble we make use of the approximation $m = m_0$ and $r = r_0$. Here we take m_0 (the number of centers of formation of the nonequilibrium bubbles) as equal to the number of complex radiation defects arising in the parts of the grain close to the boundary when fast neutrons (E < 1 MeV) interact with the crystal lattice of the material, while we take r_0 as equal to the radius of a complex defect. For a fast-neutron flux of $1.2 \cdot 10^{14}$ neutrons/cm^2 · sec [14], at the boundary of a grain of area $10^{-2} \times 10^{-2}$ cm^2 some 10-30 nuclei of helium bubbles are formed, with a mean radius of the impoverished zone equal to ~10-10^2 Å.

Using the approximation indicated and taking Eq. (3) with due allowance for (6) and the initial condition $P|_{t=0} = 0$, we obtain:

$$P(r_0, t) \doteq P_0 \frac{\delta n_0 v W}{2\eta} I_0 \sigma \frac{t^2}{r_0^2}. \quad (7)$$

Using Eq. (7), we carried out an approximate calculation of the pressure in nonequilibrium bubbles of various radii in relation to the irradiation time (Figs. 2 and 3). We assumed: boron content 0.01 wt. %, dimensions of a plane grain $s \times s = 10^{-2} \times 10^{-2}$ cm^2, thickness of boundary layer $\delta = 10^{-7}$ cm, giving for $\eta \approx \delta/s \approx 10^{-5}$; $I_0 = (0.7\text{-}1.1)10^{14}$ neutrons/cm^2 · sec [14]; $\sigma = 2 \cdot 10^{-21}$ cm^2 [15].

A calculation of the number of focusons arriving at the grain boundary (and hence the mean velocity of the helium atoms W) was carried out on the basis of the method of [13]. The depth of the filtering layer, equal to the maximum range of a focuson, equals $\sim 10^2$ interatomic distances. In calculating the number of focusons, allowance was made for direct focusing (neutron energy $E \leq 25\text{-}30$ eV) and indirect focusing ($E = 30\text{-}100$ eV) in which a "bunch" (cluster) of parallel focusons develops (10^2-10^3 focusons). As a result of this it was found that about 10^6 focusons reached the boundary of a grain $10^{-2} \times 10^{-2}$ cm^2 in size for a neutron flux of 10^{14} neutrons/cm^2 · sec. Taking the focuson distribution as uniform over the plane of the grain, we may derive the mean velocity of the helium atoms along the boundary (10^{-11}-10^{-12} cm/sec).

The focuson-helium hypothesis as to the cause of the high-temperature radiation embrittlement of metals preserves all the advantages of the helium hypothesis and eliminates its failings. In view of the fact that the boron is distributed mainly along the grain boundaries, the appearance of nonequilibrium bubbles during the irradiation of the material is mainly associated with the helium formed by the (n, α) reaction in boron, and to a lesser extent with the helium diffusing to the grain boundaries from the matrix. This evidently explains the slight dependence of the high-temperature embrittlement on the boron concentration and the absence of any link with the total amount of helium formed in the material from other elements. Clearly different forms of heat treatment of the samples after irradiation, which lead to different redistributions of the total amount of helium (redistribution and formation of equilibrium bubbles) cannot influence the high-temperature embrittlement, since the formation of new nonequilibrium bubbles is impossible owing to the absence of focusing processes, and (as follows from experimental data relating to irradiation with α-particles [1]) nonequilibrium bubbles are hardly annealed at all at the test temperatures of 700-900°C.

The change in the pressure of the nonequilibrium helium bubbles 10-100 Å in radius (Fig. 2, shaded region) agrees closely with the change in the relative elongation, expressed as a function of irradiation dose [3]; a considerable rise in the pressure in the bubble and a fall in the relative elongation appear after $\sim 10^5$-10^6 sec. It is interesting to note that the pressure in the "nonequilibrium" bubbles rises quite rapidly, and over a practical irradiation time of 10^7-10^8 sec may reach considerable levels, which leads to the weakening of the grain boundaries. Electron-microscope examination of microsections of irradiated samples [1, 2, 11] revealed not only large pores corresponding to equilibrium bubbles at the grain boundaries but also tens of fine pores with radii of 10-100 Å. However, with existing methods of preparing samples for electron-microscope investigations it is extremely hard to say whether these pores are in fact traces of nonequilibrium bubbles.

In conclusion, it should be noted that under certain conditions high-temperature embrittlement may be affected by many other processes (formation of carbides, pinning of grain boundaries, etc.); however, the process which we have just been discussing certainly makes a major contribution, even if it is not the main one in certain cases.

We have thus proposed a focuson-helium hypothesis as to the reason for the high-temperature radiation embrittlement of austenitic stainless steels and nickel alloys, based on a combination of three processes taking place during neutron irradiation: the formation of impoverished zones, constituting nuclei for helium bubbles, by the fast neutrons; the formation of helium at the grain boundaries by virtue of the $^{10}B(n, \alpha)^7Li$ reaction involving thermal neutrons; the formation of nonequilibrium bubbles from helium atoms which have received kinetic energy as a result of focusing processes; also (possibly) channeling effects when intermediate neutrons interact with atoms in the crystal lattice of the material. We have obtained an equation relating the radius of a bubble and the pressure within it to the number of helium atoms generated, the neutron flux, and other parameters. The solution of the equation subject to the approximation $r = r_0$ agrees closely with the experimental relationship between the relative elongation and the period of irradiation.

LITERATURE CITED

1. S. Mishima and P. Ishino, J. Atomic Energy Soc. Japan, 11, No. 2, 184 (1969).
2. D. Woodford et al., J. Nucl. Mater., 29, No. 1, 103 (1969).
3. S. I. Votinov et al., Transactions of the Scientific-Technical Conference of the Socialist Economic Union: Atomic Energy, Fuel Cycles, Radiation Material Sciences, Vol. III [in Russian], Izd. SÉV, Moscow (1971), p. 612.
4. D. Arkell and P. Pfeil, J. Nucl. Mater., 12, No. 1, 145 (1964).
5. R. Roy and R. Solly, J. Iron and Steel Inst., 205, 58 (1967).
6. R. Higgins and A. Roberts, ibid., 60.
7. V. S. Karasev, Dokl. Akad. Nauk SSSR, 171, No. 1, 84 (1966).
8. M. Cangilaski, Reactor Mater., 12, No. 1, 33 (1969).
9. P. Pfeil and D. Harries, Amer. Soc. Test. Mater., Spec. Tech. Publ., No. 380, 202 (1969).
10. W. Martin and I. Weir, ibid., No. 426, 170 (1968).
11. V. Levy et al., Tenth Colloquium of Metallurgy, Brittleness Tests on Irradiated Materials, Saclay, 1966, Cif-Sur-Ivette, Paris (1967).
12. I. De Pino, Nucl. Appl., 3, 620 (1967).
13. G. Duesing and G. Leibfried, Phys. Stat. Sol., 9, No. 2, 463 (1965).
14. G. Ya. Vasil'ev, K. A. Konoplev, and Yu. P. Semenov, in: Problems of Ship-Building, Series 7, Ship-Building Materials, Metallography, No. 1 (16) [in Russian]. Sudostroenie, Leningrad (1972), p. 244.
15. I. V. Gordeev, D. A. Kardashev, and A. V. Malyshev, Nuclear-Physical Constants [in Russian], Gosatomizdat, Moscow (1963).

HYDRAULIC DRAG IN TUBES HAVING GRANULAR ROUGHNESS

M. D. Millionshchikov,* V. I. Subbotin, M. Kh. Ibragimov, G. S. Taranov, and I. P. Gomonov

UDC 532.542.4

The present paper continues a complex of studies on the hydrodynamic characteristics in tubes having various forms of regular roughness produced by identical projections which are uniformly distributed over the tube surface [1-3]. These studies showed that the forms of the roughness elements and the intervals between them had significant influence on hydraulic drag. In the region of Reynolds numbers up to Re $= 1 \cdot 10^6$, there was observed practically no interval in which the square law of drag would hold. The curves λ(Re) can vary monotonically with increasing Reynolds number and have maxima and minima whose regions of distribution vary according to the Reynolds-number range while the roughness-elements shape and interval vary. This behavior of the λ(Re) curves disagrees with assumptions concerning the character of roughness influence on the flux hydrodynamics at high Reynolds numbers; these conceptions arise from experiments with sand roughness [4].

With this characteristic of the drag coefficient behavior in tubes having geometrically strictly regular roughness, it is interesting to conduct a hydraulic study of tubes in which the form and distribution interval of the roughness outcroppings is preserved only approximately, i.e., with irregularly shaped elements whose distribution density is constant only on the average.

Such rough surfaces were produced in two ways: by bonding either abrasive powder or sand grains to the tube surface.

Abrasive-type roughness was obtained by bonding a paper-backed abrasive to the inner surface of a tube having diameter 61 mm. Grinding papers having granularity No. 50 and No. 32 were used. The abrasive-grain material was electrocorundum.

*Deceased.

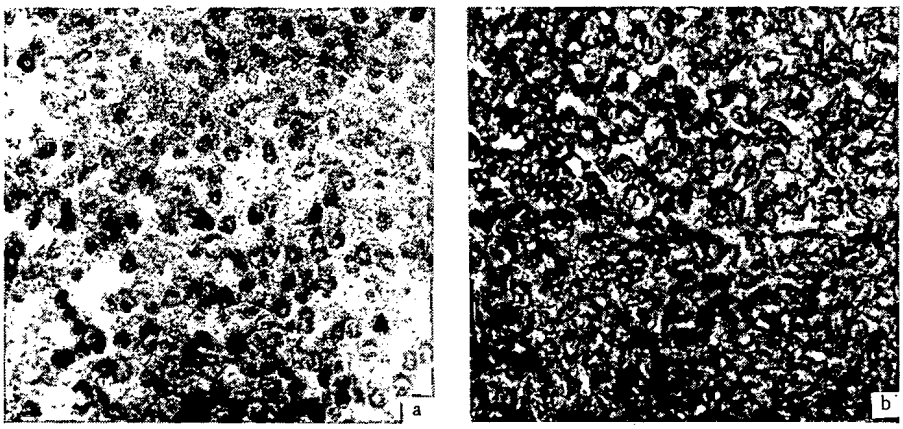

Fig. 1. Sand-grain appearance: a) sand-grain fraction 0.49 mm used for bonding; b) tube surface with bonded sand grains (R/k = 60).

Translated from Atomnaya Énergiya, Vol. 36, No. 3, pp. 186-188, March, 1974. Original article submitted September 15, 1973.

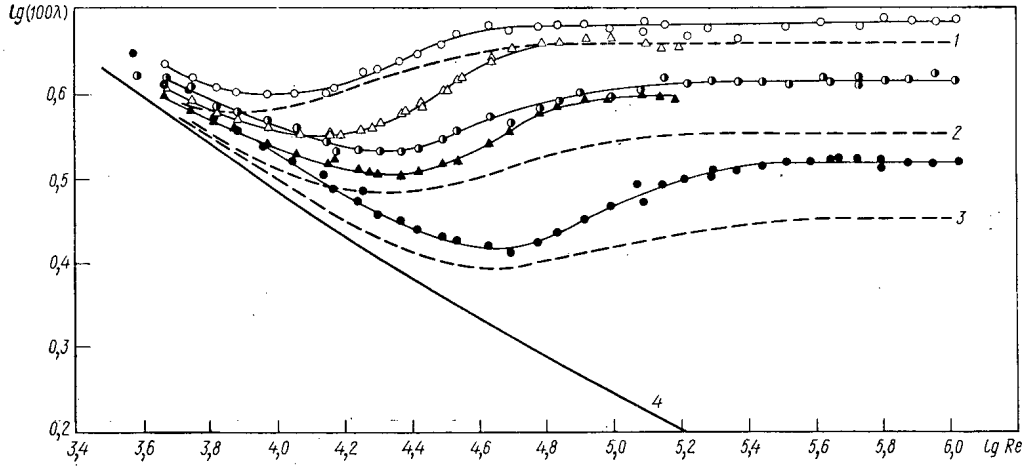

Fig. 2. Hydraulic-drag coefficients for rough tubes: Δ) abrasive cloth No. 50; ▲) abrasive cloth No. 32; ●, ◑, ○) tubes with sand grains at relative roughness 108, 60, and 39, respectively; 1, 2, 3) from data in [4] for R/k = 30.6, 60, and 126, respectively; 4) for smooth tube [8].

Definite composition by size (fractions) is allowed for abrasive powder. Thus, for powder having granularity No. 50, fractions from 0.32 to 0.8 mm are allowed. Moreover, the powder grains are not spherical and can have a ratio of their diameters of 1:3. Therefore, profilograms of the abrasive cloths were taken to determine the average grain size. The average grain height in abrasive cloth No. 50 in the profilogram can be taken as k = 0.66 mm with relative dispersion $\sigma_k/k = 0.295$. The dimensions for abrasive cloth No. 32 are: k = 0.34 mm and $\sigma_k/k = 0.285$. With the indicated dimensions, the average relative surface roughness is R/k = 45 (No. 50) and R/k = 88 (No. 32), where $R = \sqrt{V/\pi L}$ is the reduced radius determined from the rough-tube volume V and length L.

In preparing tubes with sand roughness, the sand-grain size was chosen such that we would obtain relative roughness close to those in Nikuradse's experiments [4]. For the bonding, previously washed river sand was taken and three fractions having average size 0.25, 0.49, and 0.8 mm were separated out by sifting.

Sand grains have an irregular, elongated shape. Therefore, the average grain size of the sand, separated using two sieves (a pass-through and an impassable one), can be significantly different from the sieve-opening sizes. For example, in sand sifted using sieves having openings 0.49 (pass-through) and 0.46 mm (impassable), there may be elongated grains with length up to 0.8 mm and dimension ratio 1:2; the proportion of elongated grains increases with increased time agitating the sand in the sieve. To separate out spherical grains having the least size variation, it was necessary after rough separation of the sand to pass it many times through pass-through sieves: to separate in the sifting process the passed sand into parts, to monitor the composition of the parts by grain size, and then to resift those parts where there was high percentage of grains with the desired dimensions. With such separation techniques, we were able to separate out sufficiently spherical grains for bonding (see Fig. 1). For example, the 0.49 mm sand fraction has dimensional ratio for the grains as a rule no greater than 1:0.7.

The sand was bonded to the inner surface of tube sections 59 mm in diameter and 635 mm long. Bituminous lacquer thinned with two parts turpentine was used for bonding. Thinned in this way, the lacquer left a film 0.002 mm thick on the tube and sand-grain surfaces.

Bonding was accomplished as follows: the tube was filled completely with lacquer, then emptied and held vertical until the lacquer stopped flowing; this was determined from the print of the lower tube end on paper. Then the tube was completely filled with sand and then emptied. The bonding quality, i.e., the absence of sand-free places and bulges, was determined by transillumination. A sufficiently uniform single-layer bonding of sand grains was confirmed. The tube was dried in an oven at 200°C for 50 min. After cooling, lacquer was poured into the tube, which was then emptied and again dried. The tube was cut at both ends to eliminate the irregularities in the sand layers at the ends.

The actual geometric dimensions for the roughness in tubes were determined from profilograms: for a tube with large sand grains, k = 0.755 mm, $\sigma_k/k = 0.172$, and R/k = 39; for a tube with medium sand

grains, k = 0.488 mm, $\sigma_k/k = 0.205$, and R/k = 60; for a tube with fine sand, k = 0.27 mm, $\sigma_k/k = 0.185$, and R/k = 108.

The experimental equipment allowed studies to be made in the Reynolds-number range $Re = 4 \cdot 10^3$–$1 \cdot 10^6$. The interval $Re = 4 \cdot 10^3$–$150 \cdot 10^3$ was obtained by moving air through the tubes, while higher Reynolds number were with moving water. The experiments with tubes that had paper-backed abrasive bonded to them were conducted only with air flow which, naturally, limited the Reynolds-number range. The measurement method is explained in [2].

The experimentally obtained drag coefficients are shown in Fig. 2. The surface roughness affects the drag coefficient in all Reynolds-number intervals, i.e., there is no smooth-flow mode. As in Nikuradse's experiments, at high Reynolds numbers, the drag coefficient ceases to depend on the Reynolds number, i.e., there begins a mode with a square law for drag.

The given roughnesses show significant dispersion in height and intervals. Therefore, the transition to the square-law drag mode occurs in a Reynolds-number interval significantly higher than the interval of transition to the extended-roughness mode for tubes having projections identical in height and interval. Thus, for tubes having roughness in the form of small truncated pyramids with R/k = 59 (see [3], variant 4-3 and 4-3-B), the transition to the extended-roughness mode ends at $Re \approx 40 \cdot 10^3$. The surface of these tubes were roughened by cutting multiple criss-cross threads and there is low dimensional dispersion. The transition to the extended-roughness mode for tubes with sand (R/k = 60), having dispersion $\sigma_k/k = 0.205$, appears before $Re \approx 200 \cdot 10^3$.

Quantitatively, the experiments show higher λ values than would follow from the equations in [4] for the R/k studied. The maximum dispersion, 25%, is observed for the tube with abrasive cloth No. 32. The remaining tubes have excesses of 12-17%. The quantitative deviations as a rule in the direction of excess are noted in experiments with sand roughness [5-7] and can be explained by variations in the grain sphericality, height dispersion, and also variations in grain-distribution density over the surface.

In contrast to experiments with tubes whose roughness is produced by projections identical in size and shape and equally distributed over the surface [3], in these experiments a square-law drag arises at high Reynolds numbers. This phenomenon may be explained by the geometrical nature of sand grains as roughness elements. Sand grains are poorly streamlined elements with various deviations from sphericality and, moreover, they possess local irregularity in distribution density over the tube surface. As a result, during the hydraulic manifestation of roughness, there occurs superposition of various (depending on the form of roughness and their interval) variation laws of λ and Re, which, apparently, also produces, on the average, self-similarity of the flow mode with respect to the drag coefficient.

Most papers indicate that the condition for the square-law mode to begin is the practically complete emergence of the roughness projections beyond the limits of the viscous sublayer, i.e., $k \gg \delta$, where δ is the viscous-sublayer thickness. Comparing our results and [3] shows that the single condition $k \gg \delta$ is insufficient for onset of the square-law mode. The square-law mode occurs when, besides the condition $k \gg \delta$, there is observed irregularity in the form of roughness elements and their distribution density over the tube surface.

LITERATURE CITED

1. M. D. Millionshchikov et al., Dokl. Akad. Nauk SSSR, Ser. Mekh., Fiz., No. 6, 207 (1972).
2. M. D. Millionshchikov et al., Preprint FÉI-385, Obninsk (1973).
3. M. D. Millionshchikov et al., At. Énerg., 34, No. 4, 235 (1973).
4. J. Nikuradse, Strömungsgesetze in Rauhen Rohren, VDI-Forschungsheft, No. 361 (1933).
5. A. P. Zegzhda, Similarity Theory and Calculation Methods for Hydrotechnical Models [in Russian], Gosstroiizdat, Moscow (1938).
6. F. A. Shevelev, Fundamental Hydraulic Regularities of Turbulent Motion in Tubes [in Russian], Gosstroiizdat, Moscow (1953).
7. Townes et al., Proc. American Society of Mechanical Engineers, 94, Series D, No. 2, 108 (1972).
8. M. D. Millionshchikov, At. Énerg., 28, No. 3, 207 (1970).

URANIUM IN ROCKS OF PHOSPHORITE-BEARING FORMATIONS

G. Ya. Ostrovskaya

UDC 546.791:549.01

The rocks of phosphorite-bearing formations often have high uranium concentrations, sometimes reaching commercial levels. However, in most phosphorite deposits the uranium content is too low to make it worthwhile extracting on its own and, it is therefore extracted as a byproduct in the chemical processing of phosphorite.* The uranium content of phosphorites is usually less than 0.0n%.

It is generally agreed that the uranium of phosphorite-bearing formations is syngenetic with the country rocks, although it has been subjected to redistribution in places. Karst and island phosphorites usually have only low uranium contents. The uranium content of phosphorites of alluvial beds (the upper sector of the Bown Valley formation, USA) reaches 0.01-0.02%, and phosphorites of intermontane lacustrine basins (Green River, USA, Pg_2) contain up to 0.015% uranium. However, only 0.6% of uranium-bearing phosphorites is assignable to continental formations. Marine phosphorites — the principal uranium carriers — are found in the deposits of all geological periods. They occur most extensively in Cambrian, Permian, Upper Jurassic, Paleogene, and Neogene deposits. The use of formation analysis to determine the relation between elevated uranium contents and specific types of phosphorites enables us not only to solve genetic problems, but also to assess the prospects of phosphorite-bearing deposits as a source of uranium raw material. As in the case of my communication on uranium-bearing coals [2], I have made an attempt to compare known uranium-bearing phosphorites of various countries with the existing classification of phosphorite raw material.

Of the numerous classifications of phosphorites, the most acceptable one for revealing the relation between uranium and phosphorites is deemed to be Shatskii's classification of marine phosphorites [3]; despite the fact that it does not take account of biogenic, redeposited, metamorphogenetic, and continental phosphorites, it can be used to distinguish groups and types of formations which are either promising or useless as regards uranium prospecting. This is due to the fact that, in contrast with many others, Shatskii's classification, developed on a formational basis, gives a picture of the tectonic conditions of accumulation of phosphate-bearing sediments; it is these conditions which determine many characteristics of deposits.

Shatskii [3] distinguishes 12 types of phosphorite-bearing formations, combined into three groups (Table 1, groups I-III). Deposits formed in the initial or later stages of development of geosynclines, and within young or ancient platforms, are distinguished. Elevated uranium concentrations are observed only in rocks of marginal siliceous formations. In the first group — volcanic-siliceous sediments — the geochemical paragenetic series of phosphorus may be represented as follows: P, Si, Fe, Mn, (Al)... Uranium is concentrated together with rare earths and sometimes with Sr, Zr, and Th only in deposits of the "marginal" siliceous formation of the outer troughs of geosynclinal regions (type 3). The texture of these phosphorites is solid and massive [4]. The uranium content is 0.00n-0.0n%, sometimes reaching 0.n%; the uranium reserves are considerable and in some cases may even be as high as several hundred thousand tons [5].

Despite the fact that uranium occurrences associated with this type usually have large reserves and a considerable number of ore horizons, not all the phosphorites of this formation have high uranium

*Extraction of uranium as a byproduct in the processing of phosphorites was first put into practice in September 1952 at a factory near Joliet (Illinois). Uranium is presently extracted as a byproduct from Tertiary phosphorites of Florida and Permian phosphorites of the Rocky Mountains [1].

Translated from Atomnaya Énergiya, Vol. 36, No. 3, pp. 189-194, March, 1974. Original article submitted April 19, 1973.

TABLE 1. Classification of Marine Phosphorite-Bearing Formations*

Groups of formations	Type of formations	Tectonic conditions	Type of phosphorite	Paragenesis with other ores	Scale of uranium presence	Examples of deposits, age of country rocks †
I Volcanic-siliceous group of initial and mature stages of geosynclinal development	1. Volcanic greenstone	Inner zones of geosynclinal regions ("eugeosynclines")	Phosphate dispersed over sectors in volcanites	Si Fi Mn, (Al)	–	Nassau (W. Germany), D_2-D_3 (< 0.004); Litencice and Hvaletice (Erzgebirge, Czechoslovakia); Mino (S. Japan), Pz
	2. Siliceous-schistose	Inner zones of geosynclinal regions ("eugeosynclines")	Bedded finely crystalline			Mansfield, Victoria, Cm_2; Cm_3, S. Australia, Brisbane series, Queensland, Pz_1 (Australia)
	3. Marginal siliceous	a) Inner troughs of geosynclinal regions ("mio-geosynclines" following Kaye's terminology)	Bedded oolitic granular		Ore occurrences and large deposits	Phosphoria, Rocky Mountains, USA, P_1 (0.028)
		(b) Others in inner consolidated rock masses of geosynclines			–	
II Terrigenous-carbonate (terrigenous-siliceous carbonate) group, mostly the young platform stage	4. Terrigenous ("Nubian")	Flanks of anteclises of ancient platforms	Bedded granular	Glauconitic rocks, oolitic limestones, iron- manganese and manganese-carbonate ores	Ore occurrences and large deposits	Abeokuta (Nigeria), Pg_2 (0.01); Trichinopoli (India), Cr_2^{cm} (0.01) Thies (Senegal) Pg_2-Ng
	5. Flinty-terrigenous	Flanks of ancient platforms	Granular		Ore occurrences and deposits	Safaga (Egypt) Cr_2^{cmp} (0.01)
	6. Terrigenous-calcareous ("Atlas")	Flanks of ancient platforms (a), flat troughs of Epipaleozoic platforms (b), and outer flank of foredeep (c)	Granular		Occasional ore occurrences and small deposits	Quseir (Egypt) Cr_2 (0.02); Ulad Abbu, Louis Gentile (Morocco) Cr_2^{mst} - Pg_{1-2} (0.02); Gafsa basin (Tunis) Cr_2-Pg (0.03); Tebessa basin (Algeria) Cr_2-Pg (0.01); Hawthorn series (Florida) Ng (0.03), Lind-Pernambuco (Brazil) Cr_2
	7. Calcareous ("Atlas")	Flanks of ancient platforms	Granular		Occasional ore occurrences	Nechvev (Israel) Cr_2^{cmp} (0.01); Er Ruseif (Jordan) Cr_2^{cmp} (0.01); Tennessee D (0.005)

* Classification of phosphorites of groups I-III given by Shatskii; that of group IV, and data on uranium content, supplied by the author.
† The figures in parentheses are the maximum percentages of uranium.

TABLE 1. (Continued)

Groups of formations	Type of formations	Tectonic conditions	Type of phosphorite	Paragenesis with other ores	Scale of uranium presence	Examples of deposits, age of country rocks†
	8. Cherty-calcareous	Outer and inner flanks of foredeeps	Bedded finely crystalline	—	—	—
III Glauconitic stages of ancient platforms or (as an exception) geosynclines	9. Terrigenous-glauconitic	Flanks of syneclises of ancient and Epipaleozoic platforms or (as an exception) geosynclines	Nodular	Manganese and oolitic iron ores	—	Bedford, Cambridge (England) Cr; Ardennes (Belgium) Cr
	10. Glauconitic-chalky		Nodular		—	Don Dorogan (Australia) Cr_2^{snt}
	11. Glauconitic-carbonate		Granular		Shows of mineralization	Mons and Cambrai (Belgium, France) Cr (0.004)
	12. Glauconitic-opoka		Nodular		Ore occurrences	
			Finely crystalline (bedded)		—	
IV Clayey, stages of platforms or (as an exception) geosynclines	13. Bituminous-arenaceous and arenaceous-argillaceous	Inner zones of foredeep of platform	Bones of fishes	Rare earths	Dispersed shows of mineralization and ore occurrences	
	14. Clayey and arenaceous-clayey	Flanks of anteclises in marginal zones of platforms	Bones of fishes and birds		Ore occurrences and deposits	
	15. Clayey and arenaceous	Central zones of platforms	Bones of fishes, birds, and mammals		—	—

contents. Uranium-bearing phosphorites differ from barren ones by their tectonic position. Uranium-bearing phosphorites of the Rocky Mountains type (Phosphoria, P_1, uranium content up to 0.03%) are correlated, according to M. Kaye and Shatskii [6], with the outer troughs of geosynclinal regions, corresponding to "miogeosynclines" of the initial and later stages of geosynclinal development (type 3a)*; barren phosphorites are located in inner geosynclinal systems (type 3b).

The phosphorite-bearing formations of virtually all types of the second group (terrigenous-carbonate) occupy enormous areas and are of great practical importance. Not less than 75% of the world's output of phosphorites comes from just four basins of this group (Algeria, Egypt, Morocco, and Tunis) and secondary deposits of this type. However, their uranium content is negligible, although the reserves of this element are assessed as several hundred thousand tons by some authors [7]. In some places glauconitic rocks, exhibiting transition in their facies to oolitic iron ore, iron—manganese, and manganese carbonate ores, siderites, and sometimes bauxites, form parageneses with deposits of phosphorites of the terrigenous-carbonate group.

The structural-tectonic conditions of formation of deposits of the second group are fairly diverse. According to Rusinov [4], deposits of types 6 and 8 are located in foredeeps, those of types 4, 5, and 7 are found in young platforms. Each formation is characterized by a specific texture of the phosphorite beds

*G. I. Bushinskii assumes that the Phosphoria phosphorites were deposited in the platform stage of development of this region.

(usually a thinly lammelar texture for the former, and a granular texture for the latter).

An elevated uranium concentration (0.01-0.02%) is characteristic of phosphorites of a terrigenous formation of the "Nubian" type (Abeokuta, Nigeria, Pg_2; Trichinopoli, India, Cr_2^{cm}; Thies, Senegal, Pg_2—Ng). In the siliceous-terrigenous formation the uranium content reaches 0.01% (Safaga, Egypt, Cr_2^{Cmp}), in the terrigenous-limestone Atlas type it reaches 0.01-0.03%(Quseir, Egypt, Cr_2; Ulad-Abbu and Louis Gentile, Morocco, Cr_2—Pg_{1-2}; the Gafsa basin, Tunis, Cr_2—Pg_2; the Tebessa basin, Algeria, Cr_2—Pg_2; Lind-Pernambuco, Brazil, Cr_2; the phosphorite-bearing Hawthorn series, Florida, Ng). Low contents (up to 0.005-0.01% uranium) are typical of the "Atlas" type limestone formation (Nechuev, Israel, Cr_2^{Cmp}; Er Ruseif, Jordan, Cr_2^{Cm}) and phosphoritized limestones (Tennessee, D).

Despite the nonuniformity and very low content of uranium in phosphate rocks of the terrigenous-carbonate group, they exhibit specific regularities. In this group uranium is absent from those types of formations correlated with the outer and inner flanks of foredeeps (types 6 and 8). This basic feature is even observed when the formation occurs in a known uranium-bearing province. When a formation of the terrigenous-limestone type is correlated with young platforms (type 6b), the phosphorites are always uranium-bearing. Note also the difference in texture: phosphorites of foredeeps have a thinly laminar texture, those of platforms have a granular texture.

Another regularity is distinctly observed in platform regions, namely that higher uranium concentrations are found in the flanks of anteclises, while intraplatform troughs are virtually devoid of this element. Note also that, in contrast with formation of ancient platforms (Egypt, Israel, Jordan, Ordovician and Devonian phosphate-bearing deposits in Arkansas and Tennessee), phosphorite-bearing formation of post-Hercynian (young) platforms (the Moroccan basin, and Neogene deposits in Florida and S. Carolina) have somewhat higher uranium contents. Here, as assumed by Smirnov [8], for the first group of formations a considerable part in the formation of rich commercial accumulations of uranium was probably played by secondary mobilization of dispersed uranium in the country rocks (the Hawthorn and Bown Valley formations in Florida, and phosphorites in Tennessee, Abeokuta in Nigeria, and Thies in Senegal).

Deposits of the third (glauconitic) group of formations, formed in the platform stage (and as an exception in the geosynclinal stage), exhibit a paragenetic relation with deposits of manganese and oolitic iron ores. Manganese ores are found predominantly in glauconite-opoka formations of the flanks of syneclises of ancient and Epipaleozoic (young) platforms. The phosphorites are usually concretionary, but are sometimes bedded. Of the four formations of this group, it is only in the glauconite-opoka formation (type 12) that noncommercial uranium occurrences (East European phosphorites, Pg_{1-2}) have been distinguished; in the glauconite—carbonate formation (type 11) the uranium content of the rocks is negligibly small (Belgium and the Paris basin, Cr).

In addition to these uranium-bearing formations, formed in marine basins, and the very small group of continental deposits, there exist numerous uranium-phosphate occurrences associated with the bones of large vertebrate animals, birds, and fishes. The bones of large vertebrate animals and birds are correlated with continental deposits. Their uranium content is about 0.00n%. In a few cases it reaches 0.n%, but these deposits are of no practical interest owing to their low reserves. Fish bones come within the group of marine deposits and are located predominantly on the flanks of anteclines of foredeeps. Uranium deposits which are poor in content but sometimes fairly large and also contain considerable reserves of complex ores (containing rare earths) are found in paragenesis with fish bones. For the purposes of uranium geology, it is therefore desirable to add to Shatskii's basic formation classification of marine phosphorites a fourth group, namely a clay group, formed in the platform stage (and exceptionally in the geosynclinal stage); it is subdivided into three formations: 1) bituminous—arenaceous and arenaceous—argillaceous, located in the inner zones of the foredeep of platforms (type 13); 2) arenacous—clayey, located on the flanks of anteclises and the margins of platforms (type 14); 3) clayey and arenaceous, located in the centers of platforms (type 15).

Known uranium deposits are correlated predominantly with clayey and arenaceous—clayey formations of the margins of platforms (type 14) and are associated with fish bones. The fish bones of the bituminous—arenaceous and arenaceous—argillaceous formation (type 13) have a negligibly small uranium content (0.00n%), and those of the clayey and arenaceous phosphorite-bearing formations (type 15) have no uranium.

The data show that higher uranium contents are found in phosphate deposits of various different ages and in all continents. However, a distinct relation with uranium is observed only in specific

phosphorite-bearing formations. In this connection the tectonic position of the sediments adjoining the ore is of fundamental importance. The largest uranium reserves have been found in the outer troughs of geosynclinal regions (corresponding, according to Kaye's classification, to "miogeosynclines") in phosphorites of the marginal siliceous formation (group I, type 3). Furthermore, relatively large deposits of uranium-bearing phosphates, associated with accumulations of fish bones, are also typical of the flanks of anteclises of the marginal zones of platforms (group IV, type 14).

Extensive development of ore occurrences and deposits of phosphorites with a low uranium content, but sometimes with large reserves, is typical of the flanks of anteclises and synclises of platforms. Uranium is linked by adsorption to phosphates of the bedded and nodular types (group II, types 4, 5, 6a, 6b, and 7; group III, types 11 and 12). Among platform formations, phosphorites correlated with Epihercynian (young) platforms and perhaps with activated platforms have somewhat higher uranium contents than the phosphorites of ancient stable platforms.

In phosphorite-bearing rocks of the centers of ancient stable platforms the uranium content is very low (group III). Uranium is absent from the rocks of the outer and inner flanks of foredeeps, even within known uranium-bearing provinces, just as in the presence of potentially uranium-bearing rocks of the marginal siliceous formation (group II, types 6 and 6c). An exception is the inner zones of the foredeep of platforms, where in sectors of facies change one sometimes observes slight contamination by uranium due to fish bones (group IV, type 13). Uranium is absent in phosphorite-bearing formations of the inner zones of geosynclinal regions.

There are grounds for assuming that these characteristics are due not only to the presence or absence of uranium sources, but also to the precipitation conditions of calcium phosphate and uranium. According to Krasil'nikova [9], in all probability the phosphorites in the geosynclinal basins of early epochs are predominantly chemogenic formations. The accumulation of calcium phosphate and uranium in the sediments was apparently due to various different factors: a change in the pH of the sea water, an increase in the phosphorus and uranium contents as a result of entry of these elements in water welling up from depth or of their arrival from a site of volcanic activity together with silicon, iron, and manganese, giving rise to large accumulations in volcanic-siliceous formation [10].

During the Mesozoic and Cenozoic periods phosphorite formation occurred mainly in platforms, a marked effect being exerted by the climate. Large deposits of high-grade phosphorites were formed in arid regions, poorer nodular phosphorites in humid zones. The former are frequently uranium-bearing, the latter usually contain no uranium. According to Strakhov [11], organisms in shallow waters promote saturation of sea-bed water with P_2O_5 and precipitation of phosphate where there is a change in the partial pressure of CO_2. Some authors [12] assume that phosphorus was introduced into the marine basins of platform regions as a mechanical suspension, as colloidal particles, and in the dissolved state. Its entry was probably accompanied by that of uranium from the surrounding rocks subjected to erosion by water.

Thus the source of uranium and phosphorus in uranium-phosphate rocks was disintegrated rocks. However, in certain cases these elements were of endogenous origin.

In conclusion, it must be emphasized that in uranium prospecting our attention should be primarily concentrated on phosphate deposits of two types, characterized by different formation conditions and different sources of phosphorus and uranium. The first type is most promising; it is associated with "miogeosynclines" of predominantly early epochs of extensive development of carbonate-siliceous phosphorite-bearing formations. The principal sources of phosphorus, like that of many other elements (including uranium), is volcanic, and its precipitation from sea water followed a chemical pattern.

The second one is the platform type; it was formed in later epochs, predominantly in the Mesozoic —Cenozoic. It is characterized by the occurrence of bedded-granular phosphorites in arid zones. The activity of organisms played an important part in the formation of uranium-phosphorite ores of this type [13, 14]. However, the primary sources of phosphorus, like that of uranium, was probably disintegrated land rocks.

LITERATURE CITED

1. V. N. Kholodov, Rare Elements in Sedimentary and Metamorphic Rocks [in Russian], Izd-vo AN SSSR, Moscow (1963), p. 67.
2. G. Ya. Ostrovskaya, At. Énerg., 28, No. 6, 467 (1970).

3. N. S. Shatskii, Proceedings of the Conference on Sedimentary Rocks [in Russian], Izd-vo AN SSSR, Moscow (1955), Vol. 2, pp. 7-101.
4. L. A. Rusinov, Dokl. Akad. Nauk SSSR, 124, No. 6, 1289 (1959).
5. R. Sheldon, Physical Stratigraphy and Mineral Resources of Permian Rocks in Western Wyoming, US Geol. Process. P-313B.
6. G. I. Bushinskii, The Phosphoria Formation [in Russian], Nauka, Moscow (1969), p. 42, 67-68.
7. Atomic Energy in African Countries [in Russian], TsNII Atominform., Moscow. Rev. Series AINF 113 (OB), pp. 3, 6, 23, 33.
8. V. I. Smirnov, Problems of Applied Radiohydrogeology [in Russian], Gosatomizdat, Moscow (1963), p. 29.
9. N. A. Krasil'nikova, Litolog. i Polezn. Iskop., No. 5, 156 (1967).
10. G. S. Dzotsenidze, The Role of Vulcanism in the Formation of Sedimentary Rocks and Ores [in Russian], Nedra, Moscow (1969), p. 244.
11. N. M. Strakhov, Fundamentals of the Theory of Lithogenesis [in Russian], Izd-vo AN SSSR, Moscow (1960), Vol. 2, p. 225.
12. B. I. Gimmel'farb, Laws of Location of Phosphorite Deposits in the USSR, and Their Genetic Classification [in Russian], Nedra, Moscow (1965), p. 23.
13. G. I. Bushinskii, Izv. Akad. Nauk SSSR, No. 1, 3 (1954).
14. G. I. Bushinskii, Ancient Phosphorites of Asia and Their Origin [in Russian], Nauka, Moscow (1966), p. 175.

GAS—LIQUID COLUMNS FOR REMOVAL OF RADIOACTIVE GASEOUS IMPURITIES

I. E. Nakhutin and Yu. G. Rubezhnyi

UDC 621.039.7.13:621.039.324.2

Successful use is now being made of so-called "permanent" chromatographic columns designed for removing short-lived radioactive inert gases. In these columns, radioactive decay of the gas occurs simultaneously with the chromatographic process [1]. In this article we shall discuss the possibility of using a similar principle to remove radioactive gases in counterflow gas—liquid columns.

Various types of these columns are made. For radioactive inert gases one can use an absorbing liquid such as CCl_4, etc. [2]. It would probably be more effective to use adsorption chromatographic columns for this purpose (except in the case of argon, for which the adsorption coefficients are vanishingly small).

High purification factors are attained by trapping ^{41}Ar in low-temperature columns irrigated with liquid air, with decay of the radioactive argon.

Below we give the general equations of gas—liquid separating columns with radioactive decay of the substance. As an example we shall consider the trapping of ^{41}Ar.

Let us consider an elementary volume of a counterflow mass-exchange column of height dz. Mass transfer of the radioactive substance occurs from the light phase to the heavy one.

We shall introduce the following notation: x, y are the concentrations of radioactive substance in the currents of liquid and gas respectively, in kg/m^3; y* is the concentration of radioactive substance in the light phase, in equilibrium with its concentration in the heavy phase, in kg/m^3; L, G are the flow rates of the heavy and light phases respectively, in m^3/h; q = L/G is the ratio of the phase flow rates; k_{0y} is the mass transfer coefficient in the light phase, in m/h; F_x, F_y are the cross sections occupied by each of the currents, in m^2; S is the specific phase contact surface area in m^2/m; α is the distribution coefficient; H is the height of the column in meters; and λ is the decay constant in sec^{-1}.

Suppose that at height z in the column the concentration of radioactive substance in the heavy phase is x, and that in the light phase y; correspondingly, at height (z + dz) the concentrations in the columns will be (x + dx) and (y + dy). The scheme of the calculations for the balance is shown in Fig. 1.

The equation of mass balance for a radioactive substance in the liquid phase is

$$L(x+dx)+k_{0y}\bar{S}(y-y^*)\,dz = Lx+\lambda F_x x\,dz, \tag{1a}$$

or

$$qh_{0y}\frac{dx}{dz} = -y+\theta_2 x, \tag{1b}$$

where $h_{0y} = G/k_{0y}S$ is the unit transfer height, and

$$\theta_2 = \alpha+\frac{\lambda F_x h_{0y}}{G}.$$

The equation of mass balance for a radioactive substance in the gas phase is

$$Gy = G(y+dy)+k_{0y}\bar{S}(y-y^*)+\lambda F_y \bar{y},$$

Translated from Atomnaya Énergiya, Vol. 36, No. 3, pp. 195-197, March, 1974. Original article submitted March 12, 1973.

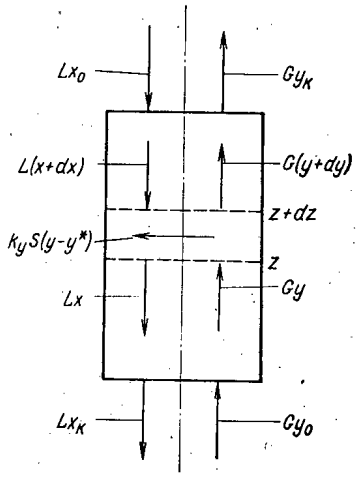

Fig. 1. Diagram for derivation of formulas.

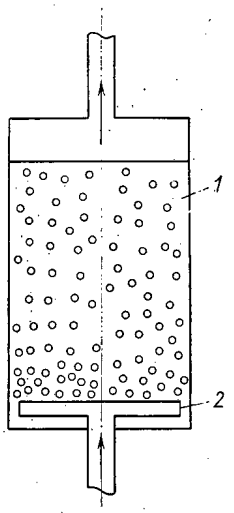

Fig. 2. Scheme of bubbler. 1) Liquid layer; 2) air distributor.

or

$$h_{0y}\frac{dy}{dz} = -y + \alpha x \tag{2}$$

(in this last equation we are neglecting the radioactive decay in the gas phase).

Let us suppose that at low concentrations of the radioactive substance, α is independent of the concentration, and hence

$$y^* = \frac{1}{\alpha}x. \tag{3}$$

By Eq. (2),

$$x = \frac{1}{\alpha}\left(y + h_{0y}\frac{dy}{dz}\right). \tag{4}$$

Putting (4) into (1) we get

$$qh_{0y}^2\frac{d^2y}{dz^2} - h_{0y}(q-\theta_2)\frac{dy}{dz} + (\alpha-\theta_2)y = 0. \tag{5}$$

The general solution of Eq. (5) (when the coefficient of dy/dz is nonzero) is

$$y = C_1 e^{\xi_1 z} + C_2 e^{\xi_2 z}. \tag{6}$$

The quantities ξ_1 and ξ_2 in the exponents are the roots of the characteristic equation

$$\xi_{1,2} = \frac{(q-\theta_2)}{2qh_{0y}} \pm \sqrt{\frac{(q-\theta_2)^2}{4q^2h_{0y}^2} - \frac{(\alpha-\theta_2)}{qh_{0y}^2}}. \tag{6a}$$

Putting (6) into (4) we get

$$x = C_1\gamma_1 e^{\xi_1 z} + C_2\gamma_2 e^{\xi_2 z}, \tag{7}$$

where

$$\gamma_i = \frac{1}{\alpha}(1 + h_{0y}\xi_i) \quad (i = 1, 2). \tag{8}$$

The coefficients C_1 and C_2 are found from a system of linear equations based on two conditions. The first is that the concentration of radioactive substance in the gas phase at the inlet to the apparatus is a constant,

$$y = y_0|_{z=0}, \quad \text{or} \quad C_1 + C_2 = y_0. \tag{9}$$

The second condition follows from the mass balance in the column:

$$Gy_0 = Gy_k + Lx_k + \frac{q(e^{\xi_1 H} - 1)(F_x\gamma_1 + F_y)C_1}{\xi_1} + C_2\frac{q(e^{\xi_2 H} - 1)(F_x\gamma_2 + F_y)}{\xi_2}, \quad (10)$$

or

$$C_1P_5 + C_2P_6 = Gy_0, \quad (11)$$

where

$$P_5 = Ge^{\xi_1 H} + L\gamma_1 + P_1; \quad P_1 = \frac{(e^{\xi_1 H} - 1)(F_x\gamma_1 + F_y)}{\xi_1};$$
$$P_6 = Ge^{\xi_2 H} + L\gamma_2 + P_2; \quad P_2 = \frac{(e^{\xi_2 H} - 1)(F_x\gamma_2 + F_y)}{\xi_2}.$$

From Eqs. (9) and (11) we find the constants C_1 and C_2 occurring in Eqs. (6) and (7):

$$C_1 = \frac{y_0(P_6 - G)}{(P_6 - P_5)}; \quad (12)$$

$$C_2 = \frac{y_0(G - P_5)}{(P_6 - P_5)}. \quad (13)$$

Let us consider the application of these relations, taking as an example the trapping of ^{41}Ar in a packed column. We shall roughly estimate the unit transfer height of the column by means of the approximate formulas in [3]:

$$h_{0y} = \frac{M_V G}{\gamma_V S k_{yv}}, \quad (14)$$

where S is the cross section of the column in m^2, M_V is the molecular weight of the vapor (gas), γ_V is the density of the vapor (gas) in kg/m^3, and k_{yV} is the volumetric coefficient of mass transfer in h^{-1}.

Then we can write

$$k_{yv} = \mathrm{Nu}\frac{D_V}{d_e^2}, \quad (15)$$

where

$$\left.\begin{aligned} &\mathrm{Nu} = 0.035\mathrm{Re}^{0.8}\mathrm{Pr}^{0.35}; \quad \mathrm{Ar} = \frac{d_e^3\gamma_V(\gamma_l - \gamma_V)}{\mu_V^2 g}; \\ &\mathrm{Re} = 0.015\mathrm{Ar}^{0.57}q_0^{-0.43}; \quad \mathrm{Pr} = \frac{3600\mu_V g}{\gamma_V D_V}. \end{aligned}\right\} \quad (16)$$

Here $q_0 = L_0/G_0$, where L_0 and G_0 are the flow rates of the heavy and light phases respectively in $kg/m^2 \cdot h$, γ_l is the density of the liquid phase in kg/m^3, μ_V is the viscosity of the vapor (gas) in $kg \cdot sec/m^2$, D_V is the diffusion coefficient of the vapor in m^2/h, V_{fr} is the free volume of the packing in m^3/m^3, and σ is the specific surface area of the packing.

Equations (14)-(16) are valid in the following range of phase current ratios:

$$0.1 < q_0 < 100.$$

Let us take the following values for the parameters (with t = −183°C) [5, 6]:

$$\gamma_V = 4.80 \text{ kg/m}^3; \quad \lambda = 1.07 \cdot 10^{-4} \text{ sec}^{-1};$$
$$\gamma_l = 861 \text{ kg/m}^3; \quad \mu_V = 7.35 \cdot 10^{-6} \text{ kg} \cdot \text{sec/m}^2;$$

$d_e = 0.025$ m; $\alpha = 10^3$; $M_V = 40$; $D_V = 0.01$ m^2/h; $F_X = 0.72$ m^2; $F_y = 5.3$ m^2. From Eqs. (15) and (16) we get: $Ar = 7.6 \cdot 10^6$; $Pr = 6.9$; $Re = 165q_0^{-0.34}$; $Nu = 3.6q_0^{-0.34}$, $K_{yV} = 284q_0^{-0.34}$.

Putting (15) into (14) we get

$$h_{0y} = 0.35 \text{ m}. \quad (17)$$

From Eqs. (17) and (6a) we find the roots of the characteristic equation:

$$\xi_1 = 3.18; \quad \xi_2 = -0.86, \quad (18)$$

and the values of γ_1 and γ_2:

$$\gamma_1 = 120; \quad \gamma_2 = 1300. \quad (19)$$

From Eqs. (11)-(13), (18), and (19), it follows that a column with a height H of about 2 m will reduce the concentration of radioactive argon in the gas current by a factor of 1000 (without radioactive decay the purification coefficient would be 15).

Gas—liquid columns can also be used to free gases from radioactive impurities in the absence of phase counterflow. Figure 2 shows a bubbler in which the gas to be purified bubbles through a closed volume of liquid (the latter is not removed from the bubbler).

Let us consider steady conditions in which the liquid is already saturated with the radioactive impurities. The mass balance in a radioactive impurity for the liquid in the bubbler is

$$Gy_0 = Gy + \lambda Vx = Gy + \alpha\eta\lambda Vy, \tag{20}$$

where $\eta \leq 1$ is a coefficient representing the degree of attainment of equilibrium between the liquid and gas.

From Eq. (20) it follows that the coefficient of purification is

$$K = 1 + \frac{\alpha\eta V\lambda}{G}.$$

Purification is of practical interest when $\alpha V\lambda/G \geq 0.5$ and η takes reasonable values; in properly constructed mass exchange apparatus, $0.5 \leq \eta \leq 1$.

Thus in a bubbler without release of liquid we can effect continuous purification from radioactive gas provided that we correctly choose the volume of the liquid ($V \geq 0.5G/\alpha\lambda$).

Let us consider a plate column with a flow of gas up the column and fixed liquid on the plates (i.e., no liquid counterflow). In such a column we cannot effect continuous removal of ordinary impurities. However, in the case of radioactive impurities, provided that we correctly choose the volume of liquid on the plate, the column can effect high coefficients of purification in continuous operation.

The equation of mass balance of impurity on a plate has the form

$$Gy_0 = Gy + \alpha Vx = Gy + \alpha\eta\lambda Vy.$$

The coefficient of purification for one plate is

$$K_p = \frac{\alpha\eta\lambda V}{G} + 1, \tag{21}$$

and the coefficient of purification for the whole column is

$$K_c = K_p^N = \left(1 + \frac{\alpha\eta\lambda V}{G}\right)^N, \tag{22}$$

where N is the number of plates in the column. If $V \geq 0.1/G\alpha\lambda$, the column can attain high coefficients of purification from radioactive impurities. For example, if air containing radioactive ^{41}Ar is passed through a plate column with liquid air on the plates, for a gas flow rate of G = 500 m^3/h with a column radius of R = 1.3 m, if N = 10 and the volume of liquid on a plate is V = 1.2 m^3, then K = 1000 (we do not calculate the plate efficiency).

Removal of radioactive gases is a complicated problem which cannot be solved by simple methods. It is especially difficult to remove radioactive inert gases.

Mass exchange with liquid air can be used to remove such gases. In the case of short-lived radioactive isotopes, this process is influenced by radioactive decay. In this article we have shown that it is in just these conditions that the columns are most effective (for example, for removal of ^{41}Ar from air).

LITERATURE CITED

1. I. E. Nakhutin and D. V. Ochkin, Inzh. Fiz. Zhurn., 9, No. 1, 112 (1965).
2. R. Mclloy et al., Second Geneva Conference, Report No. 15/P/309 [Russian translation] (1958).
3. L. A. Akopyan, A. N. Planovskii, and A. G. Kasatkin, Khim. Nauka i Prom-st', 3, No. 6, 745.
4. S. Ya. Gersh, Deep Cooling [in Russian], Pt. 1, Gosénergoizdat, Moscow—Leningrad (1957), p. 367.
5. I. I. Gel'perin, G. M. Zelinson, and L. L. Rapoport, Handbook of Separation of Gas Mixtures [in Russian], Goskhimizdat, Moscow (1953), p. 156.
6. K. F. Pavlov, P. G. Romankov, and A. A. Noskov, Examples and Problems for Course in Processes and Apparatus of Chemical Technology [in Russian], Khimiya, Leningrad (1970), p. 380.

ELECTROOSMOTIC CONCENTRATION OF ANIONS FROM EXTREMELY DILUTE AQUEOUS SOLUTIONS

L. N. Moskvin, N. N. Kalinin, and L. A. Godon

UDC 66.087.9

Present requirements imposed on the quality of water in the nuclear power industry and in several other branches of science and industry are approaching the sensitivity limits of existing methods of analysis, and on occasion even go beyond those limits [1]. In addition to improvements in methods of analysis, more accurate determinations of the concentrations of trace impurities in water could be aided by concentrating the impurities beforehand. But well known techniques for evaporating samples or for ion-exchange concentration of materials to be analyzed are not always convenient to rely upon, because of the uncontrollable losses, substantial lengthening of the time required to complete the analysis, etc.

Electroosmosis has been attracting attention among the suitable candidates as methods for removing water from solutions. Electroosmotic transport of water through simulated porous membranes in response to the charge built up on the surface of the membranes is brought about by the movement of the cation or anion forms of the elements comprising the diffuse part of the double electrical layer [2]. Concentration of ions having the same sign as the charge on the membrane can be expected in the initial solution as a result.

The present article deals with a study of the feasibility of concentrating anions from extremely dilute aqueous solutions with the aid of electroosmotic transport of water through negatively charged porous polytetrafluoroethylene membranes.

TABLE 1. Variation in Permeability of Teflon Membranes to Chloride Ions and Sulfate Ions as a Function of Ion Concentration and Mean Pore Radius in Membrane

Anion concentration in initial solution, mg/liter	Membrane characteristics			Anion concentration in electroosmotically transported water, mg/liter	Breakthrough of anion investigated, %
	mean pore radius, μ	thickness, cm	total porosity, %		
35,5 (Cl^-)	0,7	0,4	47	0,08	0,2
	0,5	0,4	42	$<$0,05	$<$0,1
	0,2	0,1	22	$<$0,05	$<$0,1
	0,04	0,1	13	$<$0,05	$<$0,1
177,5 (Cl^-)	0,7	0,4	47	9,22	5,2
	0,2	0,1	22	1,30	0,7
	0,04	0,1	13	0,10	0,06
355,0 (Cl^-)	0,7	0,4	47	19,00	5,3
	0,2	0,1	22	8,21	2,3
	0,04	0,1	13	0,90	0,2
48,0 (SO_4^{2-})	0,7	0,4	47	$<$0,3	$<$0,6
	0,5	0,4	42	$<$0,3	$<$0,6
	0,2	0,1	22	$<$0,3	$<$0,6

Translated from Atomnaya Énergiya, Vol. 36, No. 3, pp. 198-200, March, 1974. Original article submitted March 13, 1973.

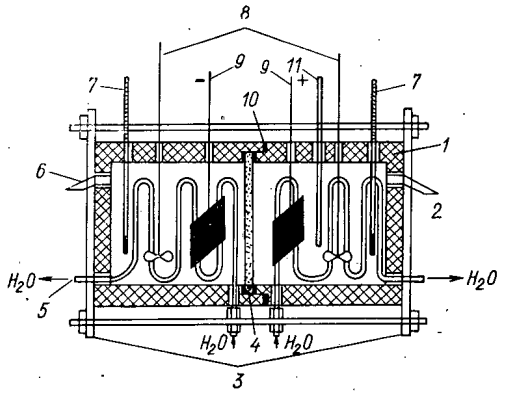

Fig. 1

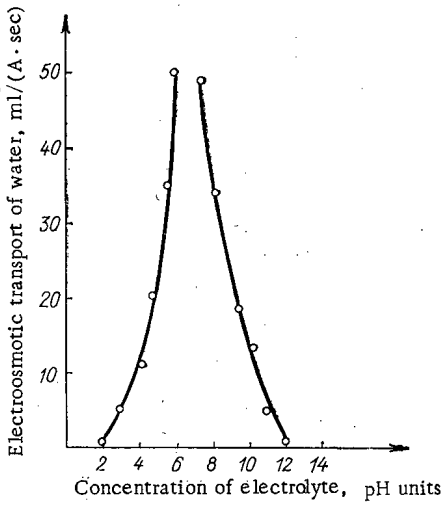

Fig. 2

Fig. 1. Diagram of electroosmotic concentration cell: 1) fluorocarbon cell housing; 2) anodic solution drainage tube; 3) tie rods; 4) polytetrafluoroethylene (Teflon) membrane; 5) coolers; 6) cathodic solution drainage tube; 7) thermometers; 8) glass agitators; 9) platinum electrodes; 10) rubber gasket; 11) tube feeding solution into anodic compartment.

Fig. 2. Dependence of electroosmotic transport of water V/J through Teflon membrane on concentration of electrolytes HCl and KOH.

The experiments were conducted in a fluorocarbon cell such as shown in the diagram in Fig. 1. The area presented by each electrode was 4 cm^2. The spacing between electrodes was 5.3 cm. The potential difference impressed across the electrode varied from 100 to 600 V. The working area of the membranes was 23.2 cm^2. The membranes were prepared from Teflon powder by a procedure described elsewhere [3], and were impregnated with desalinated water under vacuum suction until air bubbles ceased to appear on the surface. Tubes for draining the solutions in the anode and cathode compartments were set at the same level in order to keep the levels of solution identical on both sides of the membrane throughout the process. The temperature in the anode and cathode compartments was kep at 22 ± 2°C.

The concentration of the chloride ion was determined by the nephelometric method (sensitivity 0.05 mg/liter), and the concentration of the nitrate ion was determined on FÉK-60, using the sodium salt of salicyclic acid (sensitivity 0.02 mg/liter), while the concentration of the sulfate ion was determined by gravimetric means, utilizing barium chloride. The bromide ions were concentrated from water containing slight quantities of the salt KBr tagged with ^{82}Br. The dependence of the permeability of these ions on the concentration of salt in the initial solution and on the mean radius r of the pores in the membranes used was determined on KCl and Na_2SO_4 solutions.

The experiments were conducted in the following sequence. Desalinated water was poured into the cathode compartment of the cell. The anode compartment was then filled with solution taken for the investigation, after which dc potential was impressed across the electrodes. A stream of solution was passed with intense agitation through the anode space in order to keep the concentration of anodic solution constant, and the stream flow velocity was more than 20 times greater than the rate of electroosmotic transport of water. Samples of the water trickling out of the cathode compartment were taken with the velocity of the electroosmotic stream at steady state after the first two or three volumes of water, equal to the volume of the cathode compartment, had been discarded, during the first two hours.

The permeability of the membranes to chloride ions and sulfate ions was estimated from the breakthrough of the ion to be concentrated in the electroosmotically transported water, in terms of percentage of the content of that ion in the initial solution (see Table 1). For a given membrane, the increase in applied voltage in the operating range from 100 to 600 V at constant concentration of solution did not bring about any appreciable change in the amount of impurities present in the electroosmotically transported water. That is in close agreement with the conclusion advanced by O. L. Alekseev and F. D. Ovcharenko [4] to the effect that true electroosmotic transport actually depends solely on the concentration of excess

TABLE 2. Electroosmotic Concentration of Anions from Aqueous Solutions of Salts

Initial salt solution	Concentration of original solution with respect to anion, mg/liter	Specified degree of concentration	Concentration of final solution with respect to anion, mg/liter	Yield of concentrated anion, %
KNO_3	0,02 0,02 0,02	10 10 10	0,20 0,22 0,20	100±10 110±10 100±10
KNO_3	0,01 0,01 0,01	10 10 10	0,09 0,10 0,09	90±20 100±20 90±20
KNO_3	0,004 0,004 0,004	50 50 50	0,20 0,21 0,21	100±10 105±10 105±10
KCl	7,1	50	353±5	99,4±1,5
KBr (^{82}Br)	(2,30±0,04)·10^{-6} *	50	(1,16±0,02)·10^{-4} *	101±3

* Concentration of initial and final KBr solutions with respect to anion expressed in Ci/liter.

ions in the double electrical layer. Consequently, the results obtained are not referred to the applied potential difference.

It is clear from Table 1 that even at r = 0.5 μ the Cl^- and SO_4^{-2} ions practically do not penetrate into the cathodic space during the process of electroosmotic transport of water from 0.001 N solutions of KCl and Na_2SO_4. Increasing the concentration of the initial solution has the effect of raising the Cl^- concentration in the electroosmotically transported water for all the r values cited.

According to the theory of the double electrical layer, a rise in electrolyte concentration brings about compression of the diffuse part of the double layer and a concomitant increase in the fraction of volume taken up by the electrically neutral solution in the capillary [5]. The electrical neutral solution is entrained by the stream of electroosmotically transported water and is responsible for contamination of the water by dissolved electrolyte. We can similarly account for the increase in breakthrough of ions with increasing r at the same concentration of initial solution. The boundary condition for impermeability of a negatively charged membrane to anions can be taken as the condition that the radius of the capillary and the thickness of the double electrical layer be equal. In that case the water in the capillary will in practice contain ions of the same sign, which will be opposed to the sign of the charge on the membrane.

We are therefore in a position to select a membrane which will facilitate a quantitative concentration of anions from extremely dilute aqueous solutions. In order to verify the feasibility of the method we conducted experiments on concentration of NO_3^-, Cl^-, and Br^- ions, employing the cell depicted in Fig. 1 with a Teflon membrane such that r = 0.04 μ and the thickness 0.1 cm; the current density on the membrane did not exceed 2 mA/cm^2. The sequence in which the cell is filled is similar to that described earlier. The initial solution is fed into the anodic compartment via the tube 11 (see Fig. 1) at the flowspeed at which the electroosmotically transported water moves out from the cathodic compartment. The experimental results are entered in Table 2.

It is evident from the data listed in Table 2 that concentration of anions takes place with practically 100% yield, within the limits of error of the analysis.

The dependence of electroosmotic transport of water (V/J) on the concentration of electrolyte (HCl and KOH) expressed in pH units (Fig. 2) was taken in order to pinpoint the region where the electroosmotic method of ion concentration is most effectively applied. The maximum electroosmotic transport clearly corresponds to absolutely pure water. In that case the flow of water through the membrane is due to the motion of hydrated protons forming water upon dissociation, through the membrane. For example, in the case of water with electrical conductivity 1.6 ·10^{-6} mho · cm^{-1}, electroosmotic transport amounts to 50

ml/A·sec, which corresponds to the flowspeed of water streaming through the membrane ~ 200 ml/min ·dm^2. Accordingly, electroosmotic concentration of ions is carried out more feasibly from extremely dilute solutions.

LITERATURE CITED

1. I. M. Korenman, Analytical Chemistry of Small Concentrations [in Russian], Khimiya, Moscow (1967).
2. O. N. Grigorov et al., Electrokinetic Properties of Capillary Systems [in Russian], Izd-vo AN SSSR, Moscow—Leningrad (1956).
3. L. N. Moskvin, N. N. Kalinin, and L. A. Godon, Zh. Prikl. Khim., 46, 5 (1973).
4. O. L. Alekseev and F. D. Ovcharenko, Kolloid. Zh., 33, No. 1, 3 (1971).
5. K. Fetter, Electrochemical Kinetics [Russian translation], Ya. M. Kolotyrkina (editor), Khimiya, Moscow (1967).

CONDITIONS FOR THE SELF-ACCELERATION OF AN ELECTRON BEAM

N. E. Belov, A. V. Kisletsov, and A. N. Lebedev

UDC 621.384.6:621.3.638.62

One of the most important problems in the generation of high-current electron beams is increasing the electron energy to ultrarelativistic values, which is extremely important for practical applications (e.g., use of these electrons for collective acceleration).

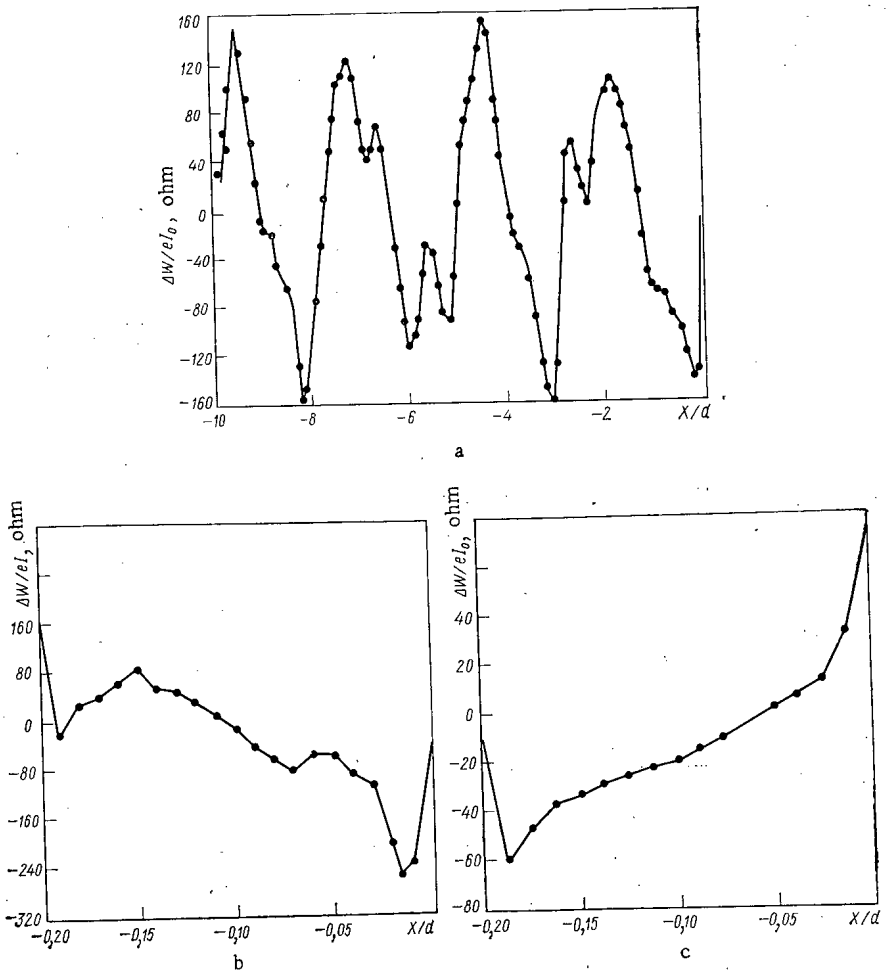

Fig. 1. Redistribution of the energy over the length of the beam. The wavelength of the basic excited mode (m = 0, n = 1) is $\lambda/d = 2.61$. a) $\gamma_0 = 5$; $R/a = 5$; $d/R = 1$; $L/d = 10$; b) $\gamma_0 = 10$; $R/a = 5$; $d/R = 10$; $L/d = 0.2$; c) $\gamma_0 = 1.1$; $R/a = 5$; $d/R = 10$; $L/d = 0.2$.

Translated from Atomnaya Énergiya, Vol. 36, No. 3, pp. 201-206, March, 1974. Original article submitted February 27, 1973.

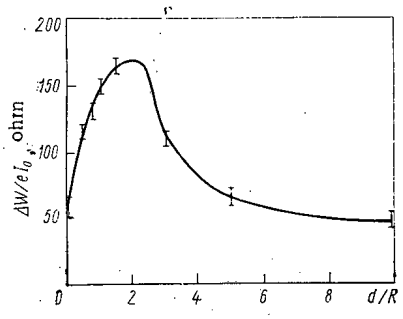

Fig. 2

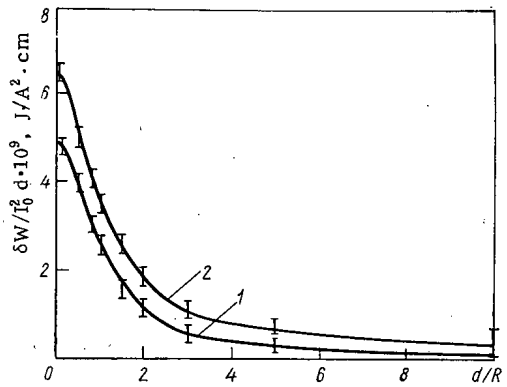

Fig. 3

Fig. 2. Dependence of the impedance upon the relative length of the resonator: L/d = 10; γ_0 = 3; R/a = 5.

Fig. 3. Dependence of the maximum losses upon the geometry of the resonator: 1) γ_0 = 3; 2) γ_0 = 50.

L. N. Kazanskii's self-acceleration concept of an electron beam has been discussed in [1]. In this case, a certain fraction of the beam electrons is accelerated by the strong electric field which is induced by the beam in a passive electrodynamic structure. The energy of the remaining particles can be greatly increased as a consequence of the reduction of the energy and the losses of the major fraction of the beam. In this fashion, it is possible to overcome the limitations which are imposed by high-voltage technology, The magnitude of the pulsed current remains constant, whereas the average current decreases.

The example of [1] concerned the self-acceleration in a passive, cylindrical resonator in the approximation of a predetermined current. The model which was adopted must be improved for two reasons: first, it is necessary to establish the optimal resonator parameters or the resonator parameters close to the optimal parameters; and second, it is necessary to investigate the possibility of cascade connections of self-accelerating elements without the approximation of the fixed current, since this approximation holds only for a single resonator.

The two problems involve extensive computational work the results of which are outlined in the present article. We considered in addition the total energy losses of the beam in the resonator. This problem is of importance for both estimating the efficiency of the system proposed and for other collective acceleration schemes, particularly when the longitudinal dimensions of the beam are much smaller than the longitudinal dimensions of the resonator.

Interaction of the Beam with a Single Resonator and Optimal Parameters

The calculation method of [1] can be used to obtain the following expressions for the energy acquired by a particle which is on the beam axis at a distance x from the origin of the beam and passes through a cylindrical resonator of radius R and length d:

$$\left.\begin{aligned}\Delta W(x)=&\frac{8eI_0\left(\frac{d}{R}\right)^2}{\pi\beta_0 C\left(\frac{a}{R}\right)}\sum_{m=0}^{\infty}\sum_{n=1}^{\infty}\frac{\mathcal{J}_1\left(\mu_n\frac{a}{R}\right)\delta_m}{\mu_n\mathcal{J}_1^2(\mu_n)}\\&\times\int f_0(\xi)\,\Phi(\nu)\,d(\xi/d);\\ \delta_m=&\left.\begin{matrix}1,\ m=0\\2,\ m\neq 0\end{matrix}\right\},\end{aligned}\right\}\qquad(1)$$

where I_0, a, and β_0 denote the maximum current, the radius, and the reduced velocity of the beam, respectively; $f_0(\xi)$ denotes the longitudinal distribution of the current density; μ_n denotes the nth root of the Bessel function of the first kind and zeroth order, i.e., $\mathcal{J}_0(\mu_n) = 0$; $\nu = \xi - x/d$; and $\xi = z - v_0 t$.

We obtain the following expressions for the kernel $\Phi(\nu)$:

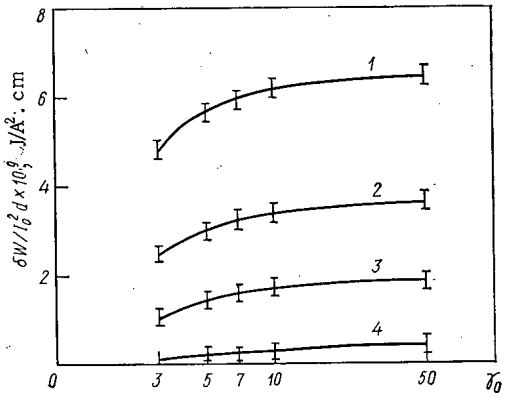

Fig. 4

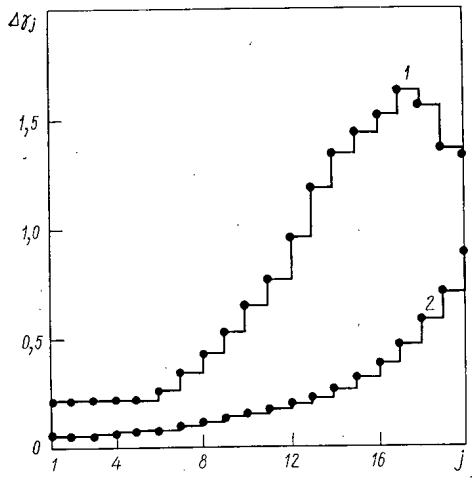

Fig. 5

Fig. 4. Dependence of the maximum losses upon the reduced energy: 1) d/R = 0.1; 2) d/R = 1; 3) d/R = 2; and 4) d/R = 10.

Fig. 5. Dependence of the reduced voltage of the resonator on 1) the number of resonators for capacitive impedances and 2) the number of resonators for inductive impedances. ($I/I_A = 2$; $\gamma_0 = 7$; 10% premodulation).

$$\Phi(\nu)=\begin{cases} -F_2\cos\Omega_\alpha\nu\,(1-\cos\pi m\,\cos\Omega_\alpha) & \text{for } \nu\geqslant 1;\\ -F_1\dfrac{1-\nu}{2}\sin\pi m\nu-\dfrac{F_2}{2}\,[2\cos\Omega_\alpha\nu-\cos\pi m\nu & \\ \quad -\cos\pi m\cos\Omega_\alpha(\nu+1)] & \text{for } 0\leqslant\nu\leqslant 1;\\ -F_1\dfrac{1+\nu}{2}\sin\pi m\nu-\dfrac{F_2}{2}\,[\cos\pi m\nu & \\ \quad -\cos\pi m\nu\cos\Omega_\alpha(\nu+1)] & \text{for } -1\leqslant\nu\leqslant 0;\\ 0, & \text{for } \nu\leqslant -1; \end{cases} \tag{2}$$

$$m=0,\ 1,\ 2\ \ldots;\qquad n=1,\ 2,\ 3\ \ldots$$

with the coefficients*

$$F_1=\frac{m}{m^2+\gamma_0^2A^2};\quad F_2=\frac{2\gamma_0^2A^2(\gamma_0^2-1)}{\pi\,(m^2+\gamma_0^2A^2)^2}, \tag{3}$$

where

$$\gamma_0^2=\frac{1}{1-\beta_0^2};\quad A=\frac{d|\mu_n}{R\pi};\quad \Omega_\alpha^2=\frac{\pi^2(m^2+A^2)}{\beta_0^2};$$
$$m=0,\ 1,\ 2,\ \ldots,\ n=1,\ 2,\ 3\ \ldots$$

After integrating the kernel $\Phi(\nu)$ over ξ/d for $-L/d \leq x/d \leq 0$ (L denotes the length of the beam), formula (1) was studied by numerical summation over both the longitudinal and transverse modes (i.e., summation over the subscripts m and n) in the case of a rectangular current distribution. Figure 1 shows the results of a calculation of the energy redistribution over the length of the beam. The increment of the particle energy after the particle's passage through the resonator is characterized by the effective impedance expressed in ohms, i.e., by the quantity $\Delta W/eI_0(x, d, R, a, \gamma_0)$.

Beams of particles whose flight time is longer than the period of the basic mode are characterized by a pronounced periodicity of the energy modulation (see Fig. 1a); the period of the modulation is close to the period of the principal mode. Transition processes and Coulomb fields which are immaterial in the central section of a long beam are very important in the case of beams the length of which is smaller than

*An error was made in [1] in the calculation of $F_{1,2}$; the error does not cause a qualitative change of the results, but reduces the useful effect.

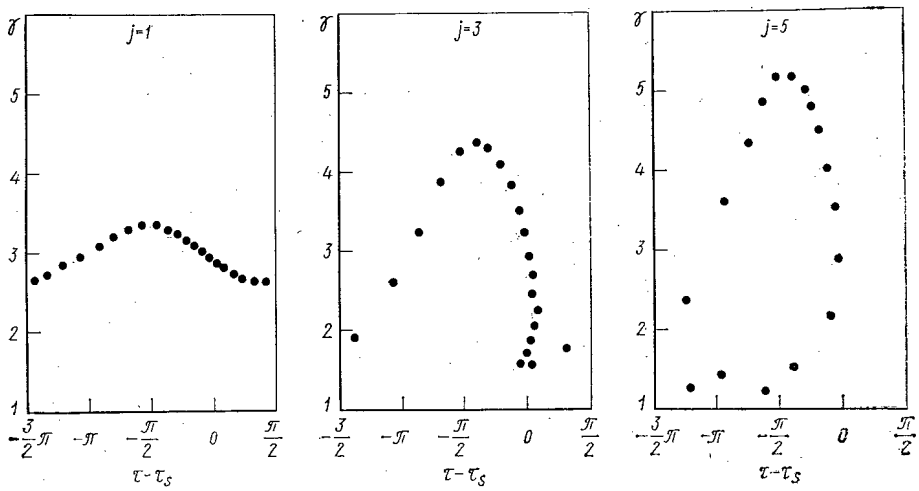

Fig. 6. Distribution of coalescing (bunching) particles in the phase plane behind the jth resonator ($I/I_A = 2$; 30% premodulation).

the length of the resonator. In the case of short, relativistic beams ($L < d$; $\gamma_0 \gg 1$), the influence of Coulomb repulsion is less noticeable than transition processes. As can be inferred from Fig. 1b, the initial portion of the beam looses energy, whereas the final portion of the beam acquires part of that energy. In slow, short beams ($L < d$; $\gamma_0 \approx 1$), Coulomb repulsion results in an acceleration of the initial portion of the beam and a retardation of its final portion (see Fig. 1c).

In order to select the optimal dimensions of a cylindrical resonator, we investigated the dependence of the maximum energy increment over the length of the beam upon the ratio of resonator length d to resonator radius R. The results of the calculations, which are shown in Fig. 2, indicate that the function $\Delta W/eI_0$ depends strongly upon the ratio d/R. At increased d/R (elongated resonator), the interaction between the field and the particles decreases, because the difference between the particle velocity and the phase velocity of the field components which influence the phase velocity plays a role. The interaction between the field and the particles decreases at small d/R values, because the interaction time is reduced. A d/R ratio which is approximately equal to 2 is closest to the optimal value (i.e., the length of the resonator is equal to its diameter).

As far as the physics involved is concerned, it is obvious that in case of operation with a predetermined current, the change of the reduced beam energy γ_0 affects mainly the Coulomb effects which rapidly decrease with increasing γ_0. Hence, at relativistic energies, a change in γ_0 is practically without influence upon the energy redistribution in the beam, as can be inferred from Eq. (3). As a matter of fact, a change in γ_0 at $\gamma_0 \gg 1$ affects only the high harmonics of the excited field; the contribution of these harmonics to the particle energy in the central section of a long beam ($L > 2d$) is small. The results of the numerical calculations fully confirm this conclusion.

Total Energy Losses in the Flight of the Particles

The quasi-periodic form of the energy redistribution curve indicates that about half of the beam particles loose energy in their flight, whereas the other half gains energy. Moreover, since the period of the basic (lowest) mode of the resonator is clearly visible in Fig. 1a, one can expect that mainly the lowest mode is excited by the beam even in the case of a rectangular current distribution which is unfavorable from this viewpoint. After the beam's passage through the resonator, there remains the excited field in the resonator and this excited field is characterized by the total energy losses of the beam and depends upon the ratio of the length of the beam to the wavelength of the basic excited mode. The expression for the losses is obtained by simple integration of Eq. (1) over the length of a particle bunch and has the form

$$\delta W = \frac{16 I_0^2 d \left(\frac{d}{R}\right)^2}{\pi \beta_0^2 c^2 \left(\frac{a}{R}\right)^2} \sum_{m=0}^{\infty} \sum_{n=1}^{\infty} \frac{\mathcal{J}_1^2\left(\mu_n \frac{a}{R}\right) \delta_m}{\mu_n^2 \mathcal{J}_1^2(\mu_n)} \Psi_{m,n}, \tag{4}$$

where $\Psi_{m,n} = F_2/\Omega_\alpha^2 (1 - \cos \pi m \cos \Omega_\alpha)(1 - \cos \Omega_\alpha L/d)$.

Equation (4) was studied by numerical summation. The results of the calculations are shown in Figs. 3 and 4. The total energy losses are characterized by the quantity $\delta W/I_0^2 d$.

The various versions of the calculations are characterized by a periodic dependence of the energy losses upon the length of the beam with the period of the basic mode (m = 0, n = 1) and by a relatively small fraction of energy of the higher oscillation modes whose frequencies are not simple multiples of the frequency of the basic mode. We have to recall that when the length of the resonator is increased and the resonator is converted into a waveguide, the energy distribution over the higher oscillation modes is more uniform so that the dependence of the total losses upon the length of the beam becomes relatively irregular in a long resonator. Apart from this, when the ratio d/R increases, the maximum of the total losses decreases and tends to the loss figure of a pointlike particle bunch; when d/R decreases, the losses increase but remain finite for d/R tending to zero (see Fig. 3). Thus, the dependence of the total losses upon the reduced energy γ_0 must vanish in the ultrarelativistic case. This conclusion is confirmed by the results of the calculation, which are shown in Fig. 4.

The absolute energy losses reach considerable values at high currents. Thus, when a bunch having the length $5 \cdot 10^{-8}$ sec, a current of 10^4 A, and a reduced energy $\gamma_0 = 3$ flies through a resonator with the parameters d/R = 1, a/R = 0.2, and d = 10 cm, the losses are $\delta W = 2$ J at a total beam energy of the order of 10^3 J. In the case of beams with a current of 10^5 A, the losses form a substantial fraction of the total beam energy. We must mention that the self-acceleration technique is not indicated with currents of this magnitude, because the voltage which is generated substantially exceeds the breakdown voltage even in short current pulses.

Self-Consistent Interaction between the Beam and a Cascade of Resonators

As has been mentioned in [1], passive elements can be connected in series so that the energy of the particles in the beam is increased at the expense of the beam intensity. The most logical series connections of self-accelerating elements are cascades of electrically disconnected passive resonators through which the beam passes. From the viewpoint of the general theory, a system of this type without a beam can be considered a periodic structure which allows the propagation of slow E waves. A homogeneous beam in such a system must be unstable in longitudinal direction at wavelengths for which the phase velocity is smaller than the beam velocity. When the wavelength is inevitably predetermined (e.g., by preliminary modulation of the beam intensity) and corresponds to a small phase velocity, one can expect a transition of the beam into the self-phased state (see the investigations of [2]). If this is not the case, the interaction must cause reabsorption of the modulation.

These concepts can be applied to the nonstationary problem of the interaction between the beam and a semiinfinite cascade of resonators when we assume that the resonators are single-mode oscillatory systems with lumped parameters. This model allows calculations of the energy which can be reached and of both the length and the time of stationary conditions in the system. The considerations are important first, from the viewpoint of the efficient use of the system and, second, due to the relatively short duration of high-current beams which are generated in practice.

In the numerical model, the beam was replaced by a sequence of "compacted" particles with the same current. The voltage induced at each resonator was calculated in the approximation of a fixed current. The interaction between a particular particle and all previously passed particles was considered in the approximation of a fixed field. Matching was obtained by phase shifts of the particles in their flight between the resonators where the motion was assumed to be a pure inertial motion. The reduced energy and phases of the particles are described by the equations:

$$\begin{gathered}\tau_{j+1,\,n}=\tau_{j,\,n}-2\pi\frac{L}{\lambda_0}\frac{\beta_{0,\,n}}{\beta_{j,\,n}};\\ \gamma_{j+1,\,n}=\gamma_{j,\,n}+\Delta\gamma_{j,\,n};\\ \Delta\gamma_{j,\,n}=-\frac{2\pi I_0\lambda_0 d}{k\beta_0 I_A S}\sum_{m=1}^{n-1}\cos\frac{\omega_{pj}}{\omega_0}(\tau_{j,\,m}-\tau_{j,\,n}),\\ I_A=\frac{m_0c^3}{e}\approx 17\text{ kA},\end{gathered}\tag{5}$$

where $\tau_{j,n}$ and $\gamma_{j,n}$ denote the phase and the reduced energy of the n-th particle in the j-th resonator, respectively; L and d denote the length of the path of flight and the size of the interaction area, respectively; S denotes the area of the capacitive part of the resonator (assumed to be toroidal); $\beta_{j,n}$ and $\beta_{0,n}$ denote the reduced velocities of the n-th particle in the j-th resonator and before the input to the first resonator, respectively; k denotes the number of particles per period; I_0 denotes the beam current; and ω_p and $\omega_0 = c/\lambda_0$ denote the intrinsic frequency of the resonator and the frequency of preliminary modulation, respectively. Both the sign and the magnitude of the detuning, $\omega_p/\omega_0 - 1$, determine the conductivity of the resonator. In a circuit with ideal conduction, we have $\omega_p/\omega_0 > 1$ (inductive conductivity) or $\omega_p/\omega_0 < 1$ (capacitive conductivity).

The system of nonlinear equations (5) was studied by solving the system numerically on a computer. The removal of particles having the kinetic energy zero was brought into account in the program. This requirement originates from the basic idea that in self-acceleration, the particles which have lost their energy in an interaction process must be removed from the beam. Since the energy of the field and of the particles is conserved, the average energy of the bunches which are formed must increase along the system. Moreover, the restrictive condition of a maximum voltage which can develop at one element of the cascade without causing electrical breakdown was introduced into the program. To do this, the tuning of the resonator was changed; the tuning adjustment was made for each individual resonator. The amplitude of the induced voltage was changed only by changing the phase relationships between the voltage at the resonator and the induction current. The changes in the amplitude of the voltage, which result from energy losses at the walls, can become effective only in sufficiently long beams in which a number of wavelengths (which are approximately equal to the Q factor) are superimposed. In the case of beams with a pulse duration of several dozen nanoseconds and a wavelength of the order of a few dozen centimeters, the attenuation resulting from purely resistive losses can be ignored.

Some results of the calculations are shown in Figs. 5 and 6. The influence of the conductivity type of the resonators upon the efficiency of particle bunching and the stability of the resulting bunches are illustrated in Fig. 5 which shows the dependence of the voltage at the resonator upon the number of the resonators for a premodulation of 10%. Curves 1 and 2, which correspond to capacitive and inductive impedances, respectively, have a clear, exponential section, a linear section, and a saturation section. Grouping of the particles and formation of bunches take place in the first section; low-energy particles which do not belong to a bunch are lost in the second section in which also the bunched particles are accelerated. The pattern of particle motion in the system becomes stationary in the saturation section and the particles perform phase oscillations in the self-phased bunches. The difference in the form of the curves for the various impedances seems to be related to various phase relationships between the modulation of the beam and the field induced by the initial particles.

The bunching processes are depicted in Fig. 6 which illustrates the behavior of the beam particles during their passage of a resonator system on the (γ, τ) phase plane. In a system with the capacitive impedance, the bunches are formed by the fifth resonator. The major fraction of the particles performs oscillations in the bunches which were formed. By giving away their energy, some particles slip from the bunches and are lost. Apart from the increase in the maximum energy in each subsequent bunch, the equilibrium energy of the bunches is increased as a consequence of the losses of particles.

The calculations have shown that when the initial beam energy is increased, the increment of the instability decreases, but the length required for establishing stationary conditions remains acceptable for beams having a duration of several dozen nanoseconds and an energy of several MeV. The increase in γ_0 extends the section of the linear increase and raises the maximum energy which is attained by the beam particles.

Thus, a noticeable increase in the energy of the beam particles is possible at currents of the order of several dozen kiloamperes. Extremely high currents cannot be employed in view of the high voltages which are induced in the resonator and in view of the possible breakdown. The energy of a fraction of the particles in a beam with an initial current of 30 kA can be increased from 2-3 MeV to 8-10 MeV, whereas the fraction of the lost particles amounts to about 50% in the particles' passage through 20 resonators.

We have to mention that removal of low-energy particles from the beam in the early stages of the deceleration of these particles would make it possible to reach higher energies of the remaining fraction of the beam particles.

LITERATURE CITED

1. L. N. Kazanskii, A. V. Kisletsov, and A. N. Lebedev, Atomnaya Énergiya, 30, No. 1, 27 (1971).
2. A. V. Kisletsov and A. N. Lebedev, Zh. Tekh. Fiz., 42, No. 4, 699 (1972).

ABSTRACTS

OXIDATION OF URANIUM MONOCARBIDE IN THE TEMPERATURE INTERVAL 300-700°C

V. G. Vlasov, V. A. Alabushev, A. R. Beketov, and A. G. Sychev

UDC 546.791.261.094.3

Modifications of the conditions under which uranium monocarbide is oxidized (state of the solid phase, temperature of the experiments, both pressure and composition of the gas) influence not only the rate of the process but also its mechanism. Research on the behavior of UC in aggressive gases has provided information on the interaction of UC with pure oxygen at 300-700°C and at gas pressures between 1.7 and 34 mm Hg. The uranium monocarbide was used in the form of granules with the composition $UC_{1.02}$ and the density 12.82 g/cm^3. The gaseous oxygen contained less than $1 \cdot 10^{-3}$% by volume admixtures. The kinetic curves are a sequence of three sections: a linear section, a parabolic section, and again a linear section. The data were evaluated with the aid of the equations

$$Q = K_0 t + Q_0; \quad (1)$$

$$Q^2 + 2K_2 Q + K_3 = 2K_1 t; \quad (2)$$

$$v = kP_{O_2}^n. \quad (3)$$

At P_{O_2} = 7.2 ± 0.10 mm Hg, the activation energy amounts to 22 kcal/mole in the temperature interval 300-450°C, and to 3 kcal/mole at higher temperatures. The exponent n in Eq. (3) is 0.1 in the first linear section, and 0.43 in the parabolic section for P_{O_2} = 1.7-20.2 mm Hg. A pressure increase raises n to 1.63. X-ray diffraction analyses of products with different degrees of oxidation have indicated the presence of uranium carbide (uranium oxycarbide), uranium dioxide, and uranium protoxide—oxide. The protoxide—oxide of uranium appears in the second linear oxidation section. The ratio of the oxide phases depends also upon the increase in the pressure of the gaseous oxidizer. Chemical analysis has established the presence of free carbon in the sample. The concentration of the free carbon depends upon the degree of oxidation. The initially adsorbed oxygen is dissolved in the carbide under the formation of oxycarbide with the maximum oxygen concentration. The oxidizing agent diffuses through a thin protective film of constant thickness. Based on Wagner's theory, and taking into account the nature of the protective UO_{2+x} film, it is possible to explain the observed influence of P_{O_2} upon the rate of the process. The activation energy which was determined is rather close to the activation energy of oxygen self-diffusion into UO_2. The oxidation of the carbon induces considerable changes in the process at temperature in excess of 450°C. The weight of the sample increases due to the association of oxygen or decreases due to the combustion of carbon and the reduction of the protoxide—oxide of uranium. Accordingly, the temperature coefficient of the reaction rate is reduced to 3 kcal/mole. Related is an increase in the coefficient n of Eq. (3) at P_{O_2} > 20 mm Hg.

Translated from Atomnaya Énergiya, Vol. 36, No. 3, pp. 207-208, March, 1974. Original article submitted April 25, 1973; revision submitted September 4, 1973.

OPTIMIZATION OF THE PROFILE OF A RADIATION SHIELD*

V. A. Zharkov, Yu. G. Akopyan, L. S. Salakatova, L. A. Filatov, and N. A. Lyapunov

UDC 621.039.-78

The radiation shield of a device employing radioactive isotopes must lower the radiation level to values ordinarily specified on the surface of the device and at a distance of 1 m from it.

Since procedures for constructing the optimum profile of a shield satisfying this condition are not available in the literature, actual shields are often unnecessarily thick in a number of directions. This leads to an unwarranted increase in the weight and size of the device, an overexpenditure of shielding materials, and an increase in transportation expenses, which is particularly important for radioisotopic power generators.

We discuss a method for calculating the optimum profile of the radiation shield for cylindrical gamma-ray or bremsstrahlung sources, applicable to radioisotopic thermoelectric generators (RITEG). The method uses a point kernel. The expression for the buildup factor entering the attenuation kernel is analyzed in detail. The required constant value of the dose rate is specified on the outer surface of the shield whose profile is being investigated. The "Gamma" and "Profile" program for an M-222 computer are based on this method.

The "Gamma" program permits the calculation of the dose rate at any point on the surface of a shield of known configuration. The "Profile" program is designed to determine the optimum configuration of the shield. The calculated results are compared with experimental data obtained on two RITEG radiation mock-ups with cylindrical ^{90}Sr sources. The mock-ups were made with nonoptimum shield profiles and then machined to the calculated optimum configuration. The dose rates were measured on the unoptimized and optimized surfaces; in both cases the calculational error did not exceed 20%.

When applied to the optimization of radioisotopic generators the method leads to weight savings of 20-40% depending on the power. The method can also be used for other radiation devices.

DISTRIBUTION OF THERMALIZED ELECTRONS IN MATTER†

A. A. Vorob'ev and A. P. Yalovets

UDC 539.124.17

The solution of a number of practical problems, such as the irradiation of polymers, ceramics, glasses, etc., requires data on the spatial distribution of charge resulting from the thermalization of fast electrons.

The distribution of thermalized electrons (DTE) with initial energies above 1 MeV was found experimentally in [1, 2]. We calculate the DTE in various materials for incident electron energies below 1 MeV. The calculation is based on a solution of the transport equation obtained within the framework of the "segments model" [3] in which a step is taken in energy, and fluctuations in energy losses are determined by fluctuations in range. The calculated and experimental DTE [1, 2] agree with the limits of experimental error. The DTE is tabulated for energies of 1, 0.7, 0.5, 0.3, and 0.1 MeV in carbon, aluminum, and copper.

*Original article submitted June 11, 1973.
†Original article submitted June 19, 1973.

LITERATURE CITED

1. T. Tabata et al., Phys. Rev., B3, 572 (1971).
2. B. Grose and K. Wright, Phys. Rev., 114, 725 (1959).
3. O. B. Evdokimov, Izv. VUZ, Fiz., No. 1, 17 (1973).

SEPARATION OF NITROGEN ISOTOPES BY THE CONTINUOUS ADSORPTION METHOD

A. V. Sarukhanov, V. E. Kochurikhin, É. P. Magomedbekov, and Ya. D. Zel'venskii

UDC 621.039.249

The separation factor of nitrogen isotopes for adsorption on zeolite NaX at a pressure of 30-720 torr and a temperature of 78°K has been measured by the method of single isotopic equilibration on a vacuum circulation assembly. The separation factor was found to be independent of pressure and equal to 1.016 ± 0.002. The separation of nitrogen isotopes by continuous adsorption on zeolite NaX was investigated at this temperature on a laboratory set-up.

Nitrogen of natural isotopic composition was used and granular synthetic zeolite NaX-ShM-61 with a grain size of 2-2.5 mm. The continuous adsorption column consisted of three main parts: the adsorber, the separating section, and the desorber. The adsorbent moved under gravity in a continuous layer from the top to the bottom of the column. Its velocity was controlled by varying the rate of rotation of the disk of a dosing apparatus located at the column outlet. The temperature of the desorber, located below the separating section, and also the temperatures of the upper and lower reservoirs for the adsorbent, were maintained between 100 and 120°C. At lower temperatures there was an insignificant adsorption of nitrogen on the zeolite NaX, leading to a decrease in the extent of separation as a result of outgoing material. All the experiments on the column were performed without outgoing material. A stationary state was reached after 4-12 h, depending on the experimental conditions.

Determinations were made of the isotopic content of gas samples withdrawn at the ends of the separation section. The ^{15}N content was determined on an MI-1305 mass spectrometer. The dependence of the extent of separation and of the height equivalent to the theoretical extent of separation (HETE) on the gas pressure in the column and the velocity of the adsorbent was studied. It was shown that when the adsorbent moves with a constant velocity of 3.2 cm/min the extent of separation as a function of the pressure passes through a maximum at a pressure of 500 torr and the HETE is 5.7 cm. When the velocity of the adsorbent is increased to 6.3 cm/min the maximum is displaced toward higher pressures (700 torr) and the HETE increases to 9.2 cm. At constant pressure an increase in the velocity of the adsorbent leads to a rapid decrease in the extent of separation and to a linear increase in the HETE. The values of 5-15 cm for the HETE obtained in the experiments are close to the values of the HETE observed in chemical isotopic exchange processes in gas—liquid systems.

The mass transfer coefficients β were calculated from the results obtained. At a pressure of 150 torr β was found to be 112,000 moles/m^3 h and independent of the velocity of the adsorbent in the velocity range investigated. It is suggested that at a pressure of 150 torr over the whole velocity range studied internal diffusion is the limiting stage of the mass-transfer process. At high pressures external diffusion exerts a significant effect on the mass-transfer process. This is probably related to the decrease in the coefficient of self diffusion of nitrogen. Thus at a pressure of 570 torr when the velocity of the adsorbent is increased from 2.0 to 7.3 cm/min β increases from 122,000 to 196,000 moles/m^3 h. The internal mass transfer coefficient was shown to be proportional to the square root of the pressure.

Original article submitted June 19, 1973.

EXPERIMENTAL DATA RELATING TO THE THERMAL NEUTRON SPECTRUM IN NUCLEAR REACTORS

S. S. Lomakin, G. G. Panfilov, and V. I. Kulikov

UDC 539.125.5

A comparison between existing theoretical and experimental data relating to the thermal-neutron energy distribution in nuclear reactors [1] proves the necessity of allowing for the very specific effects of the chemical bond and crystal structure of the moderator in order to secure a full description of the neutron-thermalization process. Existing differences between experimental and calculated values of neutron temperature [2-5] may be attributed to the fact that these effects are not allowed for in the Coveyou formula [6], based on the free gas model. It should furthermore be noted that the experimental neutron temperature T_n usually exceeds the calculated value. In this paper we shall present an empirical relationship linking the temperature of the medium and the parameter $\Sigma_a/\xi\Sigma_s$ to the neutron temperature. In order to derive this relationship, we generalized experimental T_n data obtained in the moderators of various types of reactor cells. Tables 1-3 give the hardness parameters $\Sigma_a(kT_m)/\Sigma\xi_s$ calculated for the homogenized cells of specific reactors and the corresponding values of the proportionality factor K obtained from the relation

$$T_n = T_m\left[1 + K\frac{\Sigma_a(kT_n)}{\xi\Sigma_s}\right],$$

where T_m is the temperature of the medium.

TABLE 1. Neutron Temperature in a Uranium—Water Cell

Reactor	Enrichment in ^{235}U, %	$\frac{\Sigma_a}{\xi\Sigma_s}$	T_m, °K	T_n, °K	K	Literature
VVR	10	0,145	313	400±12	1,92	[7]
MR	90	0,188	286	390±12	1,94	[7]
VVÉR	2	0,168	303	396±12	1,82	[8]
VVÉR	1,5	0,133	303	375±1	1,76	[8]
RFR	10	0,146	305	394	2,00	[9]
MELUSINE	20	0,137	300	375	1,82	[10]

TABLE 2. Neutron Temperature in a Uranium—Water—Graphite Cell

Reactor, assembly	Enrichment in ^{235}U, %	$\frac{\Sigma_a}{\xi\Sigma_s}$	T_m, °K	T_n, °K	K	Literature
1st nuclear station	5	0,1325	300	395	2,38	[4]
The same	6,5	0,191	298	445	2,58	
Assembly	2	0,0452	293	327	2,57	

TABLE 3. Neutron Temperature in a Uranium—Graphite Cell

Reactor, assembly	$\frac{\Sigma_a}{\xi\Sigma_s}$	T_m, °K	T_n, °K	K	Literature
Graphite assembly	0,076	290	360±20	3,16	[12]
Uranium—graphite assembly	0,0665	293	349±7	2,86	[13]
F-1	0,081	293	348±10	2,32	
Assembly	0,1075	293	378±11	2,69	[4]
CLEEP	0,064	293	353	3,20	[14]

TABLE 4. Neutron Temperature in a Cell with Beryllium and Heavy Water Moderators

Reactor, assembly	Enrichment in ^{235}U, %	$\frac{\Sigma_a}{\xi\Sigma_s}$	T_m, °K	T_n, °K	K	Literature
MR	90	0,0845	286	335	2,04	[7]
Heavy—water reactor	0,7	0,0204	295	318	3,68	[15]
The same	0,7	0,0253	295	321	3,36	[15]

Translated from Atomnaya Énergiya, Vol. 36, No. 3, pp. 211-212, March, 1974. Original article submitted October 23, 1972.

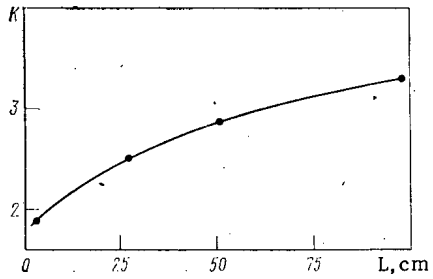

Fig. 1. Dependence of the coefficient K on the diffusion length L.

The scattering cross section Σ_s was provided with a suitable weighting factor. Calculations based on the formulas of [11] [for a uranium—water cell] showed that the weighting factor (ratio of the mean thermal neutron fluxes in the moderator and the fuel) for this particular type of reactor cell equalled 1.1. A calculation of the weighting factor was carried out in an analogous way for other types of reactor cells. The value of σ_s was taken as 20 b per hydrogen atom. The average value of K was 1.88.

Measurements of T_n were also carried out in a graphite moderator [uranium—water—graphite cell]; in these systems the water served as coolant, but its contribution to the Σ_s of the cell was also taken into account. The value of Σ_s for this type of reactor cell was provided with a weighting factor of 1.53. The average value of K for this type of reactor equalled 2.51.

The calculated value of Σ_s for uranium—graphite cells was provided with a weighting factor of 1.8. The average value of K for the uranium—graphite systems was 2.85.

Unfortunately we were unable to carry out a similar investigation for reactor cells with beryllium and heavy water moderators in view of the sparsity of published work on this subject. For these moderators we have only the individual measurements presented in Table 4.

We may also note the relationship between the coefficient K and the diffusion length L of the reactor-cell moderator in which the neutron temperature was measured (Fig. 1). The values of K in this figure represent averages.

Thus the formula here presented, together with the appropriate value of K, may be successfully used in order to calculate the value of T_n in any reactor-cell moderator.

LITERATURE CITED

1. D. R. Beister, Thermalization of Neutrons [Russian translation], Atomizdat, Moscow (1964), p. 288.
2. K. Burkhart and W. Reichhardt, Thermalization of Neutrons [Russian translation], Atomizdat, Moscow (1964), p. 314.
3. S. Kobayahi et al., J. Nucl. Sci. Technol., 4, No. 9, 451 (1967).
4. S. S. Lomakin et al., At. Énerg., 29, No. 1, 36 (1970).
5. A. Weinberg and E. Wigner, Physical Theory of Nuclear Reactors [Russian translation], Atomizdat, Moscow (1960), p. 311.
6. R. Coveyou et al., J. Nucl. Energy, 2, 153 (1956).
7. S. S. Lomakin et al., Nuclear Instrument Making, No. 17 [in Russian], Atomizdat, Moscow (1972), p. 9.
8. S. S. Lomakin et al., At. Énerg., 32, No. 3, 223 (1972).
9. D. Albert, ZFK-RN-13 (1961).
10. Neutron Fluence Measurements, IAEA, Vienna (1970).
11. G. Ya. Rumyantsev, Design of a Thermal Neutron Reactor [in Russian], Atomizdat, Moscow (1967).
12. M. Küche, Nucl. Sci. Engng., 2, 87 (1957).
13. M. Coates, Neutron Time-of-Flight Methods, Euratom, Brussels (1961).
14. E. Axton, Reactor Sci. Technol., Part A/B, 17, 125 (1963).
15. E. Sokolowski, J. Nucl. Energy, 21, 35 (1967).

HIGH-TEMPERATURE IRRADIATION OF STRUCTURAL GRAPHITE

I. P. Kalyagina, Yu. S. Virgil'ev,
V. R. Zolotukhin, V. I. Klimenkov,
V. P. Shevyakov, and T. N. Shurshakova

UDC 621.039.532.21

The construction of high-temperature uranium—graphite RBM-K type power reactors [1] has prompted a need to investigate the materials used in the construction. In particular, the graphite used must exhibit high dimensional stability when irradiated over a range of temperature from 450° to 750°C. In order to secure data on the behavior of graphite materials differing in their properties when exposed to high integrated flux levels, we undertook investigations of the materials in an SM-2 reactor.

We selected the widely popular method of irradiation in capsules, with samples of graphite heated by absorption of reactor radiation from heat-evolving inserts of such dense materials as tungsten and molybdenum. Thermal resistance was established between the specimens and the wall of the capsule, in the form of a vapor gap which underwent no change throughout the exposure. The capsules were filled with helium to prevent oxidation. The tests were conducted at temperatures 450-950°C in the research channels of the SM-2 reactor, on 5 to 15 specimens (for each experimental point), with cross section 4 × 4 mm or diameter 5 mm, and length 40 mm. The temperature was monitored by thermocouples and diamond or fusible metallic indicators. The neutron dose was arrived at on the basis of the effective exposure time and the known flux of neutrons of energies greater than 0.18 MeV.

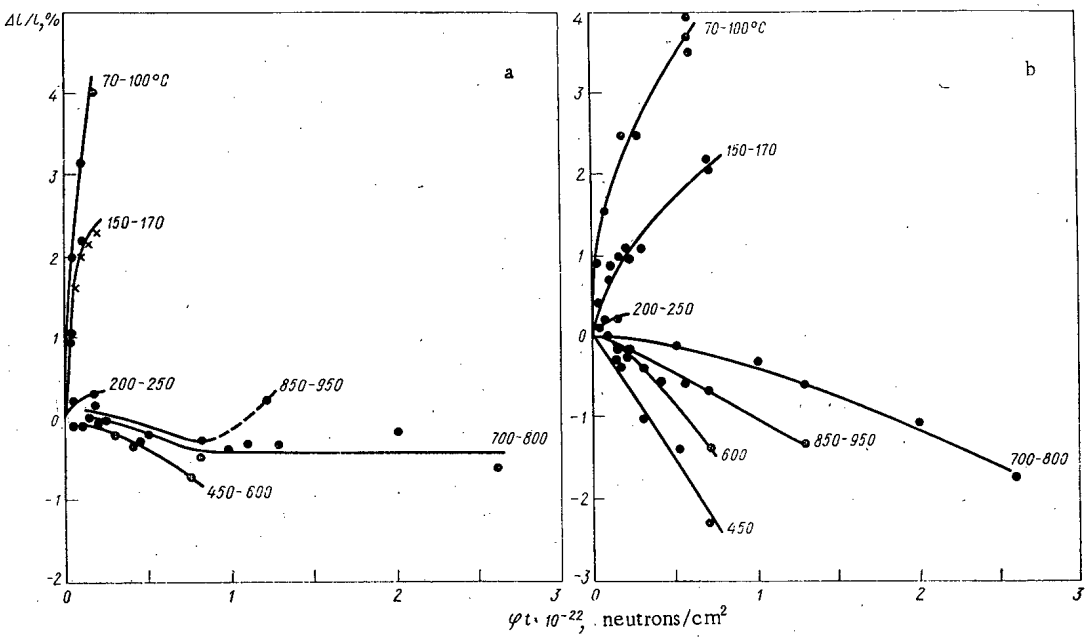

Fig. 1. Integrated flux dependence of relative change in length of grade GMZ-2400 graphite specimens irradiated at various temperatures, in perpendicular direction (a) and in parallel direction (b).

Translated from Atomnaya Énergiya, Vol. 36, No. 3, pp. 212-215, March, 1974. Original article submitted November 27, 1972; revision submitted March 2, 1973.

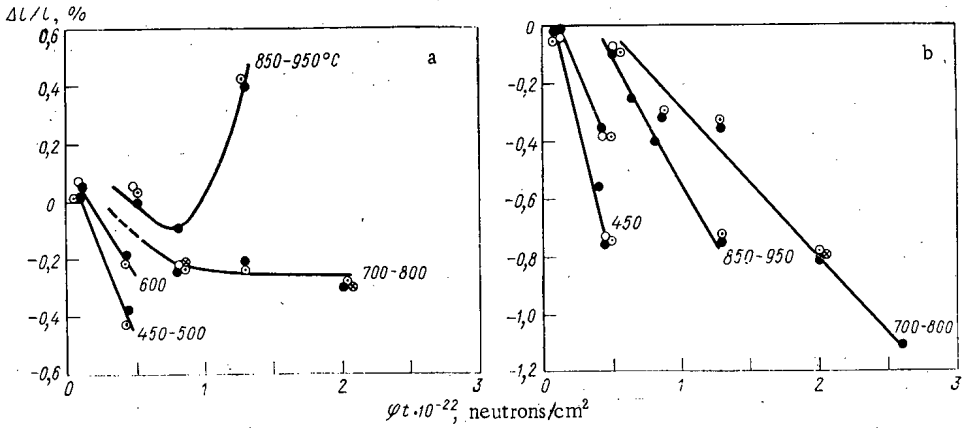

Fig. 2. Integrated flux dependence of relative change in length of specimens of grade GMZ-2800 graphite in perpendicular direction (a) and in parallel direction (b): ●) with no prior pitch impregnation; ○) with one pitch impregnation; ⊙) with two pitch impregnations; ⊗) VPG.

We investigated petroleum coke base materials differing in their fabrication technology: grade GMZ graphite with graphitization temperatures 2400° and 2800°C and different amounts of sealing impregnations with pitch, including VPG; grade KPG graphite with an uncalcined coke base; highly crystalline material with natural graphite filler (grade ER) (see Table 1).

Specimens of graphite of grades GMZ-2400, GMZ-2800 irradiated over the 450-950°C range of temperatures (Fig. 1, Fig. 2) experience shrinkage in the direction parallel and perpendicular to the extrusion

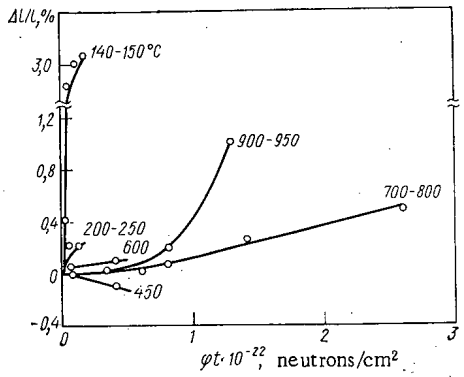

Fig. 3. Integrated flux dependence of relative change in length of specimens of grade KPG isotropic graphite irradiated at different temperatures, in perpendicular direction and in parallel direction.

TABLE 1. Physicomechanical Properties of Materials Tested

Grade of material	Graphitization temperature, °C	d_k, g/cm³	ρ, Ω·mm²/m	σ_c, kg/cm²	σ_b, kg/cm²	E·10⁻⁵, kg/cm²	α·10⁶, (°C)⁻¹	λ, kcal/m·h·deg
GMZ	2400	1,67	8,5—10,5 / 12—14,0	260—470	140—250 / 80—140	0,75—0,95 / 0,55—0,70	3,7 / 4,1	103 / 89
GMZ	2800	1,60—1,70	7,5—9,2 / 1,0—12,5	220—420	110—220 / 60—130	0,80—1,00 / 0,50—0,65	3,3—3,7 / 4,2—4,6	—
GMZ with two pitch impregnations	2800	1,80—1,85	6,0—8,0 / 8,5—10,5	450—650	220—360 / 140—230	1,11—1,13 / 0,75—0,95	3,5—4,2 / 4,8—5,1	160—180 / 90—110
KPG	3000	1,67—1,90	8—10	600—800	—	0,9—1,5	6,3 / 5,9	47 / 19
ER	2400	1,56—1,61	25—30 / 5,0—7,0	275 / 250	195 / 80	0,5—1,0 / 1,5—2,0	5,0—6,0 / 1,2—1,5	43 / 148

Note: d_k is the bulk density; σ_c and σ_b are the ultimate strengths in compression and in bending, respectively, E is the elastic modulus; α is the thermal expansion coefficient at 20-100°C; ρ is the electrical resistivity. The figures given in the numerator are for the direction parallel to the shaping axis, those in the denominator are for the perpendicular direction.

TABLE 2. Relative Change in Dimensions of Grade ER Graphite Specimens Exposed to Neutron Bombardment

Irradiation temperature, °C	Integrated flux $\varphi t \cdot 10^{-22}$, neutrons/cm^2	Relative change in length $\Delta l/l$, %	
		a*	b
700—800	1,0	−0,6	+1,0
	1,5	−1,0	+1,5
	2,0	−1,6	+2,0
	2,5	−2,4	+2,5

* Here and in Table 3: a) perpendicular to extrusion axis; b) parallel to extrusion axis.

TABLE 3. Rate of Relative Change in Linear Dimensions of Soviet and Foreign Graphitic Materials at Different Irradiation Temperatures

Grade of material	Rate of initial shrinkage, % /10^{21} neutrons/cm^2					
	400—450° C		550—600° C		750—950° C	
	a	b	a	b	a	b
GMZ-2400	−0,15	−0,35	−0,15	−0,22	−0,12	−0,15
GMZ-2800	−0,10	−0,20	−0,06	−0,15	−0,05	−0,06
VPG	−0,10	−0,20	−0,06	−0,15	−0,05	−0,06
KPG	—	−0,10	+0,02	+0,01	+0,20	+0,02
PH, PO, PR	−0,20	−0,25	−0,20	−0,25	−0,20	−0,25
PGA	−0,24	−0,30	−0,20	−0,24	−0,09	−0,20

axis. The amount of shrinkage varies inversely with the irradiation temperature. Anisotropy in dimensional variations is greater than that expected on the basis of thermal expansion coefficients [2]. "Secondary swelling," characterized by an increase in the dimensions of the specimens [3], was observed at higher temperatures in specimens cut in the direction perpendicular to the extrusion axis; the rate of compression in the parallel direction increased at the same time. Raising the graphitization temperature meant a marked decrease in shrinkage. Impregnations with anthracite pitch did not exert any substantial effects on dimensional change. Uncalcined coke materials exhibited excellent stability; e.g., the shrinkage rate is only a very weak function of the irradiation temperature in specimens of grade KPG graphite heat-treated at 3000°C (Fig. 3).

Shrinkage of grade ER highly anisotropic graphite in the direction perpendicular to the extrusion axis was slight (see Table 2).

Comparison of Soviet and foreign graphite materials developed for high-temperature power reactors and tested at temperatures to 750°C [4], and of grade PGA graphite [5], demonstrated that Soviet materials such as GMZ and KPG experience a slower rate of radiation shrinkage under the stated irradiation conditions (see Table 3).

We are led to the following conclusions:

1. The rate of radiation-induced shrinkage experienced by the specimens attains a maximum at 450°C, and slackens off as the irradiation temperature rises to 700-950°C.
2. A rise in the graphitization temperature of grade GMZ graphitic material to 2800-3000°C lowers the shrinkage rate of the material to about half.
3. Sealing impregnations with anthracitic pitch exert virtually no effect on dimensional changes.
4. Highest stability is exhibited by isotropic uncalcined coke materials.
5. At neutron doses below 10^{22} neutrons/cm^2 and at temperatures in the range 450-800°C, "secondary swelling" makes its appearance.

LITERATURE CITED

1. A. M. Petros'yants et al., At. Énerg., 31, No. 4, 315-323 (1971).
2. J. Simmons, Proc. 3rd Conf. on Carbon (1959), p. 579.
3. R. Henson et al., Carbon, Vol. 6 (1968), pp. 789-866.
4. P. Nettly et al., Atom, No. 146, 329 (1968).
5. W. Martin and A. Price, J. Nucl. Energy, 21, 359-371 (1967).

FLUCTUATION TYPE POWER AND PERIOD METER FOR NUCLEAR REACTOR

A. I. Sapozhnikov and V. I. Kazachkov

UDC 621.039.564.2

Soviet-designed nuclear reactor performance monitoring systems utilize the current method and pulsed method of measuring neutron flux density, based on measurements of the first moment of the neutron detector signal distribution. In some cases, however, it is found convenient to measure the neutron flux density and the reactor period on the basis of the variance of the ionization chamber current [1, 2].

A schematic layout of an instrument designed to measure the neutron flux density Φ and the reactor period T on the basis of the variance of the ionization chamber current appears in Fig. 1a. The fluctuation component of the ionization chamber signal IC appears on the load R_H, is amplified by the preamplifier PREAMP, and is fed to the function generator FG, in which the signal proportional to the neutron flux is separated out and its logarithm is taken. After the differential amplifier DIFAMP, we obtain a signal proportional to the reciprocal of the reactor period.

The preamplifier has the following characteristics: gain 100; gain instability over 10-40°C temperature range not more than 2%; frequency bandwidth at 0.7 level from 300 to 2000 Hz; intrinsic noise level reduced to input with input closed at 100 kΩ not more than 3 μV. The input impedance presented by the instrument is determined by the load resistance R_H, and is 100 kΩ. In order to obtain a broad dynamic range, the function generator FG is designed on the sequential summation principle [3]. The structural layout of the function generator FG is shown in Fig. 1b.

The function generator features a logarithmic channel and a linear channel. The unit module of the function generator FG consists of the amplifier AMP, linear rectifier LR, and limiter LIM. The voltages of the unit modules add, and we obtain, at the output of the summer, the signal I_{log} proportional to the logarithm of the neutron flux. The maximum relative deviation of the real logarithmic characteristic from the ideal, depending on the gain K of the unit module, appears in the form [3]:

$$\delta U_{\log} = A - [\ln(\ln K) + 1](\ln K)^{-1}/A + [1 - (\ln K)^{-1}(A \ln K)],$$

where

$$A = \sum_{i=0}^{n} \frac{1}{K^{i-1}}.$$

If we assume $\delta U_{log} \leq 10\%$, then $K \leq 5$. The module gain K and the number of modules n are related by the formula $K^n = (\Phi_M/\Phi_0)^{1/2}$, where Φ_M and Φ_0 are the maximum and minimum neutron flux, respectively. Hence, when $\Phi_M/\Phi_0 = 10^6$ and K = 3.3, the number of modules is six. The amplifier section is designed around the Spektr-ADS type operational amplifier OPAMP and offers the following parameters: gain 3.3 ± 5%; gain instability over 10-40°C temperature range not greater than 5%; maximum undistorted amplitude of output signal ±10 V at 2kΩ load; noise reduced to input not greater than 300 μV in 300-2000 Hz frequency band. The linear rectifier is a type D312 diode. The limiter is a type D106 silicon diode.

The linear channel consists of a measurement range switching unit MRSW, a square-law rectifier SQR, and the amplifier AMP. The mean across the SQR output is proportional to the neutron flux [1]. The principal reduced error in measurements on the linear scale is not greater than ±5%. A standard square-law PK type converter of the Spektr-ADS set is used as SQR. The differentiating amplifier is based on the operational amplifier OPAMP.

Translated from Atomnaya Énergiya, Vol. 36, No. 3, pp. 215-216, March, 1974. Original article submitted May 8, 1973; revision submitted September 28, 1973.

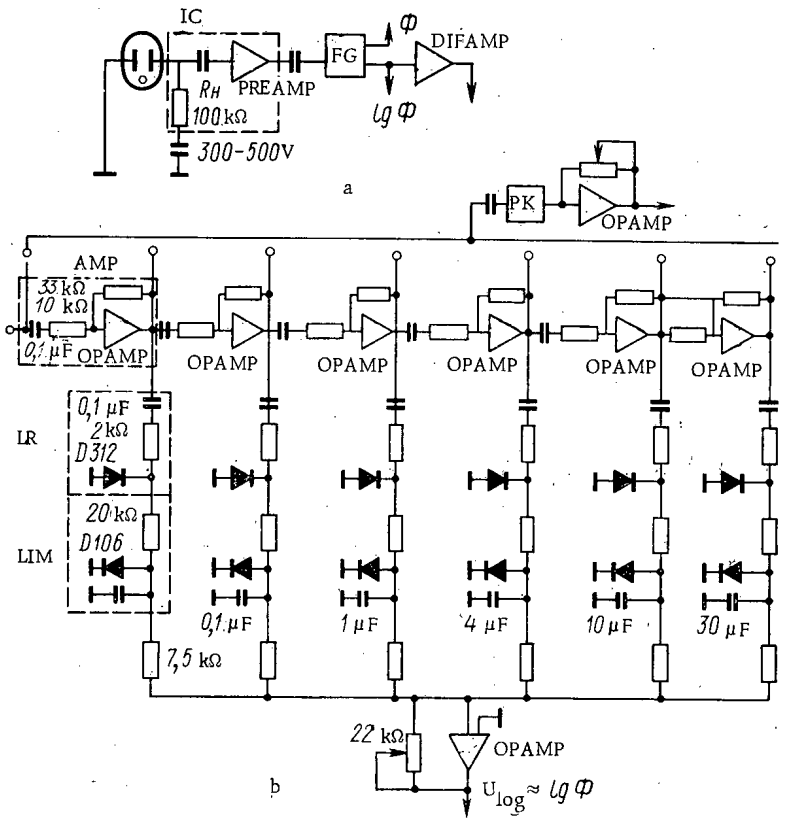

Fig. 1. Structural layout of instrument (a) and of function generator (b).

The time constants for differentiation and of the smoothing filter can be established in steps; 10 sec, 5 sec, and 1 sec. The instrument is designed to measure the reactor period over the range from 10 sec to 100 sec.

The instrument was tested in the AMBF research reactor over a neutron flux range from 10^3 to 10^7 neutrons/cm^2 · sec and against an insignificant γ-ray background, showing that the error in the neutron flux measurements did not exceed ±10% decade on the logarithmic scale. The relative error in the reactor period measurements was not greater than ± 15%.

The error in neutron flux measurements was not greater than ±10% the instrument output current on the logarithmic scale, when the instrument was tested at the IRT-2000 reactor over the neutron flux range from $5 \cdot 10^4$ to $5 \cdot 10^{10}$ neutrons/cm^2·sec and against a γ-ray background of $2\text{-}10^4$R/h. The error in the linear channel measurements was ±5%. With a γ-ray background of $3.5 \cdot 10^6$R/h, the measurement range covered $2 \cdot 10^6$ to $2 \cdot 10^{10}$ neutrons/cm^2·sec. The error in measurements of a 40 sec period was ±10%.

The KNT-54 chamber with preamplifier was coupled by a 20 m long PATRÉ cable with a 100 pF/m specific capacitance. The preamplifier and the function generator are connected by a 100 m long type RK-50 cable.

LITERATURE CITED

1. A. I. Mogil'ner and S. A. Morozov, At. Énerg., 24, No. 2, 151 (1968).
2. A. I. Mogil'ner and S. A. Morozov, At. Énerg., 26, No. 6, 491 (1969).
3. V. M. Volkov, Broad Dynamic Range Electronic Function Amplifiers [in Russian], Tekhnika, Kiev (1967).

MEASUREMENT OF PULSED NEUTRON FLUXES

M. G. Mitel'man, N. D. Rozenblyum,
N. M. Alekseev, A. A. Musatov,
I. M. Perederii, A. K. Gusarov,
V. A. Zagadkin, M. Yu. Belavin,
and A. P. Sokolov

UDC 621.039.564.2

Bock et al. [1] present data on the use of direct charge detectors (DCD) with a cobalt emitter to measure the neutron flux density in a pulsed reactor. There are two types of DCD's: an activation type using β particles produced in the ${}_{Z}A^{m}(n, \gamma){}_{Z}A^{m+1} \xrightarrow{\beta} {}_{Z+1}A^{m+1}$ reaction, and a Compton type using Compton electrons and photoelectrons produced in the interaction of gamma rays from the (n, γ) reaction with the emitter. Compton electrons also contribute to the current in an activation type DCD.

The basic equation for an activation type DCD in the one-group approximation is

$$i + \frac{1}{\lambda} \cdot \frac{di}{dt} = (f + \alpha) e \Sigma \Phi + \frac{\alpha \Sigma_e}{\lambda} \cdot \frac{d\Phi}{dt},$$

where i is the DCD current, λ is the decay constant of the β-active isotope responsible for the induced activity, t is the time, e is the charge of the electron, Φ is the neutron flux density, Σ is the macroscopic activation cross section, f is a factor taking account of the perturbation of the characteristics of the neutron distribution introduced by the detector and the decrease in current due to the incomplete utilization of β particles as a consequence of their absorption in the emitter and the insulator, and α is an analogous factor for Compton electrons and photoelectrons.

The basic DCD equation relates the detector current to the neutron flux, and permits the determination of the neutron flux in a nonstationary regime, as was shown experimentally in [2].

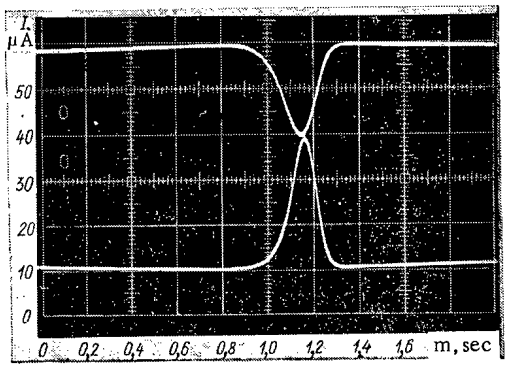

Fig. 1

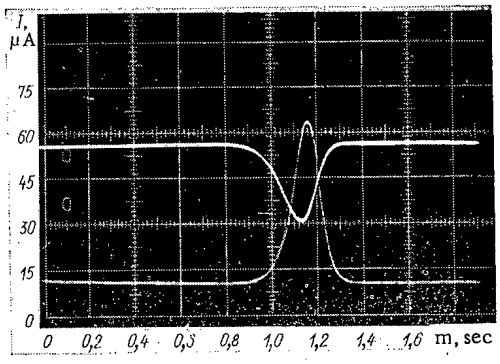

Fig. 2

Fig. 1. Oscillogram of response of a rhodium detector compared with recording of pulse by a regular instrument with an organic scintillator.

Fig. 2. Oscillogram of response of a gadolinium detector compared with recording of pulse by a regular instrument with an organic scintillator.

Translated from Atomnaya Énergiya, Vol. 36, No. 3, pp. 217-219, March, 1974. Original article submitted November 16, 1972.

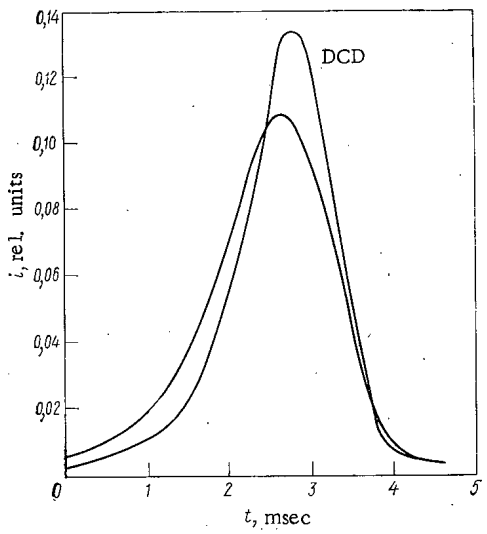

Fig. 3

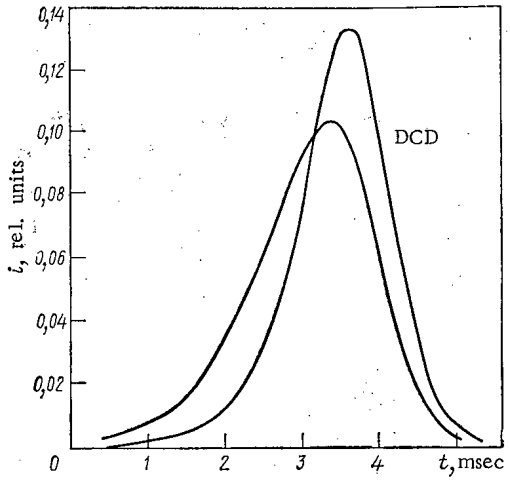

Fig. 4

Fig. 3. Experimental data normalized to the integrated responses of a rhodium DCD and a regular instrument.

Fig. 4. Experimental data normalized to the integrated responses of a gadolinium DCD and a regular instrument.

TABLE 1. Upper Limit of Pulse Duration for the Use of an Activation DCD in the Inertialess Regime

Emitter	t, sec	Emitter	t, sec
V	0,2	Gd	—
Co	10^7	Ta	10^5
Rh	0,04	W	10^3
Ag	0,02		

It is easy to show that for sufficiently short pulses the contribution of activation currents to the total DCD current can be neglected, and any DCD can be regarded as a Compton type which is inertialess with respect to the basic current generating process. The effect of the activation current can be neglected when $t \ll \alpha/\lambda f$. Table 1 lists values of t calculated under the assumption that the contribution of the activation current does not exceed 1% of the Compton current.

Figures 1 and 2 show oscillograms of the responses of rhodium and gadolinium detectors. These figures also show the pulse recorded by a regular instrument with an organic scintillator. The recording instrument was a type S-1-18 oscilloscope with a shunted input (l = 1 kΩ) ensuring a time constant of 10^{-6} sec. The traces were photographed with a "Zenith" type camera. It is clear from the oscillograms that there is good agreement between the DCD response and that of the regular instrument.

Figures 3 and 4 show experimental data normalized to the value of $\int i dt$, where i is the response of the DCD or the regular instrument. The build up of the neutron flux pulse front as measured by the DCD clearly lags that recorded by the regular instrument. The pulse width at half maximum is 0.2 msec less for the DCD than for the regular instrument. At the same time the shapes of the neutron pulse recorded by the rhodium and gadolinium DCD's practically coincide as can be seen from Fig. 5 where the curves are superposed and normalized at the maximum reading.

In discussing the experimental data it should be taken into account that the counting efficiency of organic scintillators is considerably higher for gamma rays than for neutrons [3]. The experimentally observed differences in the readings of the DCD's and regular instruments are explained by the kinetics of neutron transmission through the detector region, and are determined by the neutron slowing down time and the time of transmission to the detector.

Thermal neutrons propagate much more slowly than gamma rays. Only fast neutrons contribute initially to the rise of the pulse front in the detector response. As slower neutrons reach the detector its response shows contribution from neutrons of a broader range of energies. The cross section for the absorption of neutrons by the emitter material increases with decreasing neutron energy. Hence it follows that there is a lag in the build up of the front of the DCD response curve in comparison with the regular instrument, and also a sharper rise.

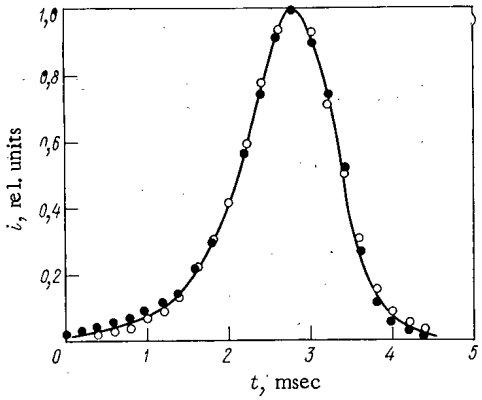

Fig. 5

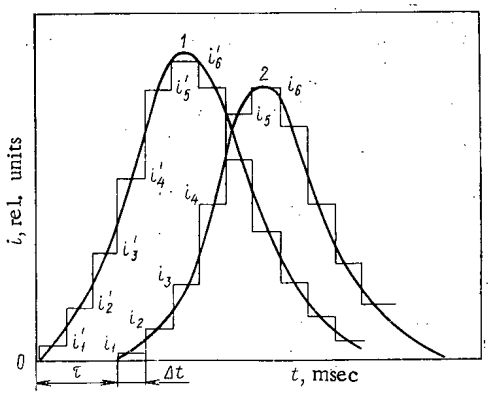

Fig. 6

Fig. 5. Recordings of neutron pulse by rhodium (●) and gadolinium (○) DCD's normalized at maximum.

Fig. 6. Recordings of neutron pulse by two identical DCD's a distance l apart.

A similar effect is noted for the fall-off of the pulse front when high-energy neutrons emerge from the detector region. This leads to a decrease in pulse width at half maximum.

The agreement of the shapes of the neutron flux pulses recorded by the rhodium (activation) and gadolinium (Compton) detectors 3 and 10 mm in diameter respectively shows that the contribution of reactor gamma radiation is small.

The rhodium and gadolinium emitters differ in size, specific gravity, and neutron sensitivity (by 50%). As indicated above the pulse shape recorded by a gamma- and neutron-sensitive detector is different.

Hence if reactor gamma rays contribute appreciably to the DCD response the pulse shapes obtained with rhodium and gadolinium detectors should be different. Since the shapes do not differ, reactor gamma rays make a small contribution to the DCD response.

The neutron flux spectrum in pulsed processes can be measured with direct charge detectors. Identical detectors 1 and 2 are placed a distance l apart in the direction of neutron propagation. As a result of the finite neutron velocities and their spectrum the pulse curves recorded by detectors 1 and 2 (Fig. 6) are displaced with respect to one another. Assuming that the neutron spectrum in the vicinity of detector 1 does not change with time, and replacing the smooth curve by a step function we have

$$i_1 = \varphi(E_1)\,\Phi(E_1);$$

$$i_2 = \frac{i_2'}{i_1'}\varphi(E_1)\,\Phi(E_1) + \varphi(E_2)\,\Phi(E_2);$$

$$i_3 = \frac{i_3'}{i_1'}\varphi(E_1)\,\Phi(E_1) + \frac{i_3'}{i_2'}\varphi(E_2)\,\Phi(E_2) + \varphi(E_3)\,\Phi(E_3);$$

$$i_n = \frac{i_n'}{i_1'}\varphi(E_1)\,\Phi(E_1) + \frac{i_n'}{i_1'}\varphi(E_2)\,\Phi(E_2) + \ldots + \varphi(E_n)\,\Phi(E_n),$$

where

$$E_1 = \frac{m}{2}\left(\frac{l}{\tau}\right)^2;\quad E_2 = \frac{m}{2}\left(\frac{l}{\tau+\Delta t}\right)^2;$$

$$E_n = \frac{m}{2}\left[\frac{l}{\tau+\Delta t\,(n-1)}\right]^2$$

and m is the mass of a neutron. We solve the n equations in n unknowns for $\Phi(E_1)$, $\Phi(E_2)$, . . . , $\Phi(E_n)$ and thus regenerate the spectrum at detector 2.

LITERATURE CITED

1. H. Bock, M. Stimler, and O. Strindehag, Nucl. Instrum. and Methods, 87, 299 (1970).
2. M. G. Mitel'man et al., Metrology of Neutron Radiation at Reactors and Accelerators [in Russian], Vol. 2, Standarty, Moscow (1972).
3. V. I. Kalashnikova and N. S. Kozodaev, Elementary Particle Detectors [in Russian], Atomizdat, Moscow (1966).

IMPROVING THERMAL INSULATION IN TOKAMAK TO-1 DURING PULSED DISPLACEMENT OF PLASMA FILAMENT

L. I. Artemenkov, P. I. Kozlov, P. I. Melikhov, and L. N. Papkov

UDC 621.039.62.12/.13

Three discharge stages are observed in Tokamak TO-1 [1]: macrounstable, "free" movement, and stage of contact with diaphragm. In the second stage, the filament is macroscopically stable, interacts weakly with the diaphragm, and is displaced towards the outside of the chamber. Meanwhile, the plasma conductivity and thermal energy, determined from the diamagnetic effect, increase. In the third stage, energy losses from the plasma increase due to contact with the diaphragm. The present paper describes experiments on improving plasma parameters by increasing the filament "free" movement time.

External control of the automatic-regulating system was used for our purposes. This system [2] consists of four independent circuits of the same type: a regulator (two-pole) and a control-winding section connected to it.

Short (several millisecond) voltage pulses can be delivered to the external regulator input — these pulses cause a current change, proportional to the input-pulse integral, in the regulator—winding section circuit. By varying the input-pulse parameters and the number of regulators to which these pulses are delivered, one can vary over a wide range the magnitude and direction of the pulsed effect on the plasma filament.

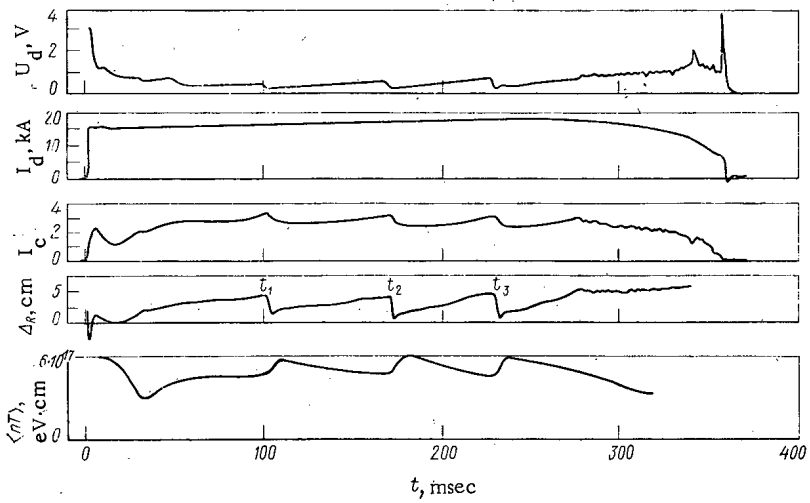

Fig. 1. Oscillograms of voltage U_d, discharge current I_d, and ampere-turns of control winding I_c. Dependence of filament displacement Δ_R and plasma thermal energy $\langle nT \rangle$, reduced to unit length plasma filament, on time.

Translated from Atomnaya Énergiya, Vol. 36, No. 3, pp. 219-220, March, 1974. Original article submitted August 10, 1973.

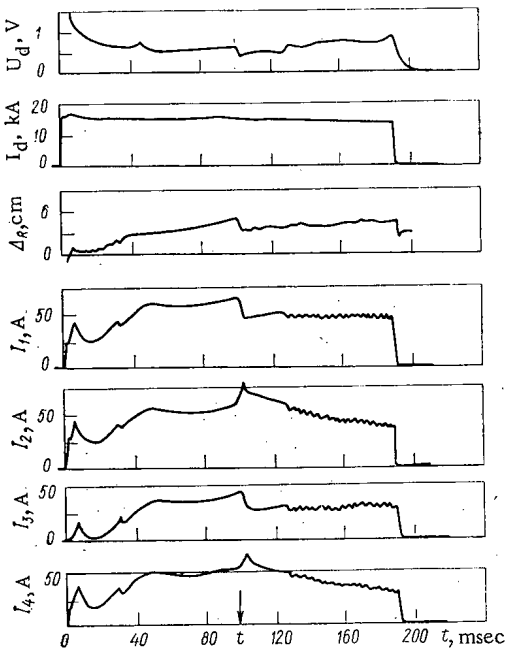

Fig. 2. Oscillograms of voltage U_d, discharge current I_d, and regulator currents I_i ($i = 1, 2, 3, 4$). Dependence of Δ_R on time.

Figure 1 shows experimental oscillograms where at instants t_1, t_2, and t_3 voltage pulses 2 msec in duration were simultaneously delivered to the external inputs of all regulators. It is clear that during the pulsed effect the filament is displaced towards decreasing the large radius R, while its conductivity and thermal energy increase. Evaluations showed that the energetic lifetime increases by a factor of 2-3. Adiabatic ion heating in the case considered is small [3] and does not exceed several percent of the initial value of $\langle nT \rangle$. After the pulse, the filament slowly returns to the initial position.

In the case (see Fig. 2), where at the instant t the voltage pulses are delivered to regulators Nos. 2 and 4 diametrically opposite to the control-winding sections, the current in these circuits increases, while in two other cases it decreases. Magnetic probes placed near the third section show (curve Δ_R) that the filament as a whole undergoes pulsed displacement towards decreasing R (the displacement is independent of the azimuthal angle with respect to the large torus circuit). The filament conductivity increases somewhat. In experiments which delivered voltage pulses to only one regulator, the plasma filament as a whole also was displaced towards the inside.

The dependence obtained in the present work between the filament — displacement increment and the total voltage supplied to the regulators is, within the limits of variation of 4 cm displacement, close to linear. This result arises from analyzing the balance of forces acting on the filament, assuming that the filament is displaced along R as a whole and the displacement velocity is much lower than drift velocity. The latter condition, which allows one to ignore the inertia term [4] is met in this case.

It is interesting to note that after the pulsed displacement of the filament inward (see Fig. 1) the sum of currents in the control-winding sections is lower than the sum of currents before the pulsed effect. This apparently is explained by increased attractive force of the filament for the magnetic conductor; this is great and can reach 70% of the electrodynamic repulsive force. Since in the balance of forces acting on the filament the contribution from the gas-kinetic pressure is small in these experiments, the average force produced by all regulators and, consequently, the sum of their currents, must decrease.

The experiments described are evidence of the possibility that filament equilibrium can be maintained at significantly greater distances between control-winding sections or even with the use of one section. Clearly, for such systems, one needs more powerful regulators with large amplification factors.

The authors thank the technical workers operating the TO-1, headed by A. P. Sabadashev, and also V. V. Arsenin for helpful discussions.

LITERATURE CITED

1. L. I. Artemenkov et al., Zh. Éksperim. i Tekh. Fiz., Pis. Red., 17, 251 (1973).
2. L. I. Artemenkov et al., Papers from the IV International Conference of the International Atomic Energy Agency on Plasma Physics and Controlled Thermonuclear Synthesis, Vienna, 1971, Report C-28/C-3.
3. K. Bol et al., Phys. Rev. Letters, 29, 1495 (1972).
4. L. A. Artsimovich, Closed Plasma Configurations [in Russian], Nauka, Moscow (1969), p. 63.

DIRECT ION ENERGY CONVERSION IN OPEN MAGNETIC TRAPS

O. A. Vinogradova, S. K. Dimitrov,
A. M. Zhitlukhin, A. S. Luts'ko,
V. M. Smirnov, and V. G. Tel'kovskii

UDC 621.039.6

The parameters of a beam at the expander exit in the recuperation system of an open type thermonuclear reactor [1] must satisfy the following constraints. Divergence angle of the particles:

$$\theta = \sqrt{\frac{W_{\perp y}}{W}} < 0.04, \tag{1}$$

where $W_{\perp y}$ is the fraction of transverse energy associated with the particles yielding the beam divergence in the collector; W is the energy associated with the ions; θ is a ratio characterizing the amount of volume charge,

$$\frac{D}{r_{di}} < 0.2, \tag{2}$$

where D is the height of the expander at the exit; $r_{di} = 0.088\ W^{3/4}\,[\text{keV}]/\sqrt{j_i\,[\text{A/cm}^2]\,Z\sqrt{A}}$ is the Debye radius of the ions, in cm; j_i is the current density of the ions; A and Z are the mass number and the multiplicity of the charge on the ions;

$$\frac{W_{\perp z}}{W} = \left(\frac{D}{r_{Li}}\right)^2 < 0.04,$$

where $W_{\perp z}$ is the portion of the energy going over into transverse energy because of the nonadiabatic discontinuity at the end of the expander;

$$\frac{W_{\perp}}{W} = \frac{W_{\perp z} + W_{\perp y}}{W} < 0.08;$$

$r_{Le}/D = vmc/eHD \ll 1$ is the condition for escape of electrons from the beam; $r_{Li}/D = vMc/eHD \gg 1$ is the condition for emergence of ions via the magnetic field, where r_{Le} and r_{Li}, m and M are the respective Larmor radius and mass of the electrons and ions respectively; v is the velocity of the particles; c is the speed of light; e is the charge on the electron; H is the magnetic field at the expander exit.

The most stringent restrictions on the expander dimensions (radius R, height D, turning angle φ) are imposed by constraints (1) and (2), from which we infer

$$D \geqslant \frac{S_0}{R\theta^2\varphi}; \qquad D \leqslant \frac{(0.088)^2 W^{3/2}\varphi R \left(\frac{D}{r_{di}}\right)^2}{I_0\sqrt{A}\,Z}, \tag{3}$$

where I_0 is the ion current from the magnetic mirror; S_0 is the area presented by the mirror. We find from inequalities (3) the minimum expander radius for Z = 1 ions:

$$R^2_{\min} = \frac{S_0 I_0 \sqrt{A}}{(0.088)^2 \varphi^2 W^{3/2} \left(\frac{D}{r_{di}}\right)^2 \theta^2} \tag{4}$$

and expander height

Translated from Atomnaya Énergiya, Vol. 36, No. 3, pp. 221-222, March, 1974. Original article submitted May 31, 1973.

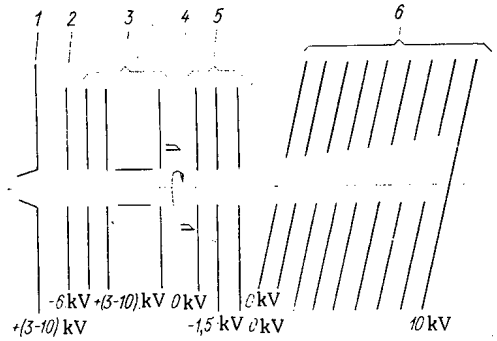

Fig. 1

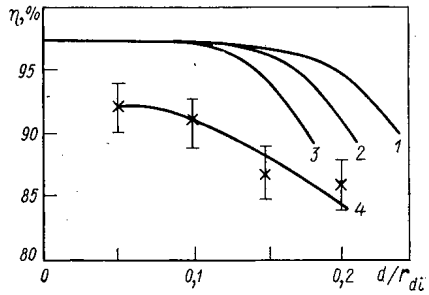

Fig. 2

Fig. 1. Diagram of experimental arrangement; 1) ion source; 2) accelerating lens; 3) focusing lens; 4) rotating Faraday cups; 5) diaphragms for removing electrons from beam; 6) system of skewed diaphragms (stops).

Fig. 2. Dependence of recuperation efficiency η on volume charge: 1, 2, 3) recuperation efficiency obtained by computer for SDS such that $\varepsilon = 2\tan^2\alpha = 0.05$ for particles of energy W = 10 keV, and accuracy of focusing interval δ L respectively 0, 0.1 L, 0.2 L; 4) average recuperation efficiency as determined experimentally.

$$D^2 = \frac{(0.088)^2 S_0 W^{3/2} \left(\frac{D}{r_{di}}\right)^2}{\sqrt{A}\, I_0 \theta^2}. \tag{5}$$

For the parameters of the reactor [2], we have W = 100 keV, I_0 = 1800 A, S_0 = 0.67 m^2, A = 2 when $D/r_{di} = 0.2$, $\theta = 0.04$, and $\varphi = \pi$ from which we get R ≈ 600 m, D ≈ 0.25 m. The radius R can be reduced by separating the stream emerging from the mirrors into layers. Then the formula for the R_{min} of an expander consisting of k layers will present the form

$$(R_{\min}{}^k)^2 = \frac{S_0 I_0 \sqrt{A}}{(0.088)^2 \varphi^2 W^{3/2} \left(\frac{D}{r_{di}}\right)^2 \theta^2}. \tag{6}$$

Here the height of each layer comprising the expander undergoes no change [cf. Eq. (5)]. Consequently, we obtain R ≈ 60 m when we increase the number of layers to ten.

Computer calculations of the energy recuperation efficiency for a high-density beam of ions η [3] in a system of skewed diaphragms (SDS) shows that the SDS can bring about a high conversion efficiency ($\eta \geq 0.9$) at $\theta \leq 0.04$, and $D/r_{di} \leq 0.2$ with prefocusing of the beam.

Experiments on recuperation of the energy associated with high-density ion beams were staged on an arrangement shown in Fig. 1. The ion beam from a duoplasmatron type source arrived, after acceleration to the appropriate energy by lenses, at the focusing lens and passed from there into the deceleration system. The diaphragm stops in the system are for removing electrons from the beam. The convergence angle, the beam density, and the beam intensity at the entrance to the deceleration system were measured with the aid of rotating Faraday cups. In a system of 26 stops, total length L ≈ 170 mm, the angle of inclination of the collector stops $\alpha = 8°46'$, the beam diameter at the entrance to the decelerator device d = 0.8 cm.

The efficiency η was determined experimentally in the 3-10 keV range of energies for the d/r_{di} ratio equal to 0.05, 0.1, 0.15, 0.26 in the circular-beam case (corresponding then to the ratio D/r_{di} = 0.35, 0.071, 0.11, and 0.14 respectively in the flat-beam case).

Figure 2 displays the dependence of the mean recuperation efficiency on volume charge, which is characterized by the ratio d/r_{di}. When the ratio $d/r_{di} = 0.2$, the efficiency drops by several percent, to 85-86%; when $d/r_{di} = 0.25$ (for 0.18 for the flat beam) and W = 5 keV, we have 85%. The beam was focused on the end of the deceleration length [3]. In the high-density case, with imprecise focusing, η drops by 10%; in the case of a sharply defined beam the focusing conditions are less critical. We realize from the experimental data that the number of collectors can be increased, emission electrons can be removed with the aid of the transverse magnetic field, and a large-angle (α) SDS can be employed, to bring the efficiency to 90-93% for Post "reactor conditions" ($D/r_{di} = 0.18$) [1].

If we establish a magnetic field H perpendicular to the electric field E in the SDS system, then the volume ion charge can be offset by streams of electrons moving on the equipotential drift trajectories. The electrons can be emitted from collector-diaphragms (secondary emission), but also from special emitters placed at appropriate potentials. When compensation is complete, the required electron current density $j_e \approx v_{dr} j_i/v$, where v_{dr} is the drift velocity. When H is directed transverse to the recuperator slit, then the trajectories of the ions become extended along the entire expander arc, and the emission current j_e is then minimized. In that case, however, compensation conditions become unstable, since the electrons leave the drift trajectories at negative pulsations of ion density to impinge on the diaphragms along the lines of force of the field H. When H is parallel to the expander slit, the electrons drift from one edge of the diaphragm to the other. The total emission current is about $\pi R/D$ times greater in this case, but the compensation conditions are stable. We then determine the dimensions of the SDS and the efficiency η for the latter case. In the case of trajectories extended along E, we have the valid constraint

$$\varepsilon_1 = \frac{W_1}{W} = \frac{\lambda}{F} \quad \text{for } \varepsilon_1 < 0.1, \tag{7}$$

where λ is the deceleration length; W_1 is the ion energy at the peak of the trajectory; ε_1 is the loss of efficiency due to the unrecuperated fraction of energy W_1; $F = 2Ec^2M/eH^2Z$ is the characteristic dimension of the ion cycloid.

$$\varepsilon_2 = \frac{m}{M} \cdot \frac{\varkappa}{2} \sqrt{\frac{F}{\lambda}} \cdot \frac{F}{D}, \tag{8}$$

where ε_2 is the fraction of the total power available for accelerating the compensating electrons; $\varkappa$ is the portion of the characteristic dimension of the electron cycloid on which the electrons pick up energy to be converted subsequently to heat ($\varkappa \leq 1$). If the electron current and ion current are not to distort the applied magnetic field, we require the constraints

$$\frac{\lambda F}{2} \ll L_i^2, \quad L_i^2 \equiv \frac{Mc^2}{4\pi e^2 Z^2 n} \tag{9}$$

(where n is the ion density), or

$$\left(\frac{D}{r_{di}}\right)^2 \ll \frac{Dc^2M}{FW} \frac{D}{\lambda}. \tag{10}$$

It is evident from formulas (7)-(9) that H must be decreased to keep ε_1 small, while H must be increased in contrast in order to keep ε_2 small and in order to minimize the effect of the intrinsic magnetic fields of the plasma. That requires minimizing the total losses $\varepsilon_1 + \varepsilon_2 + \varepsilon_3$, where ε_3 is the loss dependent upon the angle θ and the beam width D.

Computer calculations showed that at divergence $\theta = \pm 0.05$, $D/F = 0.005$, $D/\lambda = 0.1$, and $\alpha = 0$ or $\alpha = -0.45$, we can obtain $\varepsilon_1 + \varepsilon_3 \leq 0.1$. These conditions correspond to the ratios $j_i/j_e = v/v_{dr} \approx 0.45$, $(D/r_{di})^2 \ll A(500/W[keV])$, i.e., $D/r_{di} \approx 1$ for A = 2 and W = 100 keV is permissible. Losses $\varepsilon_2 \approx \varkappa/4A$, i.e., at A = 2, and $\varepsilon_2 \approx 0.01$ require that $\varkappa = 1/12$. When $\alpha = 0$, the beam is compensated by electrons emitted by the diaphragms. When $\alpha = -0.45$, all of the compensating electrons must be emitted by special emitters.

LITERATURE CITED

1. R. Post, Nucl. Fusion Reactor Conf. Proc., UKAEA (1970), p. 88.
2. I. Golovin et al., Nucl. Fusion Reactor Conf. Proc., UKAEA (1970), p. 194.
3. O. A. Vinogradova et al., At. Énerg., 33, No. 6, 969 (1972).

GAMMA AUTORADIOGRAPHY IN GLASS

V. G. Polyukhov and V. Ya. Gabeskiriya

UDC 778.35

In autoradiographic studies of highly active objects, one ordinarily employs a special emulsion layer [1, 2], the use of which involves a number of difficulties under conditions where high radioactive contamination, high humidity, or corrosive vapors are present. Glass is the most convenient radiosensitive material for use under such conditions [3]. In the present autoradiographic study of ampules irradiated in the SM-2 reactor, ordinary showcase glass (All-Union State Standard 7380-55) 5.8 ± 0.3 mm thick was used in the form of strips 30 × 500 mm in size. The diameter of the active portion of the ampules was 10 mm with lengths up to 350 mm [4]. The studies were carried out in hot cells.

In experiments with ^{226}Ra and ^{60}Co sources, it was established that the dependence of the optical density ΔS of the glass on the γ-ray exposure dose D was of the form $\Delta S = KD$, where D is expressed in roentgens and $K = (1.6 \pm 0.3) \cdot 10^{-6}\ R^{-1}$. The linear dependence was maintained up to densities $\Delta S \geq 0.6$. Photometry of the glass was accomplished with an MF-4 microphotometer having a threshold sensitivity corresponding to $\Delta S \approx 5 \cdot 10^{-4}$. The variation in optical background because of nonuniformity of the glass along a strip was $\Delta S \approx 1 \cdot 10^{-3}$. If one takes as a measure of the threshold sensitivity of the method twice the magnitude of the variation in optical background, $\Delta S \approx 2 \cdot 10^{-3}$, it is clear the linear portion of the $\Delta S(D)$ relation corresponds to a range of γ-ray exposure doses covering $1.3 \cdot 10^{-3}$–$4 \cdot 10^{5}$ R.

According to Nadler [5], the resolution for autoradiography of a ^{60}Co source having an active portion 4 mm in diameter and 4 mm long in a capsule 6 mm in diameter and 7 mm long was respectively

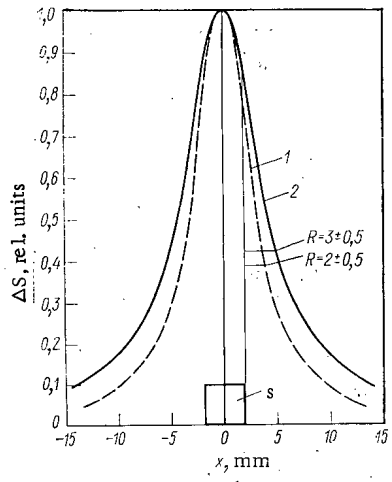

Fig. 1

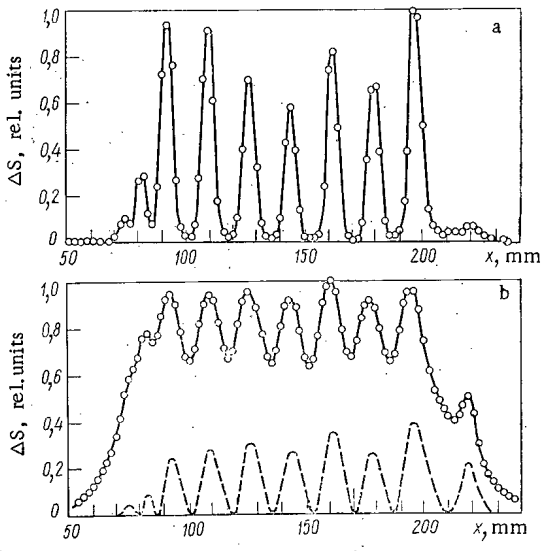

Fig. 2

Fig. 1. Comparative curves for distribution of optical density ΔS in autoradiography of a ^{60}Co source. 1) Photographic plate with a sensitivity of 6 All-Union State Standard units; 2) showcase glass; s) source.

Fig. 2. Distribution curves for γ-rays from ampules containing transuranic elements based on γ-autoradiographic data in glass.

Translated from Atomnaya Énergiya, Vol. 36, No. 3, pp. 223-224, March, 1974. Original article submitted August 15, 1973.

3.0 ± 0.5 and 2.0 ± 0.5 mm for showcase glass and an emulsion layer (Fig. 1).

Exposure of the glass in autoradiographic studies of ampules irradiated in the reactor was 10-30 min. Autoradiography of unirradiated ampules containing transuranic elements was carried out over a period of 20 h. In the latter case, an image appeared in the glass because of the intrinsic γ-radiation of transuranic elements.

Figure 2 shows curves for the relative γ-ray distributions in the same set of capsules filled with transuranic elements before and after irradiation in the reactor. Figure 2a shows the results of photometry of glass for autoradiography of unirradiated capsules placed in an aluminum container. Figure 2b shows the results for capsules loaded into a stainless steel ampule and irradiated in the reactor (the dashed curve was obtained after subtraction of a base line). The coordinates of the centers of the individual capsules agree with the design positions within ±2 mm. The base line in the curve for the distribution from the irradiated ampule (see Fig. 2b) resulted from reactor activation of the container material. During reloading from one ampule into the other, a small displacement of the capsules relative to their initial position was observed, which is clearly apparent from a comparison of the curves in Fig. 2a and 2b (see solid curves).

Advantages of autoradiography in glass are simplicity, availability of the material, ease of decontamination of glass when radioactive contamination occurs, and the capability for use under conditions of elevated humidity and corrosive environment. Deficiencies of the method are somewhat poorer resolution in comparison with an emulsion and fading of the image with time even when the glass is kept in the dark [3]. The greatest rate of fading in irradiated showcase glass was observed in the first 10 days (~15%). In approximately a month after irradiation, the optical density of the image decreased by 35%.

The method described was successfully used for remote cutting of ampules irradiated in the reactor during the process of preparing them for radiochemical experiments.

In conclusion, the authors express their gratitude to V. M. Barinov for help in photometry of the glass.

LITERATURE CITED

1. J. Boyd, Autoradiography in Biology and Medicine [Russian translation], Izd-vo Inostr. Lit., Moscow (1957).
2. N. Shassend-Barots, in: Compilation of Papers from the Symposium on Special Problems in Dosimetry (Vienna, 1960). Selected Reports of Foreign Scientists [Russian translation], Atomizdat, Moscow (1962), pp. 73-76.
3. G. V. Byurganovskaya et al., Effect of Radiation on Inorganic Glass [in Russian], Atomizdat, Moscow (1968).
4. V. A. Davidenko et al., At. Énerg., 33, 815 (1972).
5. A. Rogers, Autoradiography [Russian translation], Atomizdat, Moscow (1972).

ATMOSPHERIC PROPAGATION OF FAST NUCLEAR PARTICLES

V. S. Barashenkov, V. E. Sdobnov, and S. E. Chigrinov

UDC 539.12.17

The propagation of beams of high-energy particles in dense media has been calculated by the Monte-Carlo method [1, 2]. These calculations are based on the cascade-evaporation model for the interaction of fast particles with nuclei and make it possible to obtain flux densities, and energy and angular distributions of secondary particles in a block of material which agree with experimental values.

For practical purposes, however, it is important to know the propagation of fast-particle beams in extended gaseous media, and particularly the propagation of cosmic rays in the atmosphere of the Earth and other planets. This is needed for the solution of certain astrophysical problems, for the analysis of the structure of extensive atmospheric showers, for the evaluation of the radiation environment at great heights, and for calculating the radiation zones around high-current accelerators.

A program which makes it possible to calculate the propagation of nuclear particles in extended gaseous media by the Monte-Carlo method for particle energies from several tens of MeV to several hundred GeV was developed by the authors at the Laboratory for Nuclear Reactions at JINR. As in [1, 2], this program is based on the cascade-evaporation model for inelastic pion and nucleon—nucleus interactions. In this case, the effect resulting from the decrease in the number density of intranuclear nucleons is additionally taken into account in the course of development of the cascade shower, which is important at incident particle energies $T \geqslant 3$-5 GeV [3, 4]. The distribution of intranuclear nucleons is described by the Saxon—Woods formula without subdividing the nucleus into zones of constant density [5]. In the region of very high energies (more than several tens of GeV), the intranuclear cascades are calculated including the contribution from leader particles [6]. The decay of excited nuclei remaining after the cascade stage of the interaction process is calculated on the basis of the evaporation model. Although the conditions for the applicability of this model are not well satisfied for light nuclei, a comparison with the more exact "explosive" model of decay shows that with the correct choice of parameters characteristics of interest for secondary particles resulting from an inelastic nuclear interaction are reproduced with sufficient accuracy. This conclusion is also confirmed by comparison of calculated values with known experimental data for the group of light nuclei in photoemulsions (carbon, nitrogen, oxygen). For more detailed calculations (particularly for a study of the isotopes produced in the atmosphere, the yields of which are quite sensitive to the decay model), it is necessary to use more exact methods [7].

The phenomenological expression from [8] was used to calculate ionization losses of protons and $\pi^{\pm}$ mesons in the atmosphere. Since the ionization range of the heavy particles d, t, ^{3}He, and ^{4}He is considerably less than the nuclear range, the contribution from these particles is neglected. Protons which slow down to the "cutoff energy" $T_c = 15$ MeV are also considered to be removed from the cascade in the atmosphere and therefore their further propagation is not considered.

In the calculations, all π^+ mesons with energies $T \leq 2$ MeV are assumed to decay. The same assumption is also made for π^- mesons, which is completely valid because the atmospheric density is low and consequently the probability of nuclear absorption of a slow π^- meson is insignificant. At high energies, the competition between decay and nuclear interaction is developed in accordance with the relative values of the calculated ranges for decay and nuclear interaction (under the condition the kinetic energy of a pion at the end of the range is greater than the "cutoff energy"). All π^0 mesons not undergoing a

Translated from Atomnaya Énergiya, Vol. 36, No. 3, pp. 224-225, March, 1974. Original article submitted August 13, 1973.

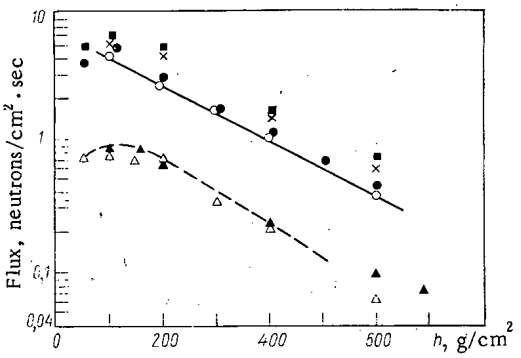

Fig. 1

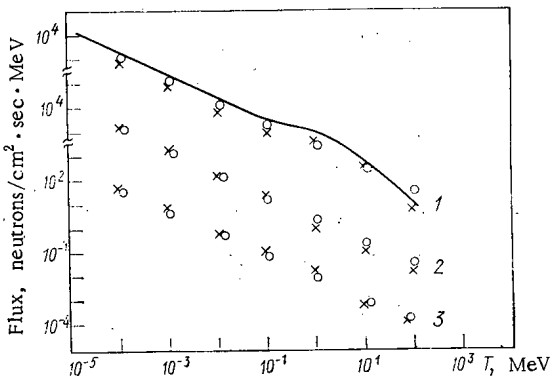

Fig. 2

Fig. 1. Neutron flux at various heights h at latitude 42°: ■) Calculated results for neutrons of all energies (present work); ×) corresponding theoretical data [16]; ●) calculated results for neutrons with energies 0-20 MeV (present work); ○) corresponding theoretical data [16]; ——) experiment [13]; ----) experimental data for neutrons with energies 1-10 MeV [14]; ▲) calculated results from this work; △) theoretical data [16].

Fig. 2. Neutron energy spectrum at various depths in the atmosphere: ○) calculated results from this work; ×) theoretical data [16]; the curve is for experimental data [15]. 1) 200 g/cm^2; 2) 400 g/cm^2; 3) 600 g/cm^2.

nuclear interaction during their lifetime in the laboratory system, $\tau = \tau_0(1-\beta^2)^{-1/2}$, are assumed to decay into two gamma rays.

The relative probability of elastic and inelastic particle interactions with a nucleus of a given type is developed in accordance with the corresponding cross sections σ_{el} and σ_{inel} taken from the monograph [9]. The elastic scattering angle is picked out in accordance with the expression [10]

$$d\sigma/d\Omega_{lab} = \sigma_0 \exp\left(-\frac{1}{3}p^2r^2\theta^2_{lab}/\hbar^2\right),$$

where σ_0 is a factor independent of θ_{lab}; p is the particle momentum; $r = Z^{1/3}\hbar/m_\pi c$; Z is the atomic number of the target. The behavior of neutrons with energies $T \leq 10.5$ MeV is described on the basis of the transport approximation in [11].

In order to illustrate the accuracy of the program, we consider the practically important case of the atmospheric propagation of primary cosmic radiation having a differential energy spectrum given by [12]

$$N(E) = \frac{0.048}{E^{2/3}(1+0.09E^{4/3})^{3/2}},$$

where E is energy (GeV), EN(E)dE is the energy (GeV/cm^2·sec·sr) carried to the Earth by protons in the energy range E to E + dE.

We assume that along the path of the primary radiation there is an infinite plane layer of air 1033 g/cm^2 thick consisting of oxygen (21%) and nitrogen (79%). The variation of pressure with height and temperature is given by the relations

$$P(h) = \begin{cases} P_0\left(\frac{t-\beta h}{t_0}\right)^{g/\alpha\beta}, & \text{if } h \leqslant 11 \text{ km}, t_0 = 288.155°\text{K}; \\ P_{11}\exp(-gh/\alpha t), & \text{if } h > 11 \text{ km}, t = 216.655°\text{K}, \end{cases}$$

where P_0 and P_{11} are the pressure at sea level and at 11 km; t_0 is the temperature at sea level; β is a coefficient characterizing the temperature gradient; g is the acceleration of gravity; $\alpha = 2.870 \cdot 10^{-6}$ ergs/g·deg is a constant associated with the choice of the system of units.

The calculations were carried out for the latitude $\lambda = 42°$, at which there are experimental data [13-15] and theoretical calculations [16]. The effect of the geomagnetic field was taken into account by particle selection with respect to energy and also with respect to polar and azimuthal angles. In this case, the cutoff energy is given in the form

$$E_\lambda(\theta) = mc^2\left(\sqrt{1+[ZP_\lambda(\theta)/mc^2]^2}-1\right),$$

where the cutoff rigidity for the dipole representation of the geomagnetic field is

$$P_\lambda(0) = 59.6\, Z \cos^4\lambda\, [1+\sqrt{1-\sin\varphi\cos\theta\cos^3\lambda}]^{-2}\ \text{GeV/c}.$$

Here, mc^2 is the mass of a cosmic particle of charge Z; λ is the geomagnetic latitude; θ and φ are the polar and azimuthal angles characterizing the particle direction.

Calculated neutron fluxes and also experimental data and calculated results from Oak Ridge are shown in Figs. 1 and 2. It is clear the present results are close to the experimental results and the theoretical data in [16].

It should be pointed out that in addition to protons, cosmic radiation contains about 6% of α-particles and a small admixture of heavy nuclei (about 1%). The contribution of this component can be taken into account if in picking out the characteristics of the secondary particles one uses the method for calculating inelastic nucleus—nucleus interactions proposed in [4, 17]; however, the contribution from α-particles and heavier nuclei is small, which agrees with the results in [16] where this problem was studied in detail.

LITERATURE CITED

1. V. S. Barashenkov et al., At. Énerg., 32, 123 (1972).
2. V. S. Barashenkov, N. M. Sobolevskii, and V. D. Toneev, Geokhimiya, 11, 1325 (1972).
3. V. S. Barashenkov, A. S. Il'inov, and V. D. Toneev, Yad. Fiz., 13, 743 (1971).
4. V. S. Barashenkov et al., Yad. Fiz., 17, 434 (1973).
5. V. S. Barashenkov et al., JINR P2-6503, Dubna (1972).
6. V. S. Barashenkov et al., JINR Report P2-6022, Dubna (1971); in: Quantum Theory of Many-Particle Systems [in Russian], Kishinev (1973), p. 83.
7. O. B. Abdinov and V. S. Barashenkov, Acta Physica Polonica, B3, 385 (1972).
8. I. K. Vzorov, JINR P1-4442, Dubna (1969).
9. V. S. Barashenkov and V. D. Toneev, Interaction of High-Energy Particles and Nuclei with Nuclei [in Russian], Atomizdat, Moscow (1973).
10. J. Geibel and J. Ranft, Nucl. Instrum. and Methods, 32, 65 (1965).
11. L. P. Abagyan et al., Group Constants for Reactor Calculations [in Russian], Atomizdat, Moscow (1964).
12. H. Neher, in: Primary Cosmic Radiation [Russian translation], Izd. Inostr. Lit., Moscow (1956), p. 79.
13. G. Boella et al., Nuovo Cimento, 29, 103 (1963).
14. S. J. Holt, Geophys. Res. 71, 5109 (1966).
15. W. Hess et al., Phys. Rev., 116, 445 (1959).
16. T. Armstrong et al., ORNL-TM-3961, Oak Ridge (1972).
17. V. S. Barashenkov et al., JINR E2-6706, Dubna (1972).

^{90}Sr AND ^{137}Cs CONTENT IN SOIL, GRAIN, FODDER, AND MILK FOR 1963-1971

Sh. Chupka and M. Petrashova

UDC 631.41:546+637.16:546

Radioactive isotopes of strontium and cesium enter the body through inhalation of aerosols in the atmosphere, but they are mainly taken in with foodstuffs. Milk is one of the main food products. The intake of ^{90}Sr with dairy products is 19%, and of ^{137}Cs 13%, of the total amount contained in food; the intake of ^{90}Sr and ^{137}Cs with farinaceous product reaches 50-60% in Czechoslovakia [1, 2].

Because of differences in the physical and chemical properties of ^{90}Sr and ^{137}Cs, they are accumulated differently in the body. ^{90}Sr mainly forms irreversible compounds in bone tissue and the skeleton is the critical organ. ^{137}Cs is predominantly stored in soft tissues and the critical organ for it is the entire body. Because the effective half-lives of these two isotopes are different (for ^{90}Sr, ~17.5 yr; for ^{137}Cs, ~70 d), their maximum permissible amounts in the body are 20 mCi for ^{90}Sr and 30 μCi for ^{137}Cs [3, 4].

Samples for the determination of ^{90}Sr and ^{137}Cs in the food chain were collected in the area around the atomic power station at Yaslova Bogunits before it was put into operation according to the following schedule: atmospheric fallout and milk were analyzed monthly at two sample collection points; alfalfa, twice a year (after the first and second mowing); wheat, once a year (after harvesting); soil, twice a year (in May and July) at four locations. After radiochemical analysis, the content of ^{90}Sr and ^{137}Cs was determined from ^{90}Y and ^{137}Cs β-activity.

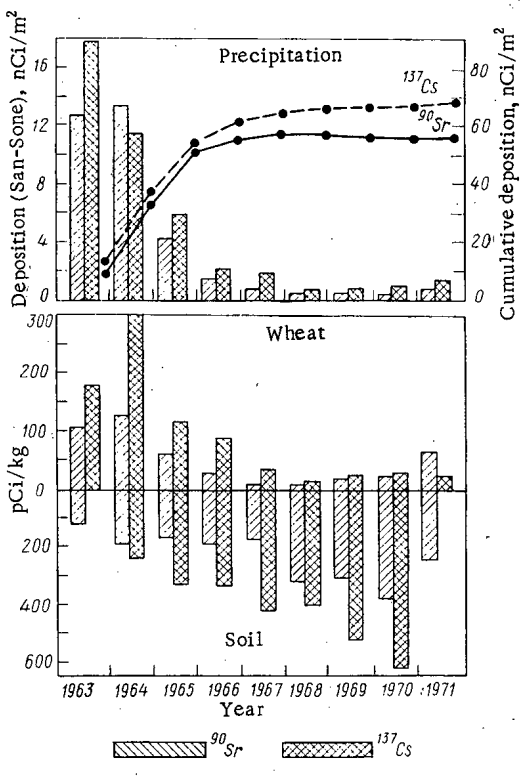

Fig. 1. ^{90}Sr and ^{137}Cs content in precipitation, wheat, and soil.

The average ^{90}Sr and ^{137}Cs content in precipitation, soil, and wheat is shown in Fig. 1. The radioactive isotopes promote the formation of condensation centers which determines a certain interrelation between radioactive fallout and precipitation. In turn, precipitation influences the sorption of the radioactive isotopes by the soil where a transition of ions from an unstable binding to a stronger binding occurs. In that case, the isotopes become less available to the root systems of plants. A close relationship is observed between cumulative fallout and the total concentration of radioactive isotopes in the soil and also between their deposition over a six-months period and their content in grains of wheat [5]. Since 1967, the rate of reduction of ^{137}Cs in grain has been greater than the rate of reduction of ^{90}Sr, and since 1971, the amount of ^{90}Sr exceeds the ^{137}Cs content. This indicates that the soil component is beginning to dominate in the contamination of grain and the plant extracts from the soil predominantly ^{90}Sr, which forms a weaker binding than ^{137}Cs with the soil complex.

A similar conclusion can also be reached for alfalfa, which is a component of fodder for dairy cattle. In comparison with wheat, alfalfa is more subject to direct contamination. The soil noticeably predominates in the contamination of alfalfa.

Regional Health Station, Bratislava, Czechoslovakia. Translated from Atomnaya Énergiya, Vol. 36, No. 3, pp. 226-227, March, 1974. Original article submitted April 11, 1973.

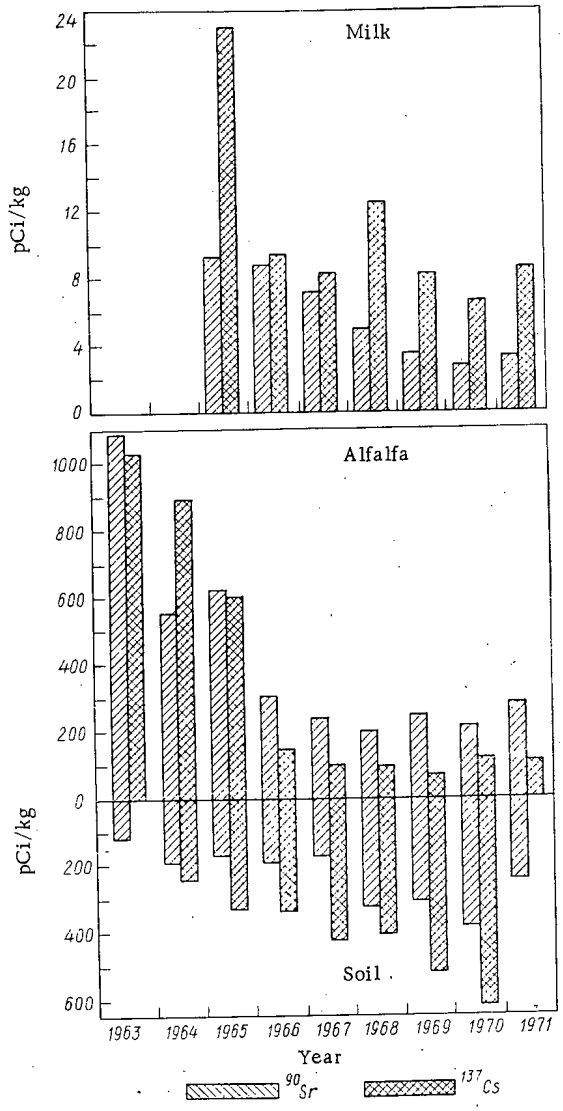

Fig. 2. ^{90}Sr and ^{137}Cs content in soil, alfalfa, and milk.

TABLE 1. Correlation Coefficients for Particular Environmental Elements

Element	^{90}Sr	^{137}Cs
Soil-precipitation	-0,636	-0,638
Wheat-precipitation	+0,904	+0,796
Alfalfa-precipitation	+0,875	+0,956
Wheat-soil	-0,502	-0,673
average value 1963-1971		
period of greatest fallout (up to 1965)	-0,214	-0,969
period of lowest fallout (after 1965)	+0,163	+0,051
Alfalfa-soil	-0,707	-0,627
average value 1963-1971		
period of greatest fallout (up to 1965)	-0,980	-0,746
period of lowest fallout (after 1965)	+0,222	-0,409
Alfalfa-milk	+0,664	+0,940

TABLE 2. Soil Contribution to the Contamination of Wheat and Alfalfa, %

Year	^{90}Sr		^{137}Cs	
	wheat	alfalfa	wheat	alfalfa
1963	6,7	12,6	20,0	6,0
1964	12,2	5,1	38,8	33,0
1965	34,6	40,4	80,3	46,7
1966	62,0	71,3	87,2	28,2
1967	84,7	89,2	78,8	35,7
1968	79,6	81,8	85,9	64,2
1969	81,2	86,7	82,8	48,5
1970	84,9	88,4	76,4	68,9
1971	71,5	79,8	68,6	40,1

The ratio of ^{90}Sr and ^{137}Cs content in milk differs from the ratio in alfalfa. This is explained by the fact that radiocesium is accumulated to a greater extent than radiostrontium in animals (Fig. 2).

On the basis of our measurements, the ratio of ^{137}Cs and ^{90}Sr content in particular areas of the environment and in milk was calculated for 1963-1971. These values are very close to the $^{137}Cs/^{90}Sr$ ratio in precipitation, which is 1.6. The lowest ratio (0.8) was found in alfalfa; it was 1.7 in soil, 1.8 in wheat, and 2.1 in milk.

The relationship between the relative isotopic content in contiguous elements of the environment is characterized by a correlation coefficient (Table 1). The transfer between two elements is greater the closer the correlation coefficient is to one. The results obtained indicate a relatively good possibility of transfer.

The overall reduction in ^{90}Sr and ^{137}Cs content in precipitation is responsible for the reduction in the content of these isotopes in all elements of the biological chain except for soil. A gradual accumulation of ^{90}Sr and ^{137}Cs in soil is typical, as a consequence of which their concentration is increasing moderately at the present time. If one compares the period of greatest radioactive fallout, which continued to the end of 1965 and the period in which the radioactivity of atmospheric fallout reached its lowest values (1965-1971), relatively different correlation coefficients are obtained. The correlation coefficients in the first period are negative. They indicate that in radioactive contamination of wheat and alfalfa the effect of radioactive fallout dominates over the component extracted from the soil. In the second period, the correlation coefficients are low. The positive values of the coefficients (except the correlation coefficient

relative to ^{137}Cs for the element alfalfa-soil) point to the predominance of soil action in the contamination of wheat and alfalfa.

The role of soil in the contamination of wheat and alfalfa is shown in Table 2. The results, which were obtained by regression analysis, demonstrate that in the period of reduction in radioactivity of precipitation, the soil contribution increased. In alfalfa, however, direct contamination by radioactive cesium in precipitation predominates over the intake of the isotope from the soil.

Thus there is an interrelation between the radioactive content in particular elements of the environment which makes it possible to predict the future level of contamination of food products.

LITERATURE CITED

1. Sh. Chupka, J. Carach, and M. Petrashova, Bratisl. Lek. Listy, 47, No. 11, 641 (1967).
2. J. Carach et al., Lek. Obzor, 19, No. 5, 229 (1970).
3. Recommendations of ICRP, Publ. 10, Pergamon Press, London (1968).
4. Radiation Protection, Recommendations of ICRP, Publ. 2, Translated from the English, Gosatomizdat, Moscow (1961).
5. Sh. Chupka, M. Petrashova, and I. Tsarakh, Gigiena i Sanitariya, No. 34, 75 (1969).

AGREEMENT ON SETTING UP THE INTERATOMENERGO INTERNATIONAL ECONOMIC ASSOCIATION

V. A. Kiselev

An agreement on setting up a body to be known as the International Economic Association on the organization of cooperation in production, deliveries of equipment, and rendering of technical assistance in building nuclear power stations, or Interatomenergo for short, was reached on December 13, 1973, between representatives of Bulgaria, Hungary, the GDR, Poland, Rumania, the USSR, Czechoslovakia, and Yugoslovia. Interatomenergo offices will be located in Moscow.

Interatomenergo activities will be directed primarily toward implementing appropriate measures in the integrated program of further deepening and improving of collaboration and development of the socialist economic integration of COMECON member-nations, and also toward the development of such collaboration between COMECON member-nations and Yugoslavia.

The basic problems to be tackled by the Interatomenergo association will be:

development of budgets of demands and production in equipment, instruments, and materials for nuclear power stations;

preparation of proposals on specialization and cooperation in production, and also on expanding the volume of production of equipment, instruments and materials for nuclear power stations by the respective industries of the contracting nations;

organization of cooperation in the production of equipment, instruments, and materials for nuclear power stations;

development of proposals on joint planning of the production of particular types of equipment, instruments, and materials for nuclear power stations;

bringing about deliveries and shipment of equipment, instruments and materials, and spare parts for nuclear power stations by the industries of the contracting nations;

making sure the necessary design and planning documentation is provided by enterprises responsible for the manufacture of the equipment, instruments, and materials;

organization of cooperation in the production and delivery of spare parts for nuclear power station equipment;

carrying out the various types of starting and adjustment work needed at nuclear power stations under construction;

production and technical training and preparation of cadres of personnel to run nuclear power stations, specialized cadres for design of nuclear power stations, and for the production and installation of power station equipment;

carrying out work on maintenance and repair of specific types of nuclear power station equipment and instrumentation;

providing the necessary technical assistance in building nuclear power stations in the territories of the contracting nations and third parties.

Translated from Atomnaya Énergiya, Vol. 36, No. 3, p. 228, March, 1974.

The members of Interatomenergo will see to it that the appropriate organizations and enterprises in their respective countries carry out the design work, preparation and deliveries of equipment, instruments, materials, and spare parts, and also render assistance and various kinds of services in the construction of nuclear power stations.

To expedite the designated economic activities, Interatomenergo will be empowered to open up, on the territories of the countries participatory to the agreement, and other agreeing countries, its representative agencies, and also to set up production and maintenance branches, scientific research affiliates, planning and design affiliates, service bodies and miscellaneous cost accounting subordinate bodies.

The activities of the association will be based on cost accounting principles. A base fund has been set up to expedite that goal. Interatomenergo income will be derived from its spectrum of economic activities.

Organizational Structure of Interatomenergo. The highest leading body of Interatomenergo is its General Council, consisting of fully authorized representatives of the members participatory to the Interatomenergo founding agreement, one for each such member. All of the representatives designated by members of the Interatomenergo association, i.e., economic organizations of any one country, have one full vote in the General Council between them.

The chairman of the General Council is to be elected periodically for a four-year term, from among the fully authorized representatives. The General Director and his immediate subordinates will be in charge of the day-by-day activities of the association. The General Director is to be designated by the General Council from among the citizens of the country in which the association is located, and his immediate subordinates from among the citizens of the member-nations participatory to the founding agreement.

The structure of the association will be determined by the General Council at one of its first sessions. The makeup of the association in terms of specialists will be in line with the resolution on the personnel of the association as approved by the General Council. Interatomenergo will maintain liaisons with the appropriate bodies of the Council for Mutual Economic Aid (COMECON), and will also be empowered to undertake business relations with international economic organizations and other organizations in the field.

The official languages of Interatomenergo will be the languages of those countries whose economic organizations are members of Interatomenergo; the working language will be Russian. The founding of Interatomenergo will contribute to the development of nuclear power in the COMECON member-nations.

SYMPOSIUM ON METHODS FOR MEASURING AND TESTING SEALED RADIOISOTOPE SOURCES OF IONIZING RADIATIONS

A. K. Zille

A symposium on methods in measurements and tests of sealed radioisotope sources of ionizing radiations was held in Moscow December 10-14, 1973.

The symposium was preceded by the elaboration and adoption of COMECON recommendations on standardization applicable to terms and definitions pertaining to sealed radiation sources, as well as work on drafting recommendations for classification and techniques in testing prototypes of sources for soundness, taking into account the pertinent documents drawn up by the International Standardization Organization (ISO).

The participants of the symposium visited laboratories of the All-Union Radiation Equipment Scientific Research Institute (VNIIRT) and exhibits of the Institute, as well as the V/O Izotop agency demonstration and exhibits hall, to familiarize themselves with the sources, radiation—protection equipment, instruments, and equipment now being manufactured in quantity lots.

Some 45 reports on two major research trends pertaining to radioisotope sources were presented and discussed at the plenary sessions: research on the stability of sources and source simulators when exposed to various external disturbances, including techniques and equipment (17 papers), and measurements of the radiation-physical characteristics of sources, including selection and use of measuring equipment and instrumentation (28 papers).

The papers contained interesting and original information on work in progress in various countries, and on results achieved in testing and measuring sealed sources and simulators of sealed sources.

Special interest was evoked by a report on studies of reliability criteria for radioisotope sources connected with the scientifically validated determination of allowable and guaranteed service terms. This is a highly promising trend of studies; its development is convenient for the practical benefit of a large number of potential users. A report on public health requirements and sealed radioisotope sources was also heard with great interest. The proposals contained in that contribution on differentiation of requirement pertaining to mechanical stability, thermal stability, and stability against corrosive attack under emergency conditions, and depending on the degree of radiation hazard presented by the sources, can provide a basis for an improved classification.

Reports on the practical state of readiness of laboratories in various countries (Hungary, East Germany, Poland, the USSR) to stage separate tests on sources and simulators of sources on specially prepared equipment, in accordance with requirements set down in draft recommendations sponsored by ISO and by COMECON, were also quite interesting.

In the future, more attention should be given to the development of faster methods for determining the stability to corrosion of sealed radiation sources.

Translated from Atomnaya Énergiya, Vol. 36, No. 3, p. 229, March, 1974.

COLLABORATION DAYBOOK

The sixth session of the Coordination Science and Engineering Council on Radiation Equipment (KNTS-RT) was held October 18-20, in Sofiya. Results of the symposium on radiation processing of foodstuffs and agricultural products, held on the even of the KNTS session, were discussed, and it was pointed out that the symposium made it possible to review the state of the art in radiation processing of food products throughout the world, perspectives for further development of that line of work, and that this constituted a major step on the way to implementing the new method of preserving food products and food resources in the COMECON nations.

Information was put forth on results of the second conference of a group of experts charged with elaborating measures to expedite the implementation of radiation processing of food products and agricultural products in COMECON member-nations, the work done to date by the group was approved, and a draft plan of the measures presented by the group for consideration was confirmed.

These measures include preparation of unique legislative proposals and stands on the marketing and disposal of products that have been radiation-processed, undertaking a broad program of research on irradiated products, working out unified procedures for public-health assessments of irradiated products, and engineering cost studies of the feasibility and advantages of implementing this new method of preserving food resources on a broad industrial scale.

A decision was adopted to convene the third conference of the group of experts in May 1974, in Czechoslovakia.

The council also heard information on the basic directions, the status, and outlook of development and research work in the field of radiation graft-polymerization, and acknowledged the need for a symposium on the problem, while confirming the sequencing of preparatory measures, and adopting a resolution on convening a symposium in October 1974.

Preliminary proposals on developing unitized modules and units of radiation equipment were discussed, and it was judged convenient to limit this program for the immediate future to unitization of such components and subsystems components of the irradiator proper, mechanisms for displacement of radiation sources, source shipping containers, and source storage facilities.

The council discussed and approved the KNTS-RT 1974-1975 work plan. The plan calls for measures to implement radiation technological processes and use of related equipment in the industry of the interested countries, to work out unified public health regulations governing the design and use of such equipment and processes, unified procedures for dosimetric monitoring of radiation technological processes, work on unitization of some individual subsystems of radiation equipment, elaborating a scientific forecast of the development of major trends in radiation equipment and radiation technology, and staging symposia on the most urgent problems in this area.

* * *

The seventh session of Interatominstrument was held in Warsaw, December 11-15, 1973. The council discussed setting up the association's own scientific and production resources base, several engineering cost criteria important in this line of work, and drawing up plans for the association's activities up to 1980. Information on preparation of draft plans for mutual deliveries of instruments and nucleonic devices for the 1976-1980 period, and agreements on specialized production of particular types and groups of products, were reported out. The council approved its 1974 work plan and a preliminary agenda for the eighth session of the council to be held in Warsaw in May 1974. D. Hancke, a member of

Translated from Atomnaya Énergiya, Vol. 46, No. 3, p. 229, March, 1974.

the council, was elected the 1974 chairman (he is currently the director of the FEB RFT Mosselektronik "Otto Schon" organization (Dresden, German Democratic Republic).

The session took place in a businesslike atmosphere, in a setting of complete mutual understanding.

IAEA SYMPOSIA ON FAST REACTOR FUELS AND FUEL ELEMENTS

Yu. K. Bibilashvili

A symposium on fuel and fuel elements for fast reactors, sponsored by IAEA, was held July 2-6, 1973, in Brussels. There were in attendance about 200 delegates from some 15 nations. A total of 49 papers was read, including three from the Soviet Union.

The reports reflected virtually all of the problems pertaining to the design of fuel elements for a fast power reactor. Corrosive interaction between the fuel-element jacket and the fuel meat, on the one hand, and fission fragments on the other, was discussed at length, as well as swelling of steel in a neutron field at high integrated flux levels, forecasts of fuel-element operating conditions, and the service life of fuel elements in-pile.

Some of the papers dealt with the fabrication of fuel elements using uranium—plutonium oxide fuel. Results of investigations on promising types of fuel (carbides, carbonitrides, uranium and plutonium nitrides) were reflected in nine of the papers.

All of the contributions on corrosive interaction of fission fragments with the fuel-element jacket and with uranium—plutonium oxide fuel pointed out that the basic element seriously influencing corrosion behavior in cesium. One particularly interesting aspect of the reactivity of cesium in this context is the fact that, with oxygen and moisture absent, cesium hardly engages in any interaction with stainless steels up to temperatures of 650°C. The reaction between cesium and austenitic steels can proceed only above a certain oxygen potential.

When the O/Cs ration is 0.04, cesium enters into a vigorous reaction with chromium contained in the steel, to form a compound close to $CsCrO_4$. Increasing the O/Cs ratio has the effect of accelerating corrosion, so that fuel of hypostoichiometric composition is recommended for use here.

One of the French contributions presented interesting data on the temperature dependence of the intensity of the interaction between the jacket and fission fragments. It demonstrated that the intensity of the interaction attains a maximum at temperatures above 650°C, and that it does not become further enhanced as the temperature is raised to 730°C. Fuel elements were irradiated to 14% heavy-atom burnup at heat loads of 520 W/cm; the fuel-element jacket temperature was 550-750°C. Interaction set in at 600°C. The maximum intensity of intergranular interaction was 120 μ. The paper offered no reason for the cessation of the increase in the intensity of the interaction in response to increased temperature.

Analysis of experimental data and predicted data presented in the papers makes it possible to arrive at the following conclusion on the corrosive interaction. The mechanism underlying the corrosive interaction between fission fragments and the fuel and jacket has not yet been studied with sufficient thoroughness. There are also some gaps in the quantitative data on hand. The problem consequently requires much further work. However, experience accumulated in testing fuel elements with uranium oxide and uranium—plutonium oxide fuel provides evidence that corrosion would not be the limiting factor in attaining the burn-up required for a fast power reactor (100,000 MW·days/ton). Reports submitted by representatives of Great Britain, West Germany, France, based on quite adequate studies of uranium—plutonium oxide fuel in the DFR, Rapsodie, and other fast reactors, pointed out that not a single reliable case of fuel-element failure due to this corrosion interaction can be exhibited to date.

J. Bishop (Britain) drew the following conclusion upon summarizing the results of the symposium at the concluding session. Fission fragments do not affect the compatibility of the fuel and jacket in

Translated from Atomnaya Énergiya, Vol. 36, No. 3, pp. 230-232, March, 1974.

carbide-fuel elements. The oxygen potential in those fuel elements is too low for complex oxides of cesium and chromium to form in them. The reaction between tellurium and the stainless steel jacket likewise becomes much less likely and less vigorous when carbide fuel is present. Formation of the complex uranium—tellurium carbide (U_2TeC_2), which binds the tellurium to the fuel, is the most likely outcome.

Absence of iodine corrosion in carbide fuel elements is accounted for by the fact that the iodine becomes bound by the cesium during the irradiation process, forming CsI. The only chemical interaction occurring between the fuel and the jacket in such fuel elements is carbidization of the jacket. The degree of carburization of the jacket depends on the fuel stoichiometry and on the rate of carbon transport through the clearance between fuel and meat and jacket.

It was pointed out, in the reports and floor discussion, that one possible limiting factor on attainment of the degree of burn-up called for by economic considerations is the swelling of steel in a neutron field. Swelling of steel in a neutron field is a topic that has received some attention in the literature, the most interesting contributions on the subject being papers by British and French specialists. Prognoses on volume measurements in the fuel assemblies of the PFR and Phoenix reactors were made in those papers on the basis of experimental data obtained in work with the DFR and Rapsodie reactors, and some views were put forth on ways of solving the problem. In particular, the British specialists entertain the view that the use of nimonic PE-16 as structural material is very helpful in reducing swelling of reactor core components. Experimental investigations have shown that nimonic PE-16 swells to a considerably lesser extent than steel of grades 316 and 318 in the cold-worked state, and much less yet than those steels in the austenitized state, over the entire temperature range typical of a fast power reactor (350-650°C).

In discussing the papers, the British specialists noted that jackets of nimonic PE-16 were employed for some of the fuel elements (~ 20%) when the set of fuel elements for the first loading of the PFR reactor was fabricated.

One of the French papers on the subject reports that direct in-core monitoring of fuel assemblies of the Phoenix reactor has been proposed in order to shed some light on the degree of warping of fuel assemblies as a result of swelling of steel, and in order to measure deviations of the heads of fuel assemblies from their initial position. A special device has been developed for the purpose, a prototype of the device has been fabricated and is currently undergoing tests. The French specialists feel that this monitoring action should be carried out on peripheral assemblies in the core. On the whole, it can be pointed out that there are as of this writing no reliable quantitative data on swelling of structural materials at high exposure dose levels, and that this problem can be investigated in detailed fashion and solved definitively after the first demonstration type pilot fast reactors, the BN-350, the Phoenix, the PFR, and others, have been started up and have been on power for some time.

Close attention is being given, in all countries, to research and development work on pilot-scale and full-scale fabrication technology of uranium—plutonium oxide fuel elements. Great progress has been achieved in Britain, France, Japan, and elsewhere in this area. We cannot omit mention of the particularly high technical level of production attained in Britain, where a 60-ton annual capacity uranium—plutonium fuel plant has been built (at Windscale). A set of fuel elements (100 assemblies, 32,500 fuel elements, $\sim 4.5 \cdot 10^6$ fuel pellets) for the first loading of the PFR reactor has been fabricated there. Work is in progress on fabricating a set of fuel elements for the next loading as well. Various experimental packages will be included in this set. A brief flowsheet of the fuel fabrication process includes the following technological operations: powder in the form of chemically coprecipitated solid solution of uranium dioxide and plutonium dioxide arrives at the "head" of the process, followed by further comminution of the powder and the introduction of binder, then compacting and granulation, pelletizing, sintering, and also grinding (the last step only to correct scrap). One typical feature of this fuel production process is the high level of mechanization of all of the technological operations, plus the automation of some process steps. Pelletizing and assembly of fuel elements is done in glove boxes with lead shielding glasses on the outside of the structures. Fuel assemblies are assembled by automatic means. When the fuel elements are hermetically sealed, they are filled with helium plus ^{85}Kr addition.

A film on a pilot facility for production of uranium—plutonium fuel in Japan was run at the symposium. At the present time, a full set of fuel elements for the JOYO Japanese experimental fast reactor is being prepared at that facility.

We can draw the following conclusions from analysis of the symposium materials and of the floor discussion following the concluding session on fuel production problems:

1. The high toxicity and activity of uranium—plutonium fuel imposes the requirement that technological processes be highly mechanized, and that individual technological operations be automated. Manual labor must be used in the repair and maintenance of equipment where unavoidable or in carrying out simple technological operations that can be completed within a short time.
2. Equipment that has been put through its paces with a high degree of attendant reliability makes it possible to fabricate fuel and fuel elements in glove boxes even when plutonium with a high content of higher-order isotopes (as much as 20-22 wt. % total) is used.
3. Technological operations involving assembly of fuel elements into fuel assemblies must be automated and must be carried out at remote distances from human personnel.
4. There are currently two concepts in fuel production. Specialists in some countries (USSR, Britain, etc.) feel that the fabrication of pellets of 90-96% of the theoretical density and with a central hole (for inserts) makes it possible to simplify the technological process and to cut down production costs. The temperature conditions of fuel element performance can be predicted with ease in such cases and axial displacement of fuel can be eliminated with guarantee. Specialists of other countries are moving ahead along lines of fabricating solid pellets of low density (82-87% theoretical density).
5. A pelletizing method has been incorporated into the production processes for fuel fabrication adopted in a number of countries, the Soviet Union included. Automatically rotary type pelletizing presses of fairly high capacity (USSR, Belgium, etc.) have been developed for these applications, as well as some multipunch vertical presses (France, Japan, etc.) with the advantage of low production costs.

The program of research being conducted by specialists of a variety of countries on forecasting operating conditions of fuel elements and the service life of fuel elements in the core covers the following points:

1) experimental work geared to refining and selecting design models of fuel elements;
2) developing fuel element design techniques;
3) analysis of experimental data secured through investigations of experimental fuel elements in hot laboratories, refinement of the design procedure and design calculation programs based on this analysis;
4) special reactor experiments and out-of-pile experiments geared to disclosing possible reasons for malfunctioning and failure of fuel elements;
5) investigation of fuels and construction materials for use in the calculation of fuel elements.

The discussion on the effects of reactor transients on fuel-element performance was also interesting. Reports by specialists from France, West Germany, and one of the Soviet reports, all based on computational investigations, showed that plastic deformations of fuel-element jackets occurring during reactor transients can be decisive in forming estimates of the useful service life of fuel elements.

One result obtained on the basis of experimental data and computational investigations should be dwelt upon at greater length.

As stated earlier, specialists of various countries recommend the use of oxide fuel of hypostoichiometric composition $(UPu)O_{1.94-1.96}$ to minimize the corrosive effects of fission fragments. But experimental investigations have shown that reduction of the oxygen ratio markedly inhibits the creep rate of fuel, i.e., the ductility of the fuel is diminished. It is evident from calculations performed by Soviet and foreign research workers that stresses due to the mechanical action of the fuel are aggravated in the fuel-element jacket in this case. A compromise solution is therefore mandatory in selecting the oxygen ratio. Specialists from Britain, the USSR, West Germany, and elsewhere take a dim view of any severe reduction in the oxygen ratio of the fuel.

Consequently, the following conclusions are in order on forecasting performance and service life of fuel elements:

1) closely similar computational models of fuel elements selected by specialists of various countries, and coinciding in their basic characteristics, still require further investigation;

2) topics involving choice of criteria for reliable performance of fuel elements governing a systematic approach to assessing the useful service life of the fuel element have not yet received sufficient study;

3) analysis of failed fuel elements still fails to yield unambiguous information on the reasons for failure of the jackets;

4) malfunctioning of individual fuel elements does not require special unplanned reactor shutdowns; the reactor can be operated with the detective fuel elements in place until the time of the planned shutdown.

The symposium confirmed the possibility of obtaining inexpensive power from the operation of nuclear power stations with a fast reactor burning uranium—plutonium oxide fuel. Fuel elements with that type of fuel ensure reactor parameters consonant with acceptable engineering costs.

Any further improvements in the engineering costs picture for fast reactors will involve utilization of more exotic types of fuel. Attention is being centered, in the various countries, on research and development work on carbide fuel, carbonitride fuel, and nitride fuel. Reports discussing research on those types of fuel covered the following principal points:

1) technology for producing original compounds and fabricating fuel meat from them;

2) compatibility of carbide and carbonitride fuel with the fuel-element jacket materials;

3) fuel-element design techniques;

4) results of fuel irradiation experiments.

The production technology of carbide, carbonitride, and nitride uranium—plutonium fuel is based on the use of both oxides (U_3O_8, UO_2, PuO_2) and metals as starting materials, but no preference is stated for any one of these methods. The recommended oxygen content in this fuel must be no greater than 0.1 to 0.15 wt. %, and any decrease below that range will improve compatibility.

French scientists are of the opinion that the fabrication costs of fuel meat made from oxygen-free compounds will be 20 to 30% higher than that made from uranium—plutonium oxide fuel.

Fuel elements with carbide, carbonitride, and nitride fuel have rendered quite impressive performance up to the required length of useful service (burn-up 7 to 10% heavy atoms), with a low degree of susceptibility to corrosion on the part of the stainless austenitic steels.

A sodium underlying layer should be used in order to attain high burn-up (over 7% heavy atoms). Segregation of plutonium from the center toward the periphery has been observed in carbide, carbonitride, and nitride fuel. Difficulties associated with the swelling, more intense than in oxide fuel (1.6 to 2% per 10,000 MW days/ton), might be coped with, in the view of specialists from many countries, by various design measures. The need to expand research on this type of fuel in order to accumulate extensive data on the durability of fuel elements under the operating conditions typifying a fast power reactor was pointed out at the symposium.

XI INTERNATIONAL CONFERENCE (PRAGUE) ON PHENOMENA IN IONIZED GASES

G. V. Sholin

The XI international conference on phenomena occurring in ionized gases was held in Prague in early September, 1973. This conference is convened every other year. The X conference in the series was held at Oxford (Great Britain) in 1971. The XI conference was organized by the Institute of Physics and the Institute of Plasma Physics of the Czechoslovak Academy of Sciences, by the departments of mathematics and physics of Charles University, and by the electrical engineering and nuclear engineering departments of the Czech Polytechnic University.

Some 600-odd scientists representing 26 countries took part in the conference.

The number of original papers submitted ran over the 500 figure, and a reporter system was adopted, following the now established tradition. There were six panels, each lasting about 50 min, running simultaneously during the second half of each session-day (30 min taken up with papers covered by the reporter and about 20 min of floor discussion). The number of panel sessions active daily was 20 to 24. The first half of the day was reserved for tutorial review papers. The organizing committee of the conference invited 13 leading scientists from various countries (including five from the socialist states) as lecturers to present review papers.

The proceedings of the conference are being published in two volumes: the first volume was in print at the start of the conference and was distributed to the participants present, with its 485 original contributions; the second volume (to be ready in early 1974) will contain tutorial review papers and papers submitted to the organizing committee of the conference after May 1, 1973.

The conference covered a very broad range of topics: elementary processes (including chemical reactions and surface phenomena), electrode phenomena; various stages of a gas discharge and different species of gas discharges; waves and instabilities in plasma; plasma emission; experimental techniques in plasma diagnostics; interaction of electromagnetic waves and beams of charged particles with plasma.

The physics of high-temperature plasma was less well represented on this occasion than earlier, apparently because of a number of conferences on the topic held within the 1973 year (see Atomnaya Énergiya 35, 289 (1973) and 35, 447 (1973)). Only two problems undergoing intensive investigation in Czechoslovakia (interaction of beams of charged particles and electromagnetic waves with plasma) were represented quite fully. A review paper by P. Sunk (Czechoslovakia) "Nonlinear effects in beam-plasma systems" and papers by K. Jungwirt et al. (Czechoslovakia) and I. F. Kharchenko et al. (USSR) offered detailed analyses of the role played by trapped particles and beam modulation in the development of a discharge. Simulation of space phenomena (polar aurorae) with the aid of a beam-plasma discharge and without a magnetic field present was reported on by I. F. Kharchenko and colleagues in their paper.

Papers dealing with interaction of RF waves and plasma centered their attention on nonlinear processes leading to anomalous dissipation, which was first detected experimentally by I. R. Gekker and G. M. Baranov (USSR). New experiments staged by I. R. Gekker excluded any effect of waveguide walls on the wave absorption effect. Analysis of backscatter spectra was presented by F. Crawford and coworkers (Britain).

The chief reason for anomalous dissipation is the parametric instability, according to most authors. G. M. Batanov and K. A. Sarkisyan put forth additional experimental evidence in support of this mechanism.

Translated from Atomnaya Energiya, Vol. 36, No. 3, pp. 232-235, March, 1974.

Inhomogeneity on the plasma boundary can bring about various effects accompanying interaction of plasma with a RF field. An understanding of these effects is of the utmost importance for laser heating of plasma to thermonuclear temperature. A report by V. I. Karpman et al. (USSR) ventured a theoretical discussion of electrostatic and magnetosonic wave packets in an inhomogeneous plasma. Results of experiments on reflection of electrostatic waves in an inhomogeneous plasma were presented by A. Ratner et al. (USA). It is clear from the experiments that long-wave oscillations are practically completely reflected off the plasma boundary, whereas oscillations with wavelengths shorter than the characteristic dimension of the inhomogeneity are practically completely adsorbed on the boundary, in contrast. The overall properties of current flow through a plasma acted upon by RF waves were analyzed by R. Klima (Czechoslovakia). The reporter demonstrated that the appearance of direct currents in toroidal systems with RF heating is always a consequence of conservation of generalized momentum.

An observation important in the interpretation of turbulent plasma experiments was made by R. Franklin, T. Smith, and S. Hamberger (Britain). They showed that the presence of even weak large-scale low-frequency fluctuations can bring about a substantial expansion of the spectrum of plasma oscillations, at the same time leading to masking of other nonlinear processes of wave interaction.

As earlier, stabilization of instabilities, above all drift waves, took the center of attention. For example, experiments conducted at the Fontenay-aux-Roses nuclear research center (by P. Brossier and colleagues, France) on stabilizing electron drift waves by the electron temperature gradient set up with the aid of local plasma heating by an external source of microwave power were reported on. Another option in stabilization was demonstrated in a contribution by S. S. Sobolev (USSR): instability of potential oscillations in a Q-machine plasma was successfully suppressed by direct magnetosonic waves. An impressive reduction in the anomalous diffusion coefficient was achieved in experiments by S. S. Sobolev, an attainment that drew comments from the specialists, and floor discussion emphasized the possible use of this effect in a number of applied problems.

The panel session on electrode phenomena occurring in plasma generated in a hot discharge discussed emission of charged particles and neutrals, stability of electrode spots and the influence of electrode spots on the pattern of three-dimensional current flow through the interelectrode gap. It is clear from the text of the reports and from the floor discussion that the use of directly and indirectly heated cathodes to generate a spatially homogeneous plasma for use in gas-discharge lasers is now a real possibility.

A tutorial review paper presented by V. Nigana (USA) pointed out the fact that instabilities appearing on electrodes and limiting the contribution made by the electrical energy to the discharge can be suppressed by generating turbulence in the stream of gas. Turbulent mixing enables USA investigators to increase the effective volume of CO_2 gas lasers with pumping, and to increase the working pressure of the mixture of gases (N_2, He, CO_2) to 200 mm Hg; the use of electron beams to preionize the gas increases the power of the light emitted as taken from a unit volume by ~10 times, and another gain of utmost importance in practice is that the system can operate at gas pressures $\geqslant$ 1 atm. The report contained an analysis of kinetic processes at work in CO_2 lasers, in particular how generating efficiency is affected by dissociation of the CO_2.

Great progress has been achieved in designing gas lasers for the production of thermonuclear plasma by a short radiation burst ($\leqslant 10^{-9}$ sec). Several reports by Soviet scientists (V. Yu. Baranov, G. A. Mesyats, V. P. Smirnov, R. I. Soloukhin, V. D. Pis'mennyi) described pulsed lasers operating on various mixtures of the gases CO_2—N_2—He at elevated pressures, using electron beams of high current density ($>10^2$ A/cm^2). Lasers with radiation outputs of 10^4 J can be designed on that basis in the near future, it appears. A molecular xenon (Xe_2, λ = 1730 Å) gas laser, first achieved in practice by N. G. Basov and colleagues in 1970, seems to offer great promise as a tool in thermonuclear research. J. Gerardo and A. Johnson (USA) investigated the performance of a molecular xenon laser at pressure ~10 atm and excitation of a relativistic (~1.5 MeV) electron beam of current ~250 A.

Advances in the design of high-output lasers became possible as a result of deeper understanding of the processes at work in a low-temperature molecular plasma. A review paper submitted by M. Z. Novgorod and N. N. Sobolev (USSR) summarized the present status of research in this area, and demonstrated, for CO_2 and CO gas lasers, the validity of a simple model to account for molecular population inversion by electron collisons. The floor discussion following presentation of this paper emphasized the need for careful investigation into the electron velocity distribution function, since even slight deformations in the high-energy tails of the distribution can drastically affect the rates of processes involving participation by electrons.

Generation of plasma through laser bombardment of a solid target or gas target is usually explained via the theory of many-photon ionization. But this generally accepted point of view is not the only plausible one. An original theory accounting for the mechanism of breakdown and ionization of the gas at the focus of laser radiation was proposed by the Canadian physicist E. Panarella. While suggesting the existence of a certain nonlinear interaction between the components of the field established by the light wave, he replaced the usual relationship between photon frequency and photon energy $\varepsilon = h\nu$ with a more general one $\varepsilon = h\nu/[1-\beta_\nu f(I)]$, where $f(I)$ is the light intensity function, and β_ν is a coefficient such that the product $\beta_\nu f(I)$ is limited away from zero appreciably only when the light intensity is high. In the same vein, E. Panarella succeeded in arriving at magnificent agreement with experimental data on breakdown and ionization without having to resort to the many-photon or cascade mechanisms.

New information on spontaneous magnetic fields in laser plasma was presented by the American scientists A. Cooper and R. Bard. Magnetic probes were used by these workers to investigate the effect of gas pressure on the magnitude of those fields and to detect any spatial periodicity of those fields.

A detailed study of this phenomenon is highly important for any understanding of the process by which laser plasma forms, and of laser plasma dynamics.

A rather large group of papers discussed at the laser plasma panel session was devoted to spectrometric measurements of parameters of a laser plasma of electron density $\geqslant 10^{19}$ to 10^{20} cm^{-3} and temperature $\geqslant 100$ eV. The intensities and profiles of lines of multiply charged ions are commonly used in diagnostics of that type of plasma. For instance, N. G. Basov and colleagues analyzed the spectral lines Al^{XIII} and Mg^{XIII}. Subsequent work will probably call for investigation of lines of even 30-fold ionized atoms.

Other spectroscopic techniques of plasma diagnostics were also given a prominent place in the agenda of the conference. The panel session on spectral lines dealt mainly with Stark broadening. Efforts of many laboratories in the USA, France, and West Germany are presently concentrating on detailed comparisons of theoretically predicted and empirically measured profiles of spectral lines for the simplest atomic systems. The purpose behind those efforts is to lay down a firm basis for calculating the parameters of lines of any atoms and ions whatever, while taking into account both pressure effects and effects of random thermal motion and turbulent oscillations. For the time being, agreement between theory and experiment still leaves much to be desired, even for the simplest L_α case.

New measurements of the L_α profile in a high-pressure capillary arc, presented by V. Ott and K. Beringer (USA), are supposedly in closer agreement with existing theoretical data than the earlier measurements of G. Boldt and V. Cooper. But the nonmonotonic pattern of asymmetry in the wings of the line is apparently indicative of a significant radial plasma inhomogeneity and of violation of conditions of local thermodynamical equilibrium. This means that the question of a divergence between theoretical and experimental results remains open for the time being. New experimental data on Stark broadening of some argon and chromium lines differing by roughly a factor of two from the theoretically calculated data were also presented at the panel. All of this suggests a need to improve upon the Beringer—Griem—Kolb—Erthely theory, the basic tenets of which have received clear confirmation on the whole. An attempt to expand the framework of this theory by taking random thermal motion of ions into account has been made by D. Vosslambert (France). But ion field rotation effects were left entirely out of account in this treatment.

A paper by A. V. Demur and G. V. Sholin (USSR) providing the first quantitative explanation of the red shifts of Balmer lines in a high-density plasma, observed experimentally, was received with great interest. The results covered in this paper are of special interest in astrophysics. The use of the polarization effect within the profile of a spectral line to analyze turbulent noise in a rarefied plasma was described in a paper submitted by M. V. Babykin et al. (USSR). An original approach to analysis of profiles of hydrogen spectral lines in the presence of self-absorption was developed by L. G. Golubchikov et al. (USSR). A detailed analysis of the asymmetry of the line underlay this approach.

A special panel session was devoted to continuum radiation. Here a lively discussion was evoked by a paper submitted by V. Vimet (Belgium) on the nature of a continuum in the visible region of the spectrum emitted by a low-temperature plasma of noble gases. Precision experiments led the author to the conclusion that the continuum is of a molecular nature in xenon, and that the use of the continuous spectrum is inadmissible in measuring electron temperature in such discharges. An insufficiency in standards for absolute measurements is felt in the case of vacuum ultraviolet, to date. V. Ott and K. Beringer (USA)

suggested using a hydrogen capillary arc with electron temperature ~20,000°K and electron concentration $\sim 2 \cdot 10^{17}$ cm^{-3} for those purposes. Another technique of calibration for use in the near ultraviolet was proposed by East German scientists. The most important finding in spectroscopic investigations of high-density plasma seems to be accumulation of data indicating the inadequacy of the model of local thermodynamical equilibrium even under conditions of an arc or plasmatron, not to mention high-frequency discharges.

The most interesting findings reported in the field of diagnostics were measurements presented by British scientists (M. Forrest, K. Murdock, H. Pinock), data on magnetic fields in a rarefied high-temperature plasma on the spectrum of scattered radiation from a ruby laser, and the application of a chemical dye laser (P. Richardson and V. Toser, Britain) in fluorescent analysis of trace amounts of impurities in plasma.

Plasma chemistry also received its due share of attention at the conference. A tutorial review paper by G. Suhr (West Germany) offered a clear sketch of the present state of research in this area. There are now two plasma chemical processes (acetylene production and ozone production processes) that have been developed for full-scale industrial use and are now being implemented for commercial purposes. Production processes for various cyanides, compounds of nitrogen with oxygen, hydrazines, and other products of ozonizing type reactions are in the implementation stage. The study of processes occurring on the surface of metals in contact with plasma also holds forth great promise for future applications. The formation of films with a variety of interesting optical, mechanical, and electrical properties under those conditions may also be of great interest for a number of technological applications. The surfaces of organic materials in contact with plasma also experience complex polymerizing processes. The basic requirements for plasma chemical reactors are: highest possible density of reactants, absence of contacts with the walls, and sufficiently long useful life. Several practical facilities of apparent long-term interest in plasma chemical engineering were also reported on at the conference: high-output stabilized microwave discharges, an arc struck in a toroidal magnetic field, and the first experimentally materialized annular stabilized arc (W. Tiller, West Germany).

Changes in rates of chemical reactions in response to deviations from thermodynamical equilibrium in plasma were the subject of papers by groups of scientists led by L. S. Polak (USSR) and J. Prajz (Czechoslovakia). A team of Italian scientists working at the center of plasma chemistry studies (P. Capesutto et al.) presented results of research on chemical processes occurring in a microwave discharge at medium-level pressures (5-7 mm Hg).

Metastable states of atoms and molecules provide additional sources of energy. They are capable of seriously influencing the electron distribution function while at the same time affecting the kinetics of plasma and the rates of the chemical reactions. These topics were addressed by a tutorial review paper authored by J. Delcroix, S. Ferreira, and A. Ricard (France) and by some original contributions made by American and French scientists. Attention in plasma chemical research is being centered at present on developing techniques for monitoring such physical variables as electron temperature and electron density, partial composition, the vibrational, rotational, and translation temperatures of molecules, and also the extent of molecular dissociation in discharges.

On the whole, the conference remains, with all of the breadth of its agenda, one of the principal forums open to scientists for presentation of findings on novel investigations, of either methodological or fundamental nature, in plasma science. The growing interest in plasma phenomena on the part of physicists engaged in the design of high-output lasers, and on the part of chemists, apparently reflecting current developmental trends in science and industry, is indicative.

The next (XII) conference on phenomena occurring in ionized gases is scheduled for Eindhoven (Netherlands) in 1975.

CONFERENCE ON APPLICATIONS OF NEW NUCLEAR PHYSICS TECHNIQUES IN SOLVING SCIENTIFIC AND APPLIED PROBLEMS, DUBNA, NOVEMBER 1973

V. S. Barashenkov

Modern nuclear physics experimental work is typified by the vigorous development of new techniques which materially expand the potentialities of measurements and improve the accuracy and precision of measurements. This is accompanied by improvements in already existing types of instruments and procedures, in turn generally accompanied by simplification and reduction in cost. This combines to create conditions favoring effective implementation and application of nuclear physics techniques in allied branches of science and engineering, and expediting the use of those methods in the solution of outstanding problems in the national economy.

The discussion of new opportunities, and shedding light on the most important and promising trends extant, consultations on the results obtained, and on research programs underway, are topics to which the conference of specialists from the ten member-nations of the Joint Institute for Nuclear Research [JINR] meeting at Dubna, at the Nuclear Reactions Laboratory, November 20-23, 1973, was devoted.

The initial assumption was that the conference would deal only with methods of activation analysis; even though it was precisely this topic that occupied the dominant position in the reports and ensuing floor discussion, the conference also went on to discuss other nuclear physics techniques which are of great interest from the vantage point of their use in solving current problems of interest to the national economies of JINR member-nations. Over 80 specialists were in attendance at the conference.

The first to take the podium at the conference were Polish and Vietnamese physicists (R. Dybezynski and Pham Rui Heing) who presented tutorial review papers on the present state of the art and on the developmental perspectives of research work in activation analysis at institutes in their respective countries. Work done at the Nuclear Physics Institute of the Academy of Sciences of the Uzbek SSR, which is the USSR's leading organization in the field of activation analysis, was covered in an exhaustive review paper presented by A. A. Kist. The Czechoslovak physicist M. Krivanek presented an interesting report on the organization of that country's activation analysis national research center.

The specialists in attendance cited numerous examples, in their reports and contributions from the floor, of applications of activation analysis in geology, metallurgy, biology, agriculture, forensic science, etc. Many of those applications have yielded impressive cost savings.

It was also pointed out that, while the activation analysis method is simple in principle, the development of concrete analytical procedure often turns out to be a rather complicated undertaking, requiring high skills and great ingenuity. This is in large measure accountable to the scarcity of high-intensity low-cost radiation costs and sensors featuring high energy resolution, so that the work of developing suitable procedures is complicated and longer lead times are required to achieve routine implementation of the procedure. Another shortcoming is that the activation analysis method is often resorted to in solving minor problems where there are no great cost savings in question, and where most of the time is taken up not in working out a suitable procedure but rather in taking into account the very specific features of the problem being tackled.

Translated from Atomnaya Énergiya, Vol. 36, No. 3, pp. 235-236, March, 1974.

The selection of the most important and pressing problems for effective application of activation analysis is currently one of the major questions confronting specialists. This point was stressed in the introductory remarks by Academician G. N. Flerov, who mapped out four major trends over the period ahead: 1) ecology; 2) monitoring the purity of materials; 3) geological exploration and prospecting; 4) process monitoring of ore mining and treatment.

A report presented by V. N. Nikitin on applications of activation analysis and radioisotope research to work at the Noril'sk mining and metallurgical combine, where such work has been undergoing intensive development since 1970 on the basis of a RG-1 nuclear reactor with a neutron flux level $2.7 \cdot 10^{12}$ neutrons /sec $\cdot$ cm^2 in the central channel, was received with great interest. This reactor features eleven experimental channels and a pneumatic shuttle system, is equipped with up-to-date multichannel analyzers with field detectors and scintillation detectors, coincidence—anticoincidence counters, and electronic data processing machinery. Neutron activation analysis is carried out in two distinct variants: a radiochemical variant using long-lived isotopes and a nondestructive variant based on short-lived emitters. The productivity of a radiochemical analysis cycle applied to the noble metals is 12-15 h, as against 10-30 min when short-lived isotopes are used, and 5-7 full days when long-lived emitters are used.

Some interesting applications of activation analysis for impurity determinations in high-purity materials were reported on by East German physicists S. Niese and H. Kleiberg.

Several papers were devoted to monitoring environmental pollution. The cited data shown that ultimate multicomponent analysis of the environmental medium into contents of harmful and hazardous elements requires radiation sensors of resolution $\lesssim 1$ keV, while in some cases important results can be secured even when using less sensitive equipment.

The symposium participants expressed the view that organization of laboratories for monitoring the state of cleanliness of the environment and for other long-term applications of activation analysis at those centers where sufficiently intense neutron sources are available would be highly desirable.

The participants paid close attention to comparative estimates of different sources by nuclear radiation, and of equipment designed for use in activation analysis. These topics were covered in review papers presented by A. S. Shtan', V. A. Yanushkovskii et al. on research and development work done at the VNIIRT radiation equipment research institute (Moscow) and at the NIIRP radioisotope instrumentation research center (Riga), and papers by S. P. Kapitsa (Institute of Physics Problems, Moscow) on microtrons and C. Simane (JINR) on the utilization of subcritical assemblies as neutron breeding facilities.

Favorable expectations are currently entertained for the use of microtrons yielding electron beams and hard γ-photon beams of intensities $\sim 10^{14}$ particles/sec, or neutron flux levels of $\sim 10^{11}$ particles/sec, and these microtrons are regarded as versatile general-purpose sources of radiation for activation analysis. As G. N. Flerov pointed out in his summarizing report, the microtron is almost a hundred times more efficient tool for use in activation analysis than is the dt-generator. The use of a breeding facility increases neutron flux by another two orders of magnitude. Experience in working with the microtron at the JINR Nuclear Reactions Laboratory has demonstrated that this accelerator operates stably and offers high beam quality.

In many cases, particularly under field conditions and under the conditions typifying small laboratories, isotope sources of types Be + Po, Be + ^{238}Pu, Be + ^{242}Cm, from which fluxes of $\sim 10^7$ to 10^8 neutrons /sec can be obtained, are found highly useful. A neutron beam almost a full order of magnitude greater can be obtained with the aid of ^{252}Cf, but this approach does not appear to be very rewarding, since the production of ^{252}Cf uses up prodigious amounts of ^{235}U and is a very expensive proposition.

A report by A. S. Shtan' et al. laid stress on the outlook for activation analysis based on reactions provoked by bombardment with 14 MeV neutrons. This approach is characterized by such advantages as high representativeness of samples, express analysis features, simplicity of fabrication of standard samples, and the option of complete automation.

As for radiation sensors, the ones currently enjoying greatest popularity in applications are the Ge(Li)-detectors. These lithium-drift detectors, with sensitive volumes from 3 to 100 cm^3, offer resolution of several kiloelectron-volts, and match the highest level found anywhere in the world in their technical ratings. For some problems in applications, however, applications in ecology specifically, a further increase in resolution to the $\Delta E \simeq 100$ eV is required. Si(Li)-detectors and detectors using pure

germanium appear to hold great promise in this regard. It is essential that conversion to the use of high-resolution detectors make it possible to get around the complicated computerized statistical processing to spectral curves to an appreciable extent.

A report by S. V. Mamikonyan (VNIIRT) dealt with the present status and developmental outlook of dispersion-free x-ray spectral analysis utilizing radioactive sources. The comparatively low cost and the compactness of the equipment render this method accessible for widespread application; the method is particularly convenient for high-precision quantitative determinations of the composition of technological products directly on stream, when automatic x-radiometric analyzers display the results of the analysis on a control panel, and are used as sensors monitoring the chemical composition in automatic process control systems.

Experience in devising automatic arrangements for activation analysis with fast neutrons was shared by colleagues of the Institute of Nuclear Physics and of the Mining and Metallurgical Academy of Krakow.

J. Knorre (East Germany) reported on an investigation of the space-time structure of neutron flux from a dt-generator.

There was keen interest shown in a report by V. S. Barashenkov and G. N. Flerov (JINR) on the outlook for practical utilization of heavy-ion beams. In view of the unique destructive capability and the possibility of implanting virtually any chemical element in the material to be bombarded, beams of heavy ions make it possible to work upon practically any material no matter what its structure or what the chemical composition of its surface and adjacent layers. Three trends in utilization of heavy ions appear currently well out in front:

1. Use of heavy ions as "microneedles" in the production of molecular-virus filters (nucleopores) with pores of identical dimensions, over a range from several tens of Angstrom units to several tens of microns. These filters can be used in ultrarefinement and ultrapurification of gases and liquids, in cold sterilization of bacteriological media and liquid foodstuffs, to take samples in ecological research, etc.
2. Use of heavy ions to form many-component alloys exhibiting such properties as superconductivity at temperatures well above the helium temperatures, and possibly well above the hydrogen temperatures. Further, implantation of heavy ions in the superconductor can keep the latter from reverting to the normal state because the critical superconducting current characteristic of each superconductor would be raised substantially through that device.
3. Use of heavy ions to simulate radiation damage (swelling) of heat-generating and structural materials in nuclear reactors and in thermonuclear fusion reactors. This effect, brought about in reactors over the course of several years in operation, can be reproduced within a few hours with the aid of a beam of heavy ions.

The radiation damage simulation problem, using heavy ions, was also discussed in a paper submitted by V. N. Bykov and Yu. V. Konobeev (FÉI, Obninsk).

The need to schedule conferences periodically on applications of new nuclear physics techniques in the national economies of JINR member-nations was stressed. The next conference is scheduled for 1975.

SEMINAR ON INTERACTION OF HIGH-ENERGY PARTICLES WITH NUCLEI, AND ON NEW NUCLEUS-LIKE SYSTEMS

I. S. Shapiro

A seminar on interactions between nuclei and high-energy particles, and also on new nuclear-like systems, was organized under joint sponsorship of GKAE SSSR [State Committee of the USSR on Peaceful Uses of Atomic Energy] and the Nuclear Physics Division of the USSR Academy of Sciences, and was held September 10-13, 1973, in Moscow. Present were some 200 physicists, including invited guests from the German Democratic Republic, Italy, the USA, and France.

One specific feature of high-energy nuclear physics of interest in this context is that this subtopic lies on the borderline between traditional physics of the nucleus and the physics of elementary particles. Relativistic accelerators materially enhance the potentialities of experimental research on the nucleus by broadening the range of particles available for bombarding the nucleus with, and broadening the range of variation in kinematic variables on which the cross sections of nuclear reactions depend (energy, transferred momentum, and so forth). On the other hand, experiments carried out using nuclear targets constitute a source of valuable information difficult to obtain by other methods, e.g., on interactions of elementary particles (e.g., short-lived particles — resonances with nucleons).

Recent years have seen new trends appear in high-energy nuclear physics. One of these is closely related to recent indications that excited states of the nucleon (nucleonic "isobars") are capable of playing a prominent role both in the properties of the lightest stable nuclei and in the course of nuclear reactions occurring at high energies, (e.g., in plastic p—d-backscattering). Furthermore, as has become clear from theoretical considerations, investigation into the existence of two-, three-, and many-baryon resonances, i.e., new unstable nuclides in which one or more nucleons are replaced by isobars, is showing itself to be of profound interest for an understanding of the physical nature of excited states of the nucleon.

Some interesting results showed up in still another new and related area several years ago: in the study of interactions between slow antinucleons with nucleons and nuclei. Theoretical work done on this topic has shown that the existence of a large number of nuclear-like bound states of antinucleons with nucleons is highly probable. The simplest of these "nuclides" would be bound nucleon—antinucleon pairs, which must be manifested in experiments as unstable heavy mesons (of mass roughly twice that of the nucleon) because of annihilation. Experimental research on annihilation of slow antiprotons in hydrogen and in deuterium, carried out in 1971-1973, yielded data arguing for the existence of such systems.

A feature common to the two fledgling trends just mentioned is the way they lay a basis for study of a new variety of nonrelativistic many-particle systems with strong interaction: nuclear-like systems differing from conventional nuclides in that one or several nucleons are replaced by other baryons (isobars, antinucleons). Still another interesting concept appears closely linked to these topics: the possible existence within nuclei of a pion condensate ("meson fluid").

The unfolding discussion on theoretical and experimental research problems pertinent to new nuclear-like systems and their role in nuclear reactions was perhaps one of the principal distinguishing features of the seminar held in September. In addition, the seminar agenda fitted in two other major topics: coherent interaction between nucleons of the nucleus and high-energy particles, and the study of the mechanism underlying direct nuclear reactions at high energies. These problems are even more frequent topics of discussion at conferences on high-energy nuclear physics.

Translated from Atomnaya Énergiya, Vol. 36, No. 3, p. 237, March, 1974.

The latest gains in the theory of coherent processes go beyond the framework of what is termed the Glauber approximation (taking account of recoil in scattering on nucleons within the nucleus, corrections for Fresnel diffraction, evaluation of the contribution of rescattering of nucleons to the amplitude of the process). What is new in the experimental research conducted is the appreciably broader investigation into processes involving inelastic scattering of high-energy particles on nuclei with excitation of low energy states. Experimental data on scattering (so far inelastic inclusive scattering) of polarized high-energy protons on nuclei have also appeared. Prominent among processes of coherent interaction between high-energy particles and nucleons within the nucleus are the quite familiar reactions involving production of particle-resonances, which enable researchers to measure the scattering cross section of those unstable particles encountering nucleons. A mark of progress in this area has been the observation of many-pion decay channels of particle-resonances generated on nuclei, as well as observation of particle production processes accompanied by simultaneous excitation of the residual nucleus on one of the low-lying energy levels (so far we are familiar with one such experiment carried out with a carbon nucleus).

Close attention is being given to experimental studies of direct reactions at high energies, specifically quasielastic scattering reactions. Discussion centers on identifying the mechanism behind the reaction. An essential shift in this trend is the staging of many experiments, suggested by theory, which are most crucial for establishing the mechanism underlying the direct process.

The work done at our institutes has made weighty contributions to the study of processes in which high-energy particles interact with nuclei. Some research efforts have been distinguished by original initiative in the statement and solution of the research problems, which has opened the way for qualitatively new and interesting physical results. In particular, Soviet experiments on identifying the mechanism underlying nuclear reactions at high energies appear to be the most comprehensive, exhaustive, and most versatile at the present time. Substantial results have also been obtained in the experimental study of processes of inelastic scattering of high-energy particles on nuclei, scattering of pions on few-nucleon systems, and in the investigation of several other specific problems.

As for the experimental data obtained at leading foreign laboratories, and discussed at the seminar, new results on the study of bound states and resonances in the nucleon—antinucleon system attracted considerable attention, as did observations of excited states of hypernuclei forming in the reaction $A(K, \pi)A^{*}_{\Lambda}$ on a beam of fast kaons, and direct indications of the presence of an isobaric impurity in the ground state of the deuteron, obtained with the aid of the quasielastic scattering reaction of pions on the intradeuteronic isobar [here we are concerned with the process $d(\pi^{+}, \pi^{+}\Delta^{+})\Delta^{0}$ at 15 GeV/c pion momentum].

The proceedings of the seminar are to be published sometime in 1974.

SESSION OF THE INDC, OCTOBER 1973

G. B. Yan'kov

The regularly scheduled (sixth) session of the International Nuclear Data Committee (INDC) was held in Vienna, October 8-12, 1973.

Traditional topics discussed at the sessions were: reports from the various countries on experimental research and data evaluation over the past year, information on new facilities, reports by standing subcommittees of INDC, reports on the activities of four neutron data centers, a worldwide list of inquiries and requests (WRENDA), the SINDA compendium, aid to developing countries in organizing research on nuclear data, summaries of recent conferences and proposals on future conferences, various aspects of the collection of nuclear data requirements, and exchange of information, plus elaboration of appropriate recommendations.

New problems prompted by the development of nuclear science and nuclear engineering make their appearance at almost every session of the committee. One such new, and unresolved, problem that turned up at the last session (see Atomnaya Énergiya, 33, 1008 (1972)) was the INDC definition of its position on nonneutron nuclear data. Increasing demands for nonneutron data needed in the solution of various practical and applied problems has led in recent years to a certain expansion of the range of topics to be handled and tackled by committees (commissions) on nuclear data of the several countries involved (Britain, USSR, USA, France, Sweden, etc.). These demands were also clearly in evidence in the work of the IAEA "Applications of Nuclear Data in Science and Industry" symposium in March 1973 (see Atomnaya Énergiya, 35, 143 (1973)). It was decided, as a result of discussions in a specially appointed INDC subcommittee and at the general session as well, that INDC will include within the sphere of its normal activities nonneutron nuclear data to be used in various applications; but the principal interests of the committee will remain focused as before on neutron data.

A certain expansion in the scope of INDC activities was reflected in the restructuring of the work being done by the standing subcommittees of INDC. Two of these subcommittees, the one on standards in nuclear data and the one on discrepancies in the basic nuclear constants, retain the same line of direction; elaboration of some recommended standards on nonneutron data is now included in the rubric of the problems handled by the standards subcommittee. Two new standing subcommittees were set up: one on nuclear data for the nuclear power industry, and one on nuclear data for applied areas exclusive of nuclear power. The purposes and problems of the first subcommittee is to draw up a list of needs and demands in all types of nuclear data for all areas of the nuclear power industry, including reprocessing of fuel and wastes, the system of guarantees, fusion reactors, and maintenance of contact and liaison between producers and consumers of nuclear data in the industry. Problems within the purview of the second new subcommittee are analogous to those tackled by the first except for the stipulation that applications be outside the nuclear power field, but do fall within the scope of normal IAEA activities (e.g., dosimetry in biology and medicine, various applications of radioactive isotopes, activation analysis, and industrial applications).

At the present writing, we still have no system for international exchange of information on nonneutron data. In the future, this type of exchange is to be carried out via the appropriate research centers or groups of scientists in countries where there are no such centers as yet. In the USSR, information on nonneutron nuclear data is being accumulated in two centers: at the Atomic and Nuclear Data Center (TsAYaD) of GKAE (I. V. Kurchatov Institute of Atomic Energy [IAE], Moscow) and at the center attached

Translated from Atomnaya Énergiya, Vol. 36, No. 3, p. 238, March, 1974.

to the B. P. Konstantinov Leningrad Institute of Nuclear Physics of the USSR Academy of Sciences (facilities located at Gatchina).

INDC recommends that IAEA schedule the first international congress of research centers (and groups of scientists) on nonneutron data in the spring of 1974, principally for the purpose of arriving at agreement on technical problems pertaining to exchanges of information on the structure of the nucleus.

A characteristic feature of work done on nuclear data in the 1972-1973 period is the fact that attention remained centered, as earlier, on basic reactor materials (fissionable materials and structural materials), and also on the characteristics of nuclear processes taken as standards. Experimental physicists working at some laboratories did not limit themselves, in their publications and contributions, to presentation of the experimental data obtained, but also ventured updated evaluations and estimates of the variable measured. The number of research efforts concerned with medical applications and thermonuclear facilities was on the increase. Estimates of nuclear data are being carried out on a broad scale. This included both the procurement of new estimated data and refinements in already available data; specifically, a fourth version of the file or library of estimated data known as ENDF/B has been proposed as a program of work for 1974 in the USA. IAEA has published a list of requests for nuclear data relating to the technical methods in the system of guarantees; demands submitted by the USSR, USA, and West Germany are included. The next edition (both old and new demands brought up to date) will be published in 1974, both in the WRENDA list and separately. A list of demands and requests for nuclear data relating to thermonuclear fusion reactors, compiled on the basis of requests submitted by Britain, the USSR, USA, France, and West Germany, has also been prepared.

The third international conference on nuclear data, scheduled for 1974, will apparently be held not earlier than 1977. An IAEA scientific conference on nuclear standards, both neutron and nonneutron, has been proposed for 1976.

The next INDC session will be held in October 1974, at the Australian nuclear research center not far from Sydney.

III INTERNATIONAL CONGRESS ON RADIATION SHIELDING (WASHINGTON, SEPTEMBER 1973)

A. D. Turkin

The III congress on radiation protection, held in Washington, September 9-14, 1973, under auspices of the International Radiation Protection Association (IPRA), attracted some 6500 members from 60 countries. Participating in the work of the congress were 891 delegates (five from the USSR) and observers from the UNO, IAEA, WHO, IRPC, Euratom, Unesco, IRRC, and also from the USAEC and USA NRPC. About 230 reports were presented (of which 42 from the USSR), covering the following major problems in the domain of radiation protection work: biological effects of ionizing radiation, including remote sequelae, uranium metabolism and metabolism of the transuranium elements, personnel dosimetry, models for computing dose in external and internal exposure, radiation safety in production, radiation emergencies, doses from sources of natural origin, doses from nuclear facilities, irradiation due to medical procedures, aerosols, models for computing radiation dose level in the lungs, determination of human body radioactivity, radioactive wastes and environmental radiation monitoring, radioecology topics, units of measurements of ionizing radiation, biological effects of nonionizing radiation (radio waves, ultraviolet radiation, etc.), training and qualification of specialists in the radiation safety field.

The topic of greatest interest at the congress was known as "radiation and humans." A review paper entitled "Effects on the population irradiation by low levels of ionizing radiation," prepared by the National Academy of Sciences of the USA, surveyed calculations of genetic damage that can victimize anywhere from 1100 to 2700 persons per year out of a population of 200 million when the dose level is 170 mrem/year. Given the same initial parameters, somatic effects can bring about 3000 to 15,000 deaths per year from cancer. The dose doubling the number of genetic damage incidences is in the 20 and 200 rem range, in the opinion of the authors of the review. The dose load comprising 5 rem per human can lead, within the span of three decades, to anywhere from 60 to 1000 genetic mutations in the first generation, or 300 to 7500 mutations in the "equilibrium number of generations" per million of the population exposed.

A dose of 1 rem would lead us to expect 1 case of leukemina; 2 to 9 cases of thyroid cancer in children; 1 terminal case of breast cancer in women; 0.2 case per million persons per year for all other forms of cancer malignancies.

The authors of the survey feel that if the population of the USA (some 200 million) are continuously exposed to a dose load of 0.1 rem/year throughout their lives, this will result in anywhere from 1726 to 9078 fatalities per year in terms of cancer, which corresponds to an increase in the natural mortality level due to cancer of 0.6 to 2.9%.

The survey takes up the question of whether the dose load to which the USA population is exposed, accountable to the nuclear power industry as it will be in the future, can be kept to within 1% of natural background, i.e., not higher than 1 mrem/year, to avoid such consequences.

In estimating the hazard of malignant tumors appearing in persons subjected to whole-body irradiation by γ-photons, S. Mace (USA) uses and analyzes data on persons who survived an atomic explosion, data on patients who have undergone x-ray therapy, and exposed radiologists, most of them from either the city of Nagasaki or radiological centers. The number of mortalities due to exposure to γ-radiation with consequent induction of malignancies from among one million persons of mixed ages, each of whom received 1 rad exposure dose over the entire body, is estimated. The author notes that, for a dose rate below 0.01 rad/min, the total number of malignant neoplasms is ten times less than for a dose rate of 10 rad/min.

Translated from Atomnaya Énergiya, Vol. 36, No. 3, p. 239, March, 1974.

Reports by N. G. Gusev et al., V. P. Rublevskii (USSR), and A. Hull (USA) cite data on radioactive discharges to the environment at nuclear power plants in the USSR and in the USA. The amount of those discharges is not in excess of levels set down in governing regulations.

Characteristic of the reports on the metrology of radiations, such as: "Equivalent dose equation" (H. Wakoff, USA), "Quality factor in IRPC interpretation" (H. Rossi, USA), "Experimental and computational program for obtaining the relationship between quality factor and linear energy loss" (J. Neufeld, USA), is the attempt to find a variable proportional to the concrete morbid or injurious effect of distinct modes of ionizing radiations. Several terms have proposed to denote this variable, including "acceptable risk dose."

A proposal voiced by a representative of the International Bureau of Measures and Weights, A. Allisi (France), to extend the international SI system to units of ionizing radiations met with no support.

OUTLOOK FOR UTILIZATION OF IONIZING RADIATIONS IN THE RUBBER INDUSTRY*

A. S. Kuz'minskii

That a whole set of valuable engineering properties marking off the various grades of rubbers in contrast to other polymeric materials has been established is due to the development of the three-dimensional spatial network in the process of rubber vulcanization. Vulcanizing agents, accelerators, activators participating in the formation of crosslinkages, and differing in their nature and in their densities, are generally introduced into the rubber being processed in order to achieve this crowning stage in the production of rubber products. The use of ionizing radiations in rubber production will make it possible to achieve fundamentally new approaches to the design of spatial crosslinked structure in elastomers.

Here we consider only applied aspects of the problem (the theoretical basis of the problem has been presented in the appropriate texts [1, 2]). First of all, when using radiations we are free to eliminate completely from the recipe for the rubbers being made any ingredients of the vulcanizing group, which then obviates any possibility of such a harmful spontaneous process as scorching (premature vulcanization) occurring. Washout and volatilization of sulfurs and accelerators so that these latter gain access to the environment, and migration of sulfur and accelerators to the surface of rubber mixes, cured rubbers, and rubber wares, are then rendered impossible. Contamination of liquids and gases in contact with the rubber by those products is often to be avoided if at all possible. The vulcanizing agents hinder the normal functioning of heat stabilizers, and that has a marked deleterious effect on the ageing resistance of rubbers. Finally, the possibility of bringing about vulcanization at room temperature would obviate generation of locked-in internal stresses and heat sets in the rubber.

It is predominantly C—C bonds that form in radiation vulcanization, and these linkages are characterized by high energy, while their density may vary over a wide range even with no change in the batch recipe. This new approach in rubber manufacturing technology can bring about a change in properties engineered in some desired and prespecified direction.

When rubbers are in service in contact with oils, greases, and other aggressive fluid media, an increase in the density of crosslinkages not only reduces the chemical relaxation rate, but also lowers the swelling limit, i.e., it has a helpful effect on the most crucial properties of the rubbers.

Various radiation-treated rubber grades boast high chemical stability to corrosive attack, frost, and wear.

Molded, extruded, and shredded products can all be fabricated by the radiation vulcanizing method. As a consequence of serious achievements in recent years in the field of radiation-processing equipment design and radiation-induced graft polymerization and sensitization, a real possibility of building continuous high-capacity production lines incorporating synchronously operating molders and electron accelerators is at hand. Sensitized radiation vulcanization is characterized by high speeds running from 2 to 40-50 m/min.

Consequently, two trends have now emerged in the utilization of radiations to cure or vulcanize rubbers: devising materials with a set of prespecified new properties and developing continuous radiation-chemical processes.

*An all-Union conference on the utilization of ionizing radiations in the rubber industry was held in Moscow, September 10 through September 13, 1973. The editors submitted a request to Professor A. S. Kuz'minskii that he give an account of the current outlook for utilization of ionizing radiations in this important branch of the national economy.

Translated from Atomnaya Énergiya, Vol. 36, No. 3, pp. 239-241, March, 1974.

TABLE 1. Radiation-Chemical Yields of Crosslinkages and Optimum Vulcanization Doses for Rubbers

Elastomer	Radiation-chemical yields, crosslinkages /100 eV	Dose, Mrad
Natural isoprene (NK)	2,0	
	1.05	
	1.4	30-40
	1.1	
	1,0-3,5	
SKI-3 (cis-polybutadiene)	1.2	30
Polybutadiene-1,4-cis (SKD)	5.3	
	3.8	
	7.1	25
	8.0	
1,2-polybutadiene (SKB)	20	20
SKS containing styrene linkages, %		
23	2.8	
28	1.7	20
38	1.55	
SKS-30	3.5	20
SKN-26	9.0	25
SKÉP	3.0	40-50
SKT	2.7	10
SKTV-1	1.7	5-7
Fluorine-containing rubber grades		
SKF-26	0.54	25-35
SKF-32	0.16	35-40

In some cases, these two trends are materialized at the same time, or in the same process. All grades of rubber other than silicones, as indicated in the accompanying Table 1, are characterized by moderate radiation-chemical yields of crosslinkages and consequently by high optimum exposure doses. Consequently, in order to achieve continuous processes, dose levels have to be brought down to 5-10 Mrad when processing these grades of rubber. This can be successfully achieved through the use of oligoester acrylates for radiation-chemical grafting in rubber media. In addition to speeding up the rate of vulcanization, the oligomers impart various important properties to the rubber mixes and finished rubbers [3]. It should be stressed that oligomers are polyfunctional not only in their structure, but also in the way they affect the untreated mixes and finished rubbers, since they do service first in the form of temporary plasticizers, and then in the form of accelerators and vulcanizing agents. An increase in processing rate, especially of rigid mixtures (mixing, injection), and a high rate of vulcanization, are combined harmonically in radiation grafting.

We also note that the use of chemical initiators calls for certain compromises given the presence of stabilizers and blacks in the mixtures, since blacks hinder normal functioning of the stabilizers. We must also deal with the fact that the ingredients selected for radiation-induced vulcanization must not increase the optimum vulcanization dose of radiation.

Suitable sources of radiation for vulcanization of rubbers are ^{60}Co and electron accelerators; each of these sources has its own advantages and disadvantages [4].

In selecting an assortment of products to be processed through radiation-induced vulcanization, we have to take into account the limitations connected with the use of the above sources. Low optimum vulcanization doses render electron accelerators economically competitive with chemical vulcanization, and technologically the electron accelerators come out ahead in the competition even when compared to existing continuous vulcanization processes (hot-air vulcanization, salt-bath vulcanization, microwave-current vulcanization, and fluidized-bed vulcanization).

We can include among the promising trends in radiation chemistry of rubbers that are undergoing encouraging development:

1) radiation vulcanization of silicons and fluorocarbon elastomers;

2) irradiation of rubber wares vulcanized chemically in either complete process or short-cut process, in order to improve physicomechanical properties, in lieu of an after-vulcanization step in vulcanizing kettles and heaters;

3) grafting of polyfunctional compounds within the bulk of the rubber mix, in order to speed up the process and improve the performance characteristics of the rubbers;

4) grafting polyfunctional compounds on the surface of the rubbers with the object of improving resistance to attack by ozone, enhancing ability to adhere to metals and fibers;

5) radiation-induced halogenation of the surface in order to lower the friction factor, which is analogous to enhancing resistance to wear;

6) radiation-chemical synthesis of rubbers from fluid crude rubbers and from monomers;

7) grafting on fibers, fabrics, metals, and fillers of vapor-phase monomers, in order to achieve modification of properties;

8) irradiation of crude rubber mixes with small doses, in order to increase cohesive strength, improve the backbone structure, and minimize heat set in extruded and calandered wares.

At the present time, many of the processes in question are being engineered into technological reality on a pilot scale and on a full production scale.

LITERATURE CITED

1. A. S. Kuz'minskii, T. S. Fedoseeva, and F. A. Makhlis, in: Radiation Chemistry of Polymers [in Russian], Nauka, Moscow (1973), p. 306.
2. A. S. Kuz'minskii, T. S. Fedoseeva, and F. A. Makhlis, Zh. Vsesoyuz. Khim. Ob-va. im. D. I. Mendeleeva, No. 3, 285 (1973).
3. A. S. Kuz'minskii, A. A. Berlin, and S. N. Arkina, in: Advances in the Chemistry and Physics of Polymers [in Russian], Khimiya, Moscow (1973), p. 239.
4. A. P. Bogaevskii, A. S. Kuz'minskii, and V. I. Treshchalov, Kauchuk i Rezina, No. 11, 4 (1972).

GKAÉ SSSR FAST REACTOR SPECIALISTS VISIT NUCLEAR RESEARCH CENTERS IN WEST GERMANY

L. A. Kochetkov

A delegation of fast reactor specialists from GKAÉ SSSR [USSR state committee on peaceful uses of atomic energy] visited scientific and industrial centers of the German Federal Republic from August 5 through August 18, 1973. This was a return visit under the terms of an understanding entertained between GKAÉ SSSR and the Ministry of Research and Technology of West Germany.

Our program included visits to scientific research centers located at Julich and Karlsruhe, the nuclear power plant under construction at Biblis, the Interatom concern in Behnsberg, the RWE concern in Essen, and the Alkem and RBG concerns in Chanau. At our concluding meeting at the Ministry, an exchange of views was held on the possible scope of further collaboration in the future in the field of fast reactors.

The Julich scientific research nuclear center was founded 15 years ago; at the present time its thirty institutes employ about 3600 personnel, including about 600 research scientists; the center's annual budget runs to 220 million marks. The varied scope of the center's activities includes research and development work on high-temperature gas-cooled thermal reactors (HTR type). Stages in this program are:

1) one reactor in operation (since 1967), the 15 MW(e) AVR;
2) the THTR reactor under construction in the Wentrop district (completion scheduled 1976), with a thorium loading to generate 300 MW(e);
3) a 1000 MW(e) reactor under development (target date 1980). A broad front of scientific research is being tackled to bring this facility into being; two variants are being worked on concurrently: one with a two-loop thermal arrangement, the other with a single-loop arrangement. A test stand for work at temperatures to 1000°C is being built to validate the latter concept, and to finalize the design of individual loop components (bellows, thermal insulation) and power and loop equipment, including turbines.

The directors of the research center view the HTR reactor as West Germany's front-running reactor type, since it is simple, features low operating costs, and requires only modest makeup of fissionable materials, while being distinguished by great operational safety, and does not require sources of water to carry off low-temperature process heat. Under the conditions prevailing in West Germany, that is of fundamental significance, since readily accessible water resources will be used up in West Germany within a space of about ten years. Moreover, this type of reactor promises to be also efficient in its use for chemical engineering and industrial purposes, as for example in gasification of brown coal grades. These aspects of the HTR concept are being worked on diligently.

Impressive advances have been achieved in the HTR design. We were most impressed by the fabrication of spherical fuel elements designed by Professor Schultin; by the continuous reloading system serving the reactor, with remote automatic monitoring of the soundness of the fuel elements and of the percentage burn-up; by the ability of the core to withstand very heavy damage with both gas blowers shut off even at full power level, and even with the reactor emergency protection system malfunctioning because of the maintenance of low excess reactivity and high temperature effect.

The leading figures at the research center do not put much hope on the gas-cooled fast reactor, because of the high heat loads required in its core.

Translated from Atomnaya Énergiya, Vol. 36, No. 3, pp. 241-242, March, 1974.

The national atomic research center at Karlsruhe was founded in 1956, and is responsible for training cadres and for fundamental research in the fields of physics, biology, and environmental protection; there are 4000 or so personnel employed here. The total budget is figured at 280 million marks; 25% of the budget is allocated to work on the sodium-cooled fast reactor program, 5% to work on the fast reactor concept with steam-and-gas cooling. The principal research trends in the domain of fast reactor studies are: development of overall strategy and policies regarding fast reactors; safety problems; experimental and theoretical reactor physics; the fuel cycle, including development and regeneration of fuel elements; special materials studies; heat transfer research, and sodium technology; development of wastes disposal techniques.

In addition to the Karlsruhe research center, there is also independent work on fast reactors being done by the Interatom concern. This international organization (with affiliates in the Netherlands, and Belgium, as well as West Germany), employs 1200 and 67% of the budget goes into faster reactor development. The firm is responsible for planning and design work, and for developing and testing reactor system equipment. To accomplish those tasks, it has at its disposal an up-to-date complex of sophisticated experimental facilities, including a set of large and small sodium loops.

At the present time, an extensive research program on fast reactors with oxide fuel and sodium coolant is underway in West Germany. This program includes both development of fast reactor projects (the KNK-II by 1975, the SNR-300 by 1979-1980, the SNR-2000 by 1985), and execution of scientific research and experimental design work, including building the KNK-I sodium-cooled thermal reactor (1969). The chief purpose of this program, at the present time, is to build the SNR-300 demonstration reactor near Kalkar, construction work on which was begun in April 1973. We can safely assume that the basic theoretical and experimental work in progress at the present time is geared to the validation of solutions for the SNR-300 concept.

The SNEAK fast physical assembly (Karlsruhe) with core volume 22 m^3, core equipped with top and bottom reloading machines, and automatic reloader for experimental fuel assemblies which is controlled by electronic computer, a neutron source (10^9 neutrons/sec), and an oscillator, has been built to facilitate physical experiments. The assembly is provided with 300 kg plutonium and 1200 kg ^{235}U.

While there is no doubt about the choice of fuel for the facility (a mixture of uranium oxide and plutonium oxide), selection of materials for the hexahedron and jacket of the fuel elements could still profit from some further refinement after radiation tests have been completed. At the present time, preference is being given to 1.4948 steel* for the reactor pressure vessel, to 1.4981 steel* (15% cold-worked) for the fuel-element hexahedron, and to 1.4988 steel* for the fuel-element jackets. The criteria followed in selecting the fuel-element jacket material (cladding) are durability, creep behavior, response to corrosive attack from the inside. The last criterion is viewed by Karlsruhe specialists as the principal factor in any attempts to obtain better than 8% burn-up.

In terms of heat transfer and fluid dynamics, the brunt of the work is placed on detailed studies of thermal and hydrodynamical processes occurring within the fuel assembly when different departures from the normal in the geometry and output of the fuel elements prevail, and also when the total flowrate through the fuel assembly experiences changes. Processes at work in local and overall boiling of sodium in the fuel assembly are also being looked at closely. Highly impressive and important advances have been achieved in this area as well. We formed the impression, on the basis of the work done at Schleisig, that local damage done to the fuel element (meltdown of the fuel element) does not lead to propagation of the disturbance along a chain. We also attach importance to the conclusion that overheating and failure of fuel elements in response to boiling of the sodium cannot be avoided through detecting pressure fluctuations originating in the collapse of sodium bubbles, since this process takes place at an extremely rapid pace (~1 sec).

We should also mention the concept developed by West German specialists (Eitz, Traube, et al.) concerning the safety of fast reactors and other reactors. Existing nuclear power station projects have recently been reexamined and revised in West Germany with the purpose of effecting substantial improvements in the safety of the facilities, and setting up safety margins and standby solutions. This is part of an effort to achieve reliable performance on the part of those facilities while preparing public opinion for more widespread acceptance of nuclear power plants. In particular, personnel safety requirements and

* Designations adopted in West Germany for certain steel grades.

environmental safety requirements imposed on nuclear power station projects call for safe operation in the face of earthquakes of up to 8 points severity (on the Richter scale), a head-on crash of a modern airplane on the power plant building, explosion of the gas cloud forming when two tankers collide, maximum emergency damage with complete interruption of the heat removal system, plus failure of the emergency protection (scramming) system to function, and so on and so forth. A system of step-by-step permits or licenses is introduced into nuclear power plant building practice, at the discretion of a specially appointed governmental monitoring agency which is empowered to forward or withdraw approval of the contractor's work. For example, permission to proceed to the first stage of the construction program (first out of five eventual stages) was given in the case of the SNR-300 reactor project, with 97 conditions which required, all told, a 20% increase in the original one-billion-mark budget drawn up. Satisfaction of similar requirements, in a similar way, increased the capital construction costs for the second unit of the Biblis nuclear power station by a factor of one and a half.

We could not close without mentioning the kind attentiveness and friendly welcome we were privileged to experience throughout our visit.

RRPS-1 RADIOISOTOPE RELAY DEVICE WITH SCINTILLATION DETECTOR MODULE

V. M. Iryushkin, S. B. Maslennikov,
Yu. A. Skoblo, and V. B. Timofeev

This new device was developed at the All-Union Scientific-Research Institute for Radiation Equipment (VNIIRT). It is intended for widespread use in various branches of the national economy (as an on-off controller of the interface between two media, a contactless limit switch, an on-off thickness gage, density gage, and so forth). The RRPS-1 features broad control ranges for its basic parameters (response threshold, dropout threshold, time constant, hysteresis) which is helpful in expanding the range of problems that can be successfully tackled with the aid of the device, and in enhancing the versatility of the device. Reliance on a scintillation detector boasting a high efficiency in recording γ-radiation, and the stable basic parameters of the device, render it useful in solving problems where there is a small radiation flux density drop, and when sources of low-level γ-radiation are employed. As performance tests have revealed, the RRPS-1 arrangement is useful in solving problems where the radiation flux density drop (ratio of maximum to minimum value) is as low as 1.25.

The RRPS-1 arrangement consists of three functional modules designed separately: a radiation source module, a detection module, and a radio electronics module.

Series-manufactured É1M-É4M model units containing sealed ^{60}Co γ-emitting sources (exposure dose rate $1.2 \cdot 10^{-8}$ to $1.2 \cdot 10^{-7}$ r/sec at a distance of one meter) or ^{137}Cs γ-emitting sources (exposure dose rate $1.2 \cdot 10^{-7}$ to $4.7 \cdot 10^{-4}$ r/sec at a distance of one meter) are used as the radiation source module in the RRPS-1.

The scintillation detection module comes in two variants: the normal GDS-2 variant and the special explosionproofed GDS-2V variant. The sensitivity of the detection module is not less than $6 \cdot 10^9$ pulses/r. The length of cable joining the detection module to the radio electronics module can be increased to 300 m.

The BR-2 radio electronics module is designed to process the signal arriving from the detection module, and to shape a control command to be sent to the executive relay, with simultaneous annunciation

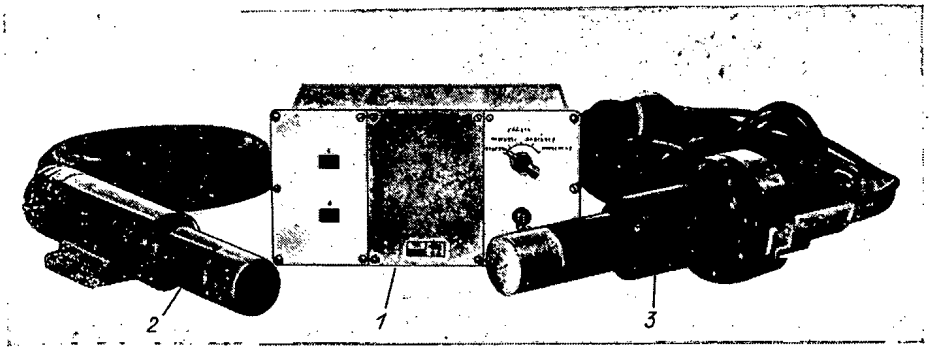

Fig. 1. General view of the RRPS-1 device: 1) BR-2 radio electronics module; 2) GDS-2 detection module; 3) GDS-2V explosionproofed detection module.

Translated from Atomnaya Énergiya, Vol. 36, No. 3, pp. 242-243, March, 1974.

of the state of the relay by visual light signal. The device is also provided with a contactless output terminal with a 0-5 mA current signal. The electrical response threshold can be set anywhere from 10 to 20,000 pulses/sec. The basic generalized instability of the response and dropout thresholds is not greater than 6%. The time constant of the device is regulated anywhere from 0.1 to 10 sec, hysteresis anywhere from 0.4 to 0.9. The device can be operated in either positive or negative mode. The power that can be switched amounts to 500 W at 300 V ac voltage, with current to 5 A. The range of operating temperatures extends from —40° to +50°C. The additional generalized threshold instability in response to temperature changes is not greater than ± 0.3% per 1°C.

The device has successfully passed state licensing tests and performance tests. Series manufacture of the instruments is being planned.

The reader can examine a general view of the BR-2 radio electronics module, and the GDS-2 and GDS-2V variants of the detection module, in Fig. 1.

STEREO TV FOR NUCLEAR ENGINEERING

É. M. Afonin, Yu. A. Gerasimov,
G. P. Malyuzhonok, and A. I. Lunin

Work with radioactive materials and in locations of high-intensity radiation is usually limited in time or outright forbidden. All kinds of remote handlers and manipulators are used in such situations. Glass windows, periscopes, liquid windows, mirror systems, TV devices, and other arrangements are used for observation.

Most versatile are TV devices which frequently are the only means for transmitting visual information which allow the operator to be at any distance from the handled material and to be protected by any desirable shield. However, the absence of depth perspective makes it impossible for the operator to determine the actual distance between the slave mechanism of the manipulator and the handled object.

Especially effective is the use of stereoscopic TV devices which provide a three-dimensional image of objects in the field of view of the transmitting stereo TV camera.

Specially designed stereo TV devices, based on the two-channel closed-circuit TV principle, are used at the I. V. Kurchatov Institute of Atomic Energy and the Serpukhovo proton accelerator. By means of an optical system consisting of two objective lenses and focussing and convergence units, the object image is projected onto the left and right targets of two vidicon tubes. The tubes convert visual information into a video signal which is transmitted through a cable to two 35LK4B kinescope picture tubes where it is converted back into an image. The screen of one picture tube is directed towards the operator, the other screen lying horizontally at an angle of 90° to the first. A semitransparent mirror is placed at an angle of 45° between the two screens. The two images pass through perpendicularly polarized filters onto the semitransparent mirror. One image passes through the mirror, while the other is reflected towards the operator. The operator is equipped with polaroid eyeglasses which reconstruct a three-dimensional image of the object in the screen plane. The TV set includes the transmitting stereo camera on a rotatable mounting, a channel unit, a power supply unit, a video monitor, operator eyeglasses, and a set of connecting cables (Fig. 1). The stereo camera is radiationproof.

The TV set has been designed at the Special Design Bureau of the Institute of High Temperatures, Academy of Sciences of the USSR.

Technical Specifications. Image scanning is interlaced at 625 lines and 25 frames per second. The resolution with an LI-409 vidicon tube, as measured on the video monitor screen with a fixed 0249 test pattern (illumination 10 lx in the target plane), was 500 lines at the center and 450 lines at the edge of the vertical wedge. The image brightness corresponds to a discernibility of at least six gradations including the test pattern background. The set can be fitted with one of the following three stereo cameras: a camera with exchangeable remote-controlled optics for work in air, with exchangeable remote-controlled optics for work in magnetic fields, and a miniature camera for underwater work.

Maximum length of cable connecting the camera to the video monitor is 300 m. The cameras are fitted with Zh-49 and Zh-51 objective lenses with focal lengths 22 and 50 mm respectively. The aiming mechanism provides remote control of the camera rotation through an angle ± 135° in the horizontal plane and ± 45° in the vertical plane. At an object illumination of 1500 lx, the matching error of the Zh-49 and Zh-51 lenses is less than 3 and 2 mm respectively for a depth of 1 m, and 12 and 5 mm respectively for a depth of 2 m. With an object illumination of 2000 lx, the matching error in water is 3 and 7 mm at a depth of 1 m for the Zh-49 and Zh-51 lenses respectively, and 15 mm at a depth of 2 m for the Zh-51

Translated from Atomnaya Énergiya, Vol. 36, No. 3, pp. 243-245, March, 1974.

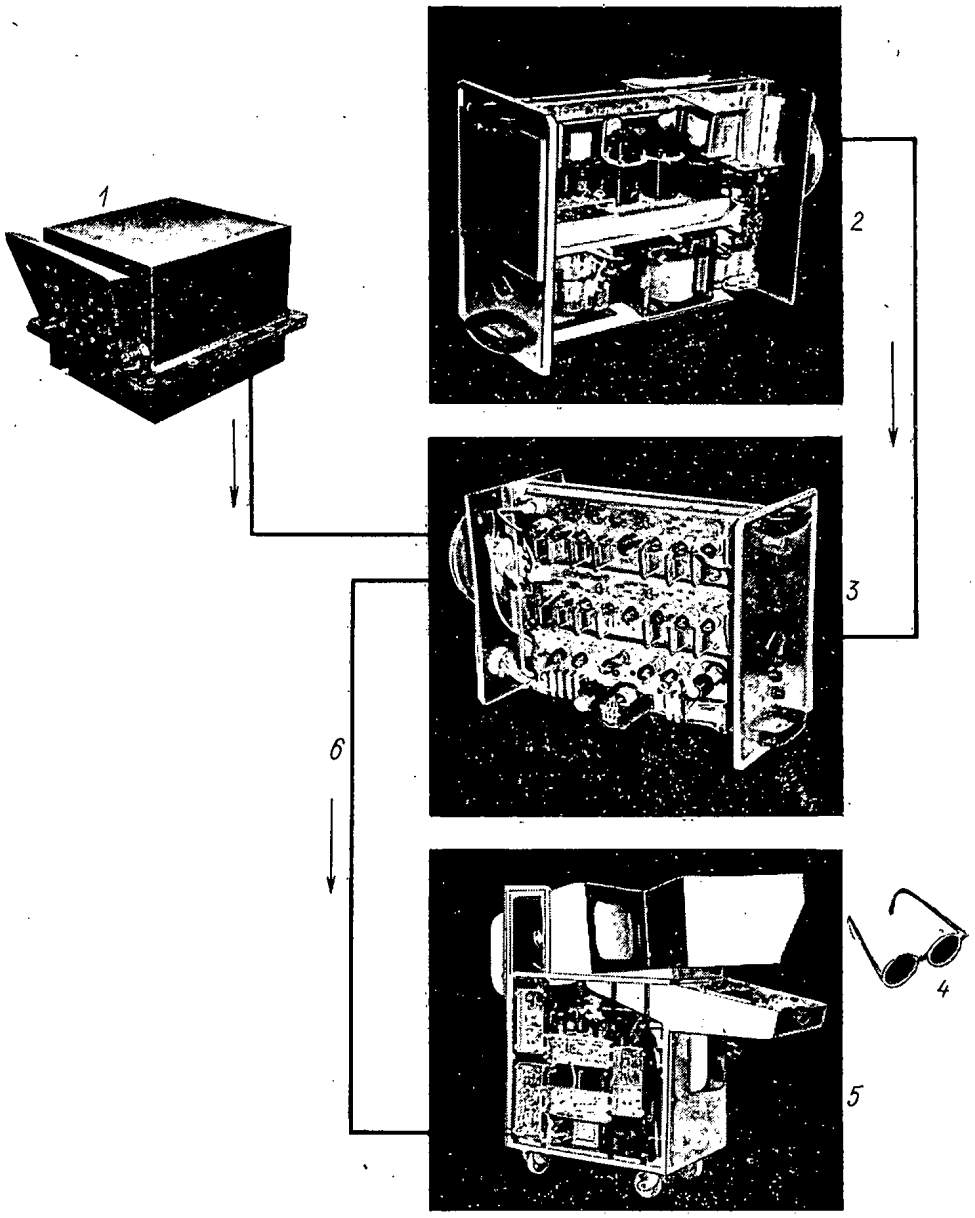

Fig. 1. Stereo TV set for nuclear engineering: 1) stereo camera; 2) power supply; 3) channel unit; 4) polarized eyeglasses; 5) video monitor unit; 6) connecting cable.

objective lens. Total power consumed by the set is 0.9 kW. The set is fed from a 220 V, 50 Hz power line. The dimensions of the individual units composing the set are:

Air camera	510 × 450 × 220 mm
Underwater camera	310 × 128 × 55 mm
Channel unit	690 × 270 × 380 mm
Power supply unit	690 × 270 × 380 mm
Video monitor	1300 × 485 × 1270 mm
Connecting cable diameter	22 mm

The stereo TV set allows individual and group observation with a single video monitor, while its relative operating simplicity allows widespread application in industrial conditions. Of special importance is the application of the stereo set in nuclear engineering for remote controlled maintenance, disassembly, and preventive operations.

A stereo TV set with a remote camera on a mobile stand allows reloading operations to be carried out remotely practically without errors, place dosimetric instruments in dangerous locations, investigate damaged regions, convey service tools to locations where work is to be carried out, install and set into operation various instruments, collect spillovers of radioactive products, move radioactive materials from place to place, etc.

The availability of remote-controlled exchangable optics in the stereo camera ensures versatility and improves the accuracy of operations.

The use of stereo TV significantly reduces the maintenance time, increases the safety of the conducted operations, improves the reliability, and allows considerable economical gain.

PRELIMINARY INFORMATION

THIRD SCIENTIFIC CONFERENCE ON POWER ECONOMICS OF THE ZITTAU HIGHER SCHOOL OF ENGINEERING

To commemorate the 25th Anniversary of the German Democratic Republic, the Third Scientific Conference on Power Economics will be held at the Zittau Higher School of Engineering on November 13-15, 1974. As all former Conferences, the Third Conference will be attended by many local and foreign scientists.

The first day of the Conference is to be devoted to a plenary session which will be addressed by the Minister of Coal and Power Industries of the GDR, Mining Engineer K. Siebold and by the Deputy Minister of Power Engineering and Electrification of the USSR, H. D. Mal'tsev. The plenary session will be followed by meetings divided into four sections:

1) problems and methods of increasing the generation of electrical power from an organizational point of view;
2) problems concerning the design, installation, and exploitation of power plants;
3) improving the efficiency of construction and operation of electrical power plants;
4) improving the efficiency of power utilization.

The prorector of the Higher School of Engineering, Prof. Dr. H. Schumann will be responsible for organizing the Conference.

A debate on nuclear power engineering and a discussion devoted to education in the field of power economy will be held (for participants with special invitations) in the course of the Conference.

For further information and invitations to the Conference please apply to Ingenieurhochschule Zittau, DDR 88 Zittau, Strasse der Jungen Pioniere 2.

Translated from Atomnaya Énergiya, Vol. 36, No. 3, p. 245, March, 1974.

A. G. Kharlamov

MEASUREMENTS OF HEAT CONDUCTION IN SOLIDS*

Reviewed by S. A. Skvortsov

The text describes existing methods in experimental determination of the thermal conductivity of solids. One remarkable feature of the book is the fact that the range of topics covered includes in-pile measurements in subloops and capsules in various (predominantly research) nuclear reactors.

The inclusion of this topic in the text stems from the fact that several new materials in use in modern nuclear reactors have properties, thermal conduction in particular, which depend on the irradiation conditions, and that these dependences can be determined solely on the basis of in-pile tests.

Consequently, the content of the book is in line with a special trend rendering the text interesting to workers in nuclear industry responsible for the operation of nuclear power plants, as well as to research scientists. It therein differs substantially from similar current texts describing methods used in thermal conductivity measurements.

The author takes up various measurement techniques in a rather exhaustive treatment, as we see it, reflecting an up-to-date coverage of the experimental methods in use. It also seems that the descriptions presented in the text fall short of adequate coverage for practical needs, and that the research scientist interested in comparing some of those methods for use in his work will still have to turn to the specialized literature on the topic. Moreover, the book offers too limited space to accommodate fuller and more detailed descriptions. It is worth noting that the author presents a generous bibliography (319 titles), so that the reader can orient to the necessary sources with ease.

On the whole, the book is written on a sufficiently high scientific level; it will undoubtedly be useful to a broad range of research scientists, designers, and engineers, particularly any persons concerned with reactor materials science, and will also be found useful by college students majoring in the appropriate subjects.

One shortcoming that should be pointed out is the incompleteness of the analysis in the presentation, so that the reader does not obtain a clear picture of which of the methods described would be preferable in what applications.

In his discussion of nonstationary methods, the author does not consistently stipulate for what sets of conditions the basic equations used in the determinations were solved. It seems to us that many of the equations were derived for the condition λ = const, but the author frequently omits mention of this. The author does not go into sufficient detail on how to determine the power released in specimens and structures in in-pile experiments.

The book is not free from misprints, occasionally rather vexing ones. Diagrammatic illustrations are often marred by obscurities.

All of these defects should be eliminated in subsequent editions of the book.

*Atomizdat, Moscow, 1973.

Translated from Atomnaya Énergiya, Vol. 36, No. 3, p. 246, March, 1974.

A. I. Klemin

ENGINEERING PROBABILISTIC CALCULATIONS IN NUCLEAR REACTOR DESIGN*

Reviewed by S. V. Bryunin

This book deals with the methodology of probabilistic-statistical computations involving the solution of crucial problems in nuclear reactor design, in particular forecasting the reliability of a reactor and of nuclear power station equipment, estimating the radiation safety of a nuclear power station, planning and staging tests and experiments and processing their results in the validation of a reactor installation project, estimating the accuracy of reactor design calculations, and of calculations underlying the fabrication of reactor components and subsystems, selecting appropriate solutions where indeterminacies exist in the initial information. The book is in five sections and fourteen chapters.

The first section can be treated as an introductory section devoted to elements of the theory of probabilities and mathematical statistics. Basic concepts and methods cited in the text are used in subsequent sections when applied to specific engineering problems.

These problems are divided up into three categories: problems arising in the design and calculations of reactors (second section), staging of experimental research (third section), and construction of the reactor and fabrication of reactor components (fourth section). In all cases the author strives to lend the topics a concrete character and to keep the treatment as close to an engineering approach as possible. This portion of the book contains numerous examples illustrating applications of the methods described.

The fifth section offers a review and analysis of current sophisticated statistical techniques available for use in reactor design in the solution of engineering problems under conditions where the initial information contains uncertainties. This section is clearly method-oriented, and can apparently be treated as the first step in investigations in this intriguing and important area.

The appendices are also quite interesting, and offer in addition to the usual mathematical tables reference data on the rate of failure of components of reactors and nuclear power station equipment, as well as initial foreign statistical data for reliability and safety forecasts of reactors of various types. While securing these data, the author studied and analyzed a large volume of Soviet and foreign investigations (the total bibliographic list contains 130 titles, and over half of these are translated and foreign publications). The text contains 32 illustrations and 53 tables of data; there is also a subject index.

While intended for a broad range of specialists working in reactor engineering, A. I. Klemin's book can serve as a handbook on the use of the methods of probability theory and mathematical statistics in solving practical problems in reactor design. There is no question as to the value of the book, which the intended reader will find highly interesting.

*Atomizdat, Moscow, 1973.

Translated from Atomnaya Énergiya, Vol. 36, No. 3, pp. 246-247, March, 1974.

B. B. Kadomtsev (Editor)

LASERS AND THERMONUCLEAR FUSION (A COLLECTION OF TRANSLATED ARTICLES)*

Reviewed by D. A. Shcheglov

At the present time, research on laser applications in the generation and heating of plasma has acquired a broad scope in our country and elsewhere. This has led to a marked increase in the number of publications scattered among the wildest variety of sources. The appearance of the collection of articles now being reviewed reflects the essential need to select and review the scientifically most important research reflecting the experience amassed by leading foreign laboratories.

The articles in this collection are grouped by topic. The first of the four sections discusses the possibility, in principle, of solving the problem of controlled thermonuclear fusion with the aid of high-power lasers. Estimates of the parameters of laser arrangements of different types are cited, special features of laser-generated plasmas are discussed, forecasts on the future outlook of research in this domain are ventured.

The next section groups together theoretical contributions devoted to the interaction between laser radiation and plasma. Also covered are absorption of high-level laser radiation, and topics involving plasma heating and expansion of plasma in space.

The third and fourth sections include articles which contain experimental research findings on the generation and heating of plasma by laser radiation, and also on the behavior of laser-generated plasma in strong magnetic fields. Some of these articles are of greater interest from the vantage point of the diagnostic techniques described in them, such as holographic interferometry, high-speed photography using electronic image converters, and recording of x-radiation and neutrons.

The collection starts with an introductory article (by B. B. Kadomtsev, N. G. Koval'skii, and A. F. Nastoyashchii) entitled "Lasers and thermonuclear fusion," which offers a concise presentation of the basic experimental, theoretical, and engineering topics pertaining to this problem.

Since research on utilization of lasers to solve the problem of controlled thermonuclear fusion continue on a course of vigorous exploration and development, the publication of similar topical collections of articles in the future can only be encouraged.

The book under review here can be useful to research scientists and engineers working in the field of plasma physics and controlled thermonuclear fusion, and to specialists on interactions between high-output laser radiation and matter, as well as to graduate and undergraduate students majoring in those areas.

*Atomizdat, Moscow, 1973.

Translated from Atomnaya Énergiya, Vol. 36, No. 3, p. 247, March, 1974.

N. Z. Bitkolov, V. S. Nikitin, and
A. I. Burnazyan (Editor)

LABOR CONDITIONS AND VENTILATION OF RADIOACTIVE-ORE MINE WORKINGS*

Reviewed by B. D. Chizhov and N. I. Chesnokov

The specific weight of minerals mined by the open-pit method is considerable at the present time and is increasing from one year to the next. Ore mined in open-pit quarries is cheaper; there are greater opportunities for the application of highly productive machinery and better working conditions for the miners. As open-pit workings are driven deeper into the earth, however, the natural turnover of air slackens, with the result of increasing dust load and atmospheric gas load at the worksites. We can therefore only welcome the appearance of a book generalizing and reviewing Soviet and foreign practice in improving open-pit working conditions.

In this sense, the book under review here is most timely, and constitutes an excellent practical handbook for production experts and planners. The text rather exhaustively covers available experience in this area, and offers recommendations on achieving appropriate public-health standards in working conditions.

It is vitally important in this context that the book pays close attention to forecasting the composition of the atmosphere in open-pit quarry workings through a coverage of geographical, geological, meteorological, and technological factors, as well as justification of the requisite techniques and equipment for rendering working conditions healthy in planning open-pit mining operations.

With this highly positive assessment of the content of the book, as well as its style, the great detail in its treatment of a broad range of topics, and the practicalness of the recommendations offered, we feel free to venture a few comments.

The content of the book is actually broader than the title would indicate: the text describes not only problems in the ventilation of open-pit workings, but also ways of dust and gas control at the worksites, and the treatment extends beyond uranium quarries to open-pit work on coal deposits other than uranium.

It can be stated that the content of radon and radon daughters (which the authors incorrectly refer to on p. 12 as "emanations") in the atmosphere of uranium ore quarries is always well below the permissible concentration levels, and only in isolated quarries with high-grade uranium ores do we find recordings of enhanced γ-radiation, a specific feature and problem that is not mentioned by the authors.

More attention should have been given in the text to experience in artificial ventilation of quarries and open-pit workings, a topic which is only partly elucidated in the technical literature appearing in recent years.

*Atomizdat, Moscow, 1973.

Translated from Atomnaya Énergiya, Vol. 36, No. 3, p. 247, March, 1974.

The Plenum/China Program.

An event of singular importance for international science and technology.

Following closely upon the appearance of the first scientific periodicals in China since the Cultural Revolution, Plenum proudly announces the publication of authoritative, cover-to-cover translations of the major, primary journals from China, under the Plenum/China Program imprint.

These authoritative journals contain papers prepared by China's leading scholars and present original research from prestigious Chinese institutes and universities.

In addition to the biomedical and geoscience journals listed for 1974, the Plenum/China Program will publish cover-to-cover translations of periodicals in physics, chemistry, computer science, automation, mathematics and the engineering disciplines. The translations will be prepared by a large team of experts selected especially for the program, and each journal will be under the direct supervision of an outstanding authority in the field.

The first issue of each of the translation journals will be published in early 1974, and, as with our Russian periodicals under the Consultants Bureau imprint, the translations of the Chinese journals will be available within six months following the appearance of the original Chinese edition.

Subscriptions are now being accepted. Examination copies will be available in early 1974.

available in 1974	Subscription Rates*
Acta Botanica Sinica (2 issues)	$ 75
Acta Entomologica Sinica (2 issues)	$ 55
Acta Geologica Sinica (2 issues)	$ 75
Acta Geophysica Sinica (1 issue)	$ 27.50
Acta Microbiologica Sinica (2 issues)	$ 55
Acta Phytotaxonomica Sinica (4 issues)	$125
Acta Zoologica Sinica (4 issues)	$125
Chinese Medical Journal (12 issues)	$195
Geochimica (4 issues)	$110
Kexue Tongbao—Scientia (6 issues)	$ 90
Scientia Geologica Sinica (4 issues)	$125
Vertebrata PalAsiatica (2 issues)	$ 60

forthcoming

Acta Astronomica Sinica (2 issues)

Acta Biochimica et Biophysica Sinica (2 issues)

Acta Mathematica Sinica (4 issues)

Genetics Bulletin (4 issues)

Huaxue Tongbao—Chemical Bulletin (6 issues)

*These prices are for the 1973 Chinese volumes which will be published in translation during 1974. Prices somewhat higher outside the U.S.

plenum
PLENUM PUBLISHING CORPORATION
227 West 17 Street, New York, N.Y. 10011
In United Kingdom: 8 Scrubs Lane, Harlesden, London, NW10 6SE, England

Declassified and Approved For Release 2013/01/25 : CIA-RDP10-02196R000400030003-5

breaking the language barrier

WITH COVER-TO-COVER ENGLISH TRANSLATIONS OF SOVIET JOURNALS

in physics

Title	# of Issues	Subscription Price
Astrophysics *Astrofizika*	4	$120.00
Fluid Dynamics *Izvestiya Akademii Nauk SSSR mekhanika zhidkosti i gaza*	6	$180.00
High-Energy Chemistry *Khimiya vysokikh énergii*	6	$155.00
High Temperature *Teplofizika vysokikh temperatur*	6	$150.00
Journal of Applied Mechanics and Technical Physics *Zhurnal prikladnoi mekhaniki i tekhnicheskoi fiziki*	6	$175.00
Journal of Engineering Physics *Inzhenerno-fizicheskii zhurnal*	12 (2 vols./yr. 6 issues ea.)	$175.00 ($87.50/vol.)
Magnetohydrodynamics *Magnitnaya gidrodinamika*	4	$125.00
Mathematical Notes *Matematicheskie zametki*	12 (2 vols./yr. 6 issues ea.)	$185.00
Polymer Mechanics *Mekhanika polimerov*	6	$140.00
Radiophysics and Quantum Electronics (Formerly Soviet Radiophysics) *Izvestiya VUZ. radiofizika*	12	$180.00
Solar System Research *Astronomicheskii vestnik*	4	$ 95.00
Soviet Applied Mechanics *Prikladnaya mekhanika*	12	$175.00
Soviet Atomic Energy *Atomnaya énergiya*	12 (2 vols./yr. 6 issues ea.)	$175.00 ($87.50/vol.)
Soviet Physics Journal *Izvestiya VUZ. fizika*	12	$180.00
Soviet Radiochemistry *Radiokhimiya*	6	$165.00
Theoretical and Mathematical Physics *Teoreticheskaya i matematicheskaya fizika*	12 (4 vols./yr. 3 issues ea.)	$160.00

Back volumes are available. For further information, please contact the Publishers.

SEND FOR YOUR FREE EXAMINATION COPIES

PLENUM PUBLISHING CORPORATION
227 WEST 17th STREET
NEW YORK, N. Y. 10011
Plenum Press • Consultants Bureau
• IFI/Plenum Data Corporation

In United Kingdom: 4a Lower John Street, London W1R 3PD, England